33447000036248

MIRL Report No. 71

# Petrologic And Geochemical Characterization Of The Red Dog And Other Base-Metal Sulfide And Barite Deposits In The Delong Mountains, Western Brooks Range, Alaska

By

Larry Lueck
Mineral Industry Research Laboratory

School of Mineral Engineering
University of Alaska-Fairbanks
Fairbanks, Alaska 99775-1180

February, 1986

State of Alaska / DNR
Division of Geological &
Geophysical Surveys
3354 College Road
Fairbanks, AK 99709-3707
ADGGS Library

ABSTRACT

Low Cu content, lead isotope ratios, mineralogy, stratigraphy, geochemistry, and morphology of the stratiform Red Dog and Drenchwater Zn-Pb-Ba deposits are consistent with a syngenetic, submarine-exhalative origin in a Carboniferous back-arc or epicontinental rift basin. Red Dog apparently formed without vulcanism from ocean-floor hot springs like those active in the Guaymas Basin today, while submarine eruptions accompanied or followed Drenchwater sulfide emplacement. Story Creek and Ginny Creek epigenetic Zn-Pb mineralization is hosted in older sediments of the same basinal sequence. Lead isotope ratios from all four deposits are virtually identical, averaging $Pb^{206}/Pb^{204}$ = 18.408, $Pb^{207}/Pb^{204}$ = 15.598, $Pb^{208}/Pb^{204}$ = 38.250. These values fit the plumbotectonics lead growth curves for the orogene. This lead similarity also implies that the Ginny Creek and Story Creek occurrences are genetically related to Red Dog and Drenchwater, by remobilization or as parts of a regional 'plumbing system' that fed the exhalative deposits.

TABLE OF CONTENTS

LIST OF FIGURES

LIST OF TABLES

ACKNOWLEDGMENTS

I am grateful to many people for help and encouragement on this thesis: my faculty committee, P.D. Rao, Chairman, D.B. Hawkins, and S.E. Swanson; the Mineral Industry Research Laboratory of the University of Alaska, Fairbanks, for logistical, financial, and other support during the first year of thesis work and subsequently; WGM, Inc. and the U.S. Bureau of Mines for helicopter transport in the field; W.J. Nokleberg for microprobe analyses; C.F. Mayfield for samples; the Geophysical Institute of the University of Alaska, Fairbanks, for financial assistance toward SEM work; these and numerous other geologists, professors, and fellow graduate students for encouragement and many fruitful discussions; Mary Albanese for an important critical review; my friend Stephen Cowdrey for assistance with photography; and the D.G.G.S. cartographic staff for advice on drafting. Perhaps most importantly, I could not have completed this work without the patience of my wife Karen Burke, who put up with the obsession for so long and frequently made suggestions from a fresh, non-geologist's point of view.

# I. INTRODUCTION

Within the last fifteen years deposits and geochemical anomalies of Zn-Pb-Ag and barite have been discovered over a wide area in a single largely sedimentary rock sequence in the DeLong Mountains portion of the western Brooks Range, northwestern Alaska (Fig. 1). Despite certain differences among them, the Red Dog, Drenchwater, Ginny Creek, and Story Creek deposits have some important features in common. This thesis presents geological, geochemical, and lead isotope data that suggests that these widely spaced mineral occurrences may have had a common origin in one large mineralizing event.

When study for the thesis began in 1978, little was known about the Red Dog Zn-Pb-Ag-Ba deposit (Fig. 1). Plahuta (1978) published a preliminary map, cross sections, sample descriptions, and selected geochemical analyses from the deposit. Since then, at least one paper has concluded that Red Dog mineralization is of submarine exhalative origin (Plahuta and others, 1983), and one paper has drawn a connection between the sulfide mineralization and supposed volcanic activity in the Red Dog area (Lange and others, 1981). Information presented in the thesis supports and refines the syngenetic submarine exhalative mode of formation for Red Dog but argues against the volcanogenic hypothesis. Detailed studies of the Red Dog ore and country rock presented here disclose features compatible with an origin in an immature submarine spreading center or failed rift zone.

Lange and others (1981) and Nokleberg and Winkler (1982) conclude that the Drenchwater Zn-Pb-Ba deposit (Fig. 1) is of submarine volcanogenic origin, perhaps of Kuroko type, mainly because of a close spatial association between exposed igneous rocks and sulfide mineralization at this location. However, this deposit has mineralogical and geochemical features and lead isotope ratios nearly identical to those of the non-volcanogenic Red Dog deposit. It will be shown that the Drenchwater deposit, as it currently exists, may have resulted from the superimposition of a volcanic event upon a sedimentary exhalative mineralizing event.

The Ginny Creek Zn-Pb-Ag occurrence (Mayfield and others, 1979) and the Story Creek Pb-Zn-Ag occurrence (Jansons and Parke, 1981; Ellersieck and others, 1981) are epigenetic sulfide deposits that occur in the same basinal rock sequence that hosts the Red Dog and Drenchwater mineralization (Fig. 1). The sulfide mineral suites and lead isotope ratios at Story Creek and Ginny Creek are nearly identical to those found at Red Dog and Drenchwater. This very close mineralogical and lead isotope similarity between the four deposits is unlikely to be due to chance. The argument is made in the thesis that epigenetic deposits like those at Ginny Creek and Story Creek could

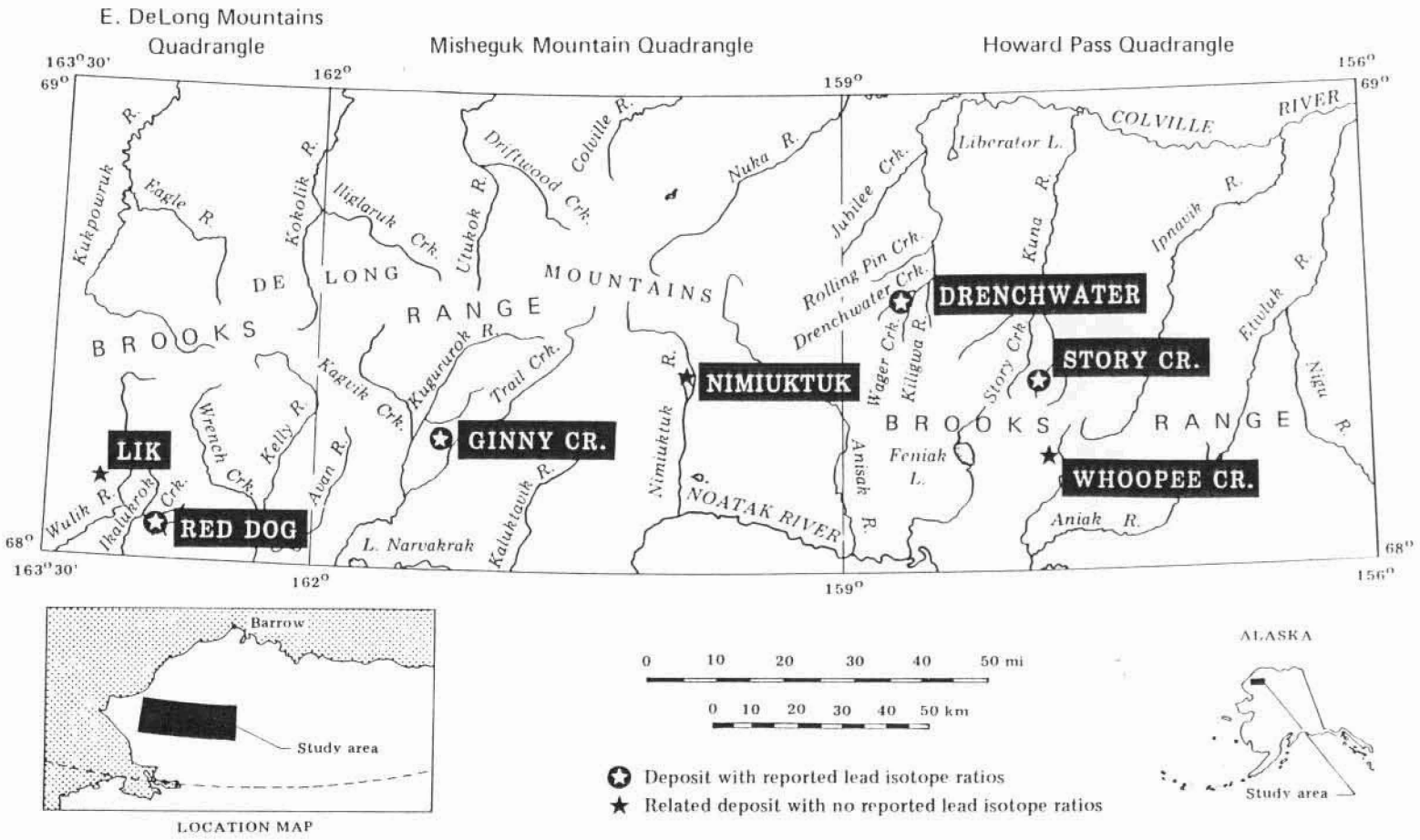


Figure 1. Location map of important base-metal and barite deposits in the DeLong Mountains, northwestern Brooks Range, Alaska.

have formed from the same source and at the same time as did syngenetic deposits like Red Dog and Drenchwater, or might have been emplaced by remobilization at a later time.

All of the authors cited above present geochemical data from mineral and rock samples from the four deposits. Metz and others (1979a) report analyses of soil samples from Red Dog and Drenchwater. The thesis presents selected semiquantitative trace element analyses of sulfide, barite, and host rock samples from all four deposits, with emphasis on Red Dog. These analyses add to the data base on the DeLong Mountains mineral deposits and suggest possible avenues for further research.

Access to Red Dog is by light plane or helicopter from Kotzebue, about 90 km south, to bush strips near the deposits. Winter travel from Kotzebue by tracked vehicle, snow machine, or ski plane is possible. A mining haul road from the coast to Red Dog is planned to be installed in the next few years. No access to Drenchwater other than small plane or helicopter is feasible at present. These are also the only reasonable means of reaching Ginny Creek, the Nimiuktuk River and the Story Creek-Whoopee Creek area.

The DeLong Mountains is a region of gently rolling hills and modest mountains with a relief of up to about 1,500 meters. Though treeless, the country is largely covered with tundra, patterned ground, and talus on lower slopes, with alder thickets in some stream valleys. Permafrost is continuous and thaws little during the short summer, depending on soil cover, plant cover, and drainage; frost boils are common. Annual precipitation is on the order of 50 to 80 cm. The region is usually only snow-free from about mid-June through August. Thus rock weathering is probably dominated by mechanical processes most of the year. Animal life, including grizzly bears, caribou, and smaller forms, is locally abundant.

## II. METHODS AND ANALYTICAL TECHNIQUES

### A. Field sampling

Several hundred hand specimens of sulfide ore, barite, gangue, and country rock for thesis work were collected at the Red Dog deposit. Sampling was done at measured ten-foot intervals through the zone of visible mineralization on the main fork of Red Dog Creek and one of its tributaries. Ore was sampled, if present, at each ten-foot location, plus or minus two feet up- or downstream. In some locations it was necessary to dig through several feet of overburden to obtain a sample.

Sample locations and brief outcrop descriptions were plotted in the field on a hand-drawn strip map at a scale of 1 inch = 10 feet. This strip map was keyed to: U.S.G.S. 1:40,000-scale black and white air photos of the area; a north-south, east-west square sample grid on 250' centers that had been surveyed over the orebody for sampling and other purposes (Metz and others, 1979a); and to a DeLong Mountains A-2 1:63,360 quadrangle map. Sample locations transferred from this strip map are shown on a portion of the geological map of Plahuta (1978) in Appendix A of the thesis.

Samples were collected at the Drenchwater Creek deposit by the author and P.A. Metz. Outcrops at Drenchwater, especially outcrops containing visible sulfide minerals or barite, are much scarcer than at Red Dog and do not necessarily occur in or near the creek. Sample locations were keyed to 1:40,000-scale air photos, to a surveyed 1000' x 1000' square grid (Metz and others, 1979a), and to a photoreduced copy of the Drenchwater geological map by Nokleberg and Winkler (1982). Locations of samples used in the thesis are shown on a portion of this map in the chapter on Drenchwater. Still later, C.F. Mayfield of the US Geological Survey contributed several grab samples of representative sulfide ore from the Ginny Creek and Story Creek occurrences, and one of barite from the Nimiuktuk barite deposit.

### B. Mineralogy and petrology

110 polished sections were prepared from selected hand specimens of Red Dog sulfide ore. These were studied and photographed under reflected light using mainly Zeis microscope equipment. Fifty thin sections of rock and sulfide samples were also prepared and studied under transmitted light with the same microscope. When samples became available from the other thesis deposits, thin and polished sections were similarly prepared and examined.

Pyritized sponge spicules were separated from Red Dog host rock

with hot hydrofluoric acid. These spicules were further studied and photographed with a JEOL JSM35 scanning electron microscope and standard techniques at the Electron Microscope Laboratory of the Geophysical Institute, the University of Alaska, Fairbanks.

Four selected polished sections of ore from Red Dog and one from Drenchwater were sent to the US Geological Survey in Menlo Park, California for electron microprobe analysis of sphalerite. Analyses were performed by W.J. Nokleberg, using an Applied Research Laboratory S.E.M. instrument and a theoretical corrections program developed by the US National Bureau of Standards, as modified by M.H. Beeson and L.C. Calk (Nokleberg and Winkler, 1982). The general operating conditions were 15-kV accelerating potential, 0.02 to 0.03 A sample current, fixed-beam current integration times of about 10 seconds, subtraction of background counts, and use of natural or synthetic standards similar in composition to the unknowns.

Two separates each of Red Dog sphalerite and galena were analyzed by X-ray diffraction. Analyses were performed at the laboratory of the Alaska Division of Geological and Geophysical Surveys, Fairbanks, with standard powder camera X-ray diffraction methods.

## C. DC-arc emission spectroscopy

Mineral and rock samples were semiquantitatively analyzed using DC-arc emission spectroscopy. Instrumentation consisted of a Jarrell-Ash 1.5-meter Wadsworth grating spectrograph, a model JA 43-650 Spectro-Varisource, a model JA 17325 microphotometer, and a model JA 34-300 photo-processor. The technique is described in detail by Stevens (1971).

Samples of ore, barite, host rock, and granular quartz rock were selected for emission spectrographic analysis from among several hundred Red Dog hand specimens. Ore samples were crushed to about 1 mm and hand picked under a binocular microscope to separate mineral phases. In most cases, at least two or three grams of sample were carefully separated in this way, never less than about half a gram. During fine grinding in a Wiggle Bug each sample was thoroughly homogenized. Although this process should minimize the effects of contamination by mineral inclusions, a certain amount of cross-contamination of each separated mineral sample by other mineral grains is inevitable. The problem cannot be prevented completely because of the nature of the materials and the necessity for mechanical separation. The same contamination would occur regardless of the analytical technique used.

Sphalerite is represented by the most emission spectrographic analyses from Red Dog because it is more abundant and more often

coarse grained than the other sulfides, which makes it both more important and easier to separate. Although there could be trace element differences between pyrite and marcasite, these two minerals could not be distinguished well enough under the binocular to make separation possible. Therefore they were analyzed together as Fe sulfide.

Samples of Red Dog host rock to be analyzed by emission spectrography were selected by examining polished sections to choose samples that were relatively free of disseminated sulfides and gangue. Five- to ten-gram pieces were then broken off the corresponding hand specimens. These pieces were hand crushed in stages to disclose any internal concentrations of extraneous material. Granular quartz rock samples were similarly chosen and crushed to remove coarse impurities, although most samples contained small to moderate amounts of fine barite which it was not feasible to separate out; this material is therefore designated "quartz-barite rock" in Table 2 and Appendix B.

## D. Lead isotope analyses

Lead isotope compositions were determined for six samples of galena separated by the author. Three of these analyses are from three different types of Red Dog sulfide ore, and one each from Drenchwater, Ginny Creek, and Story Creek. Geospec Consultants, Limited, of Edmonton, Alberta, report that analyses were performed by the silica gel-phosphoric acid technique, that the data were corrected for mass discrimination by comparison to the NBS SRM-981 common lead standard, and that comparison with the standard indicates a precision of better than 0.1% per mass unit (vendor's report, 1981).

## III. REGIONAL GEOLOGY

### A. Background

All of the ore occurrences discussed in this thesis (Fig. 2) are found in one large arcuate belt of genetically related rocks termed the Brooks Range allochthon (Mayfield and others, 1983)("Brooks Range allochthon" should not be confused with "Brooks Range," a possibly unfortunate overlap in nomenclature). This group of rocks was named the Brooks Range sequence by Martin (1970) because of its widespread occurrence throughout the northern and western parts of the Brooks Range. The same rocks have also been called the Foothills sequence (Tailleur and others, 1966) and the Endicott sequence (Mull and others, 1982). A structural sequence of Upper Mississippian to Lower Cretaceous rocks corresponding to much of the Brooks Range allochthon has been described as the Kagvik sequence by Churkin and others (1979). Kagvik sequence nomenclature and interpretation have been

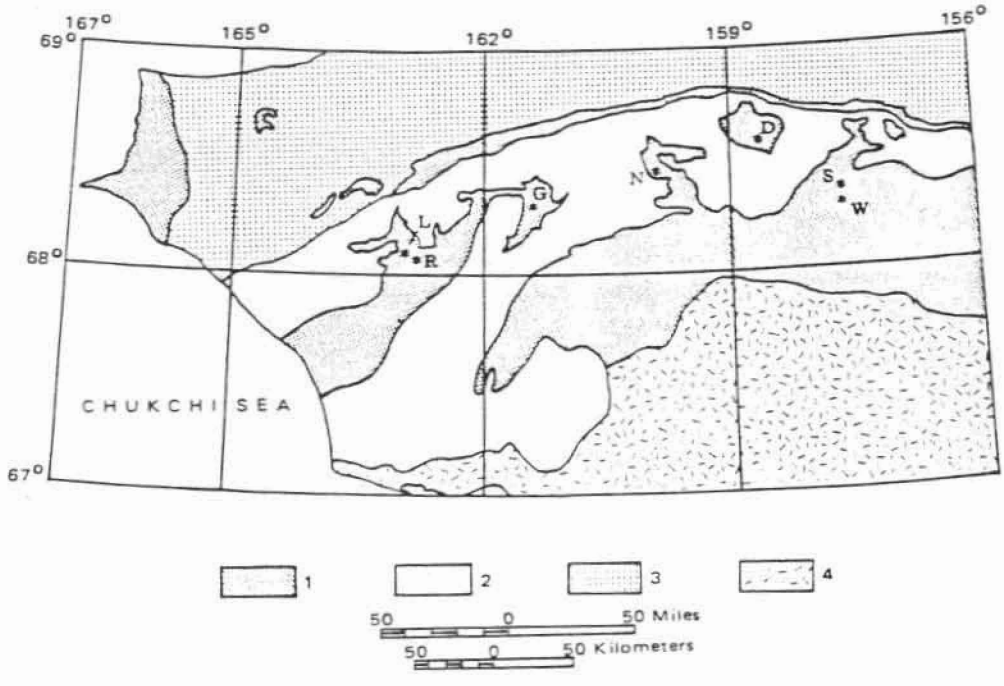


Figure 2. Map (after Mayfield and others, 1982) of the western Brooks Range showing: 1, Brooks Range allochthon; 2, other allochthons; 3, autochthonous rocks of Cretaceous age; 4, autochthonous rocks of Paleozoic and Precambrian(?) age. Asterisks represent deposits: L = Lik; R = Red Dog; G = Ginny Creek; N = Nimiuktuk; D = Drenchwater; S = Story Creek; W = Whoopee Creek.

questioned on various grounds by Crane (1980), Dutro (1980), Mayfield (1980), Metz (1980), Mull (1980), and Nelson (1980), but further defended by Nokleberg and Churkin (1980). The Kagvik controversy is part of a complex debate concerning the depositional setting and tectonic evolution of rocks in the western Brooks Range, the central question being whether these rocks were deposited on oceanic crust in a deep-ocean environment or within an intracontinental basin.

Mayfield and others (1983), in constructing their synthesis of Brooks Range stratigraphy and tectonics, draw on a much larger body of data than was available to Martin (1970). In their terminology "allochthon" is substituted for Martin's "sequence" to emphasize the allochthonous nature of these rocks. Allochthon rather than Kagvik terminology is adopted for the thesis because it encompasses a larger area in a single system, and because it is newer, incorporating information not available to Churkin and others (1979). Although the thesis includes the Drenchwater Creek area within the Key Creek sequence, this is not the view of some published authors on the Drenchwater deposit (Lange and others, 1981; Nokleberg and Winkler, 1982) who refer exclusively to the Kagvik sequence.

## B. Brooks Range allochthon and Key Creek sequence

There are seven allochthons in the western Brooks Range and one group of pre-Cretaceous autochthonous or parautochthonous rocks (Mayfield and others, 1983). These authors describe ways in which the Brooks Range allochthon can be clearly distinguished from the other six allochthons (Fig. 2).

The Key Creek sequence of the Brooks Range allochton (Fig. 3) was named by Curtis and others (1982) for exposures at Key Creek in the DeLong Mountains A1 Quadrangle. Most of the rocks of the Brooks Range allochthon, except for those of the Lisburne Peninsula and a narrow strip of Ivotuk sequence rocks on the northeast edge of Figure 2, belong to the Key Creek sequence. This sequence differs from the other two sequences of the Brooks Range allochthon in several distinctive ways and can be clearly recognized in the field (Mayfield and others, 1983).

The other two structural sequences of the Brooks Range allochthon, the Ivotuk sequence and the Lisburne Hills sequence lie structurally below the Key Creek sequence (Mayfield and others, 1983), and are not reported to host significant sulfide deposits. Distinctive Mississippian carbonates of the Ivotuk sequence appear, west of longitude 158°W, to grade into lithologies characteristic of the Key Creek sequence. The Lisburne Hills sequence is cut off from other allochthonous sequences in the western Brooks Range by a belt of Cretaceous clastic rocks, but it is assigned to the Brooks Range

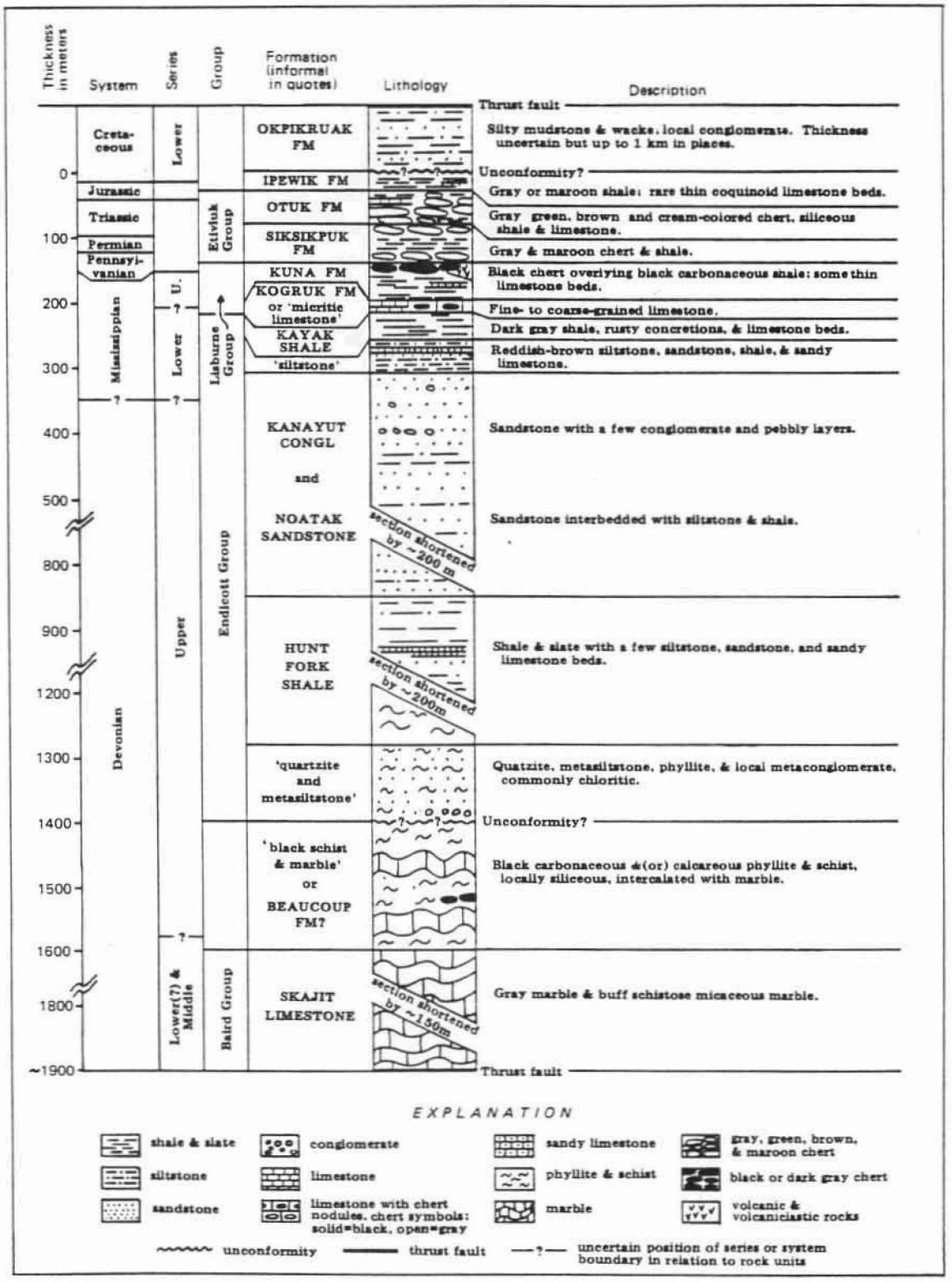


Figure 3. Columnar section of the Key Creek sequence of the Brooks Range allochthon (after Mayfield and others, 1983).

allochthon because its lithology and distinctive tectonic history are similar to those of the other sequences in the allochthon.

C. Kuna Formation

The Kuna Formation, host to the Red Dog and Drenchwater Creek deposits, was defined and named by Mull and others (1982). It overlies the Lower Mississippian Kayak Shale of the Endicott Group, and underlies the Pennsylvanian to Triassic Siksikpuk Formation of the Etivluk Group (Fig. 3). In its type section, the Kuna Formation consists of about 65 m of dark to black interbedded shale and chert, and occasional lenticular dark gray limestone beds up to a few meters thick. Elsewhere it probably ranges from about 45 to 100 m thick, though folding and thrusting locally make it appear thicker. The name Kuna Formation replaces the names Tupik Formation, Kogruk Limestone, Utukok Formation, and Nasorak Formation in locations to which the new terminology applies. In the DeLong and Endicott Mountains the Kuna Formation is in either disconformable or conformable contact with the overlying Siksikpuk Formation, depending on location. In the western Endicott Mountains the Kuna Formation gradationally overlies the Kayak Shale, uppermost formation of the Endicott Group. Elsewhere it intertongues with carbonate rocks of the Lisburne Group that depositionally overlie the Endicott Group. A lower gradational relationship with underlying units is characteristic, and no thrust contacts or unconformities are mentioned by Mull and others (1982).

D. Summary of geologic history

The entire Brooks Range allochthon, including the Key Creek sequence, was originally deposited in an ensialic basin south of an autochthonous platform at the same time that most of the other allochthons were forming further offshore to the south (Mayfield and others, 1983). Plahuta and others (1983) agree that the Red Dog deposit appears to have formed in an epicontinental setting. The north-south compressional event which created most of the Brooks Range orogen (cf. "orogene" in chapter VII) is believed to have begun in Middle Jurassic time, about 170-150 m.y. ago (Tailleur and Brosgé, 1970; Roedder and Mull, 1978). Closing of the basin in which sediments of the Brooks Range allochthon were deposited reached completion at about 110-100 m.y. ago in Early Cretaceous (Albian) time; isostatic readjustment in the Baird Mountains and folding with minor faulting in the DeLong and Endicott Mountains continued through Middle and Late Cretaceous time (Mayfield and others, 1983).

Local geology of the mineral occurrences discussed in this thesis has, with the exception of the Drenchwater deposit, been reported to fit within the Key Creek sequence. That exception arises because

Nokleberg and Winkler (1982), in describing Drenchwater Creek geology, employ Kagvik sequence terminology. The rocks themselves also fall within the Key Creek sequence. Published descriptions of the other deposits reported on here are very brief but host rock units appear to be well identified and to belong to the Key Creek sequence.

# IV. RED DOG

## A. Background

Red Dog Creek (Fig. 4A,B) heads on the western flank of Deadlock Mountain in T31N, R18W, Kateel River Meridian in the DeLong Mountains quadrangle, and flows first north, then northwest about 6 miles to the Ikulukrok River, a tributary of the Wulik River (Fig. 5). Four tributaries flow into Red Dog Creek from the east. The middle two are mineralized, the northern and southern ones apparently are outside the ore zone. Several small intermittent tributaries (Fig. 4C) enter Red Dog Creek from the west within the study area. These intermittent streams are highly iron-stained, discharging yellow and orange limonitic sediments that color the rocks on the western side of Red Dog Creek for a considerable distance down stream. Colorful "kill zones" devoid of vegetation make the study area highly visible from the air.

Geochemical anomalies and the iron staining were first recognized at Red Dog Creek in 1968 by Tailleur (1970). There is some controversy over who first "discovered" the deposit (McQuat, 1982), but it was initially staked in the mid-1970's and mapped at a scale of about 1:22,200 by Plahuta (1978).

Figure 5 is an enlarged portion of the geologic map of Plahuta (1978) showing the main Red Dog deposit. The map has been simplified somewhat but units and contacts are as on the original. Much additional work, including drilling, has been done on the deposit since thesis field work in 1978. However, this is still the most recently published geologic map of the area and gives a fair idea of the local geology. Sulfide mineralization occurs mostly in units Pss and Mtc in or near Red Dog Creek itself and in the two eastern tributaries for a few hundred meters upstream. The correlation, in the explanation to Figure 5, of Key Creek sequence units with the units of Plahuta (1978) is solely my suggestion, although Plahuta and others (1983) state that the ore host rock, units Pss and Mtc, belongs to the Kuna Formation. Locations of samples shown or referred to in the thesis are given on this same map in Appendix A.

Mapping and drilling in the last few years has delineated two separate ore bodies at Red Dog. The "main" deposit (Figure 5) is reported to contain 85 million tons of ore grading 17.1% zinc, 5.0% lead, and 2.4 oz/ton silver (Jones, 1982). The "hilltop" deposit, about 1/2 mile southwest from the section corner, is thought by Plahuta and others (1983) to be a klippe of the main orebody and contains substantial undisclosed reserves. Hereafter all discussion of Red Dog in this thesis refers to the main deposit, unless otherwise stated, because the hilltop ore is poorly exposed and its importance

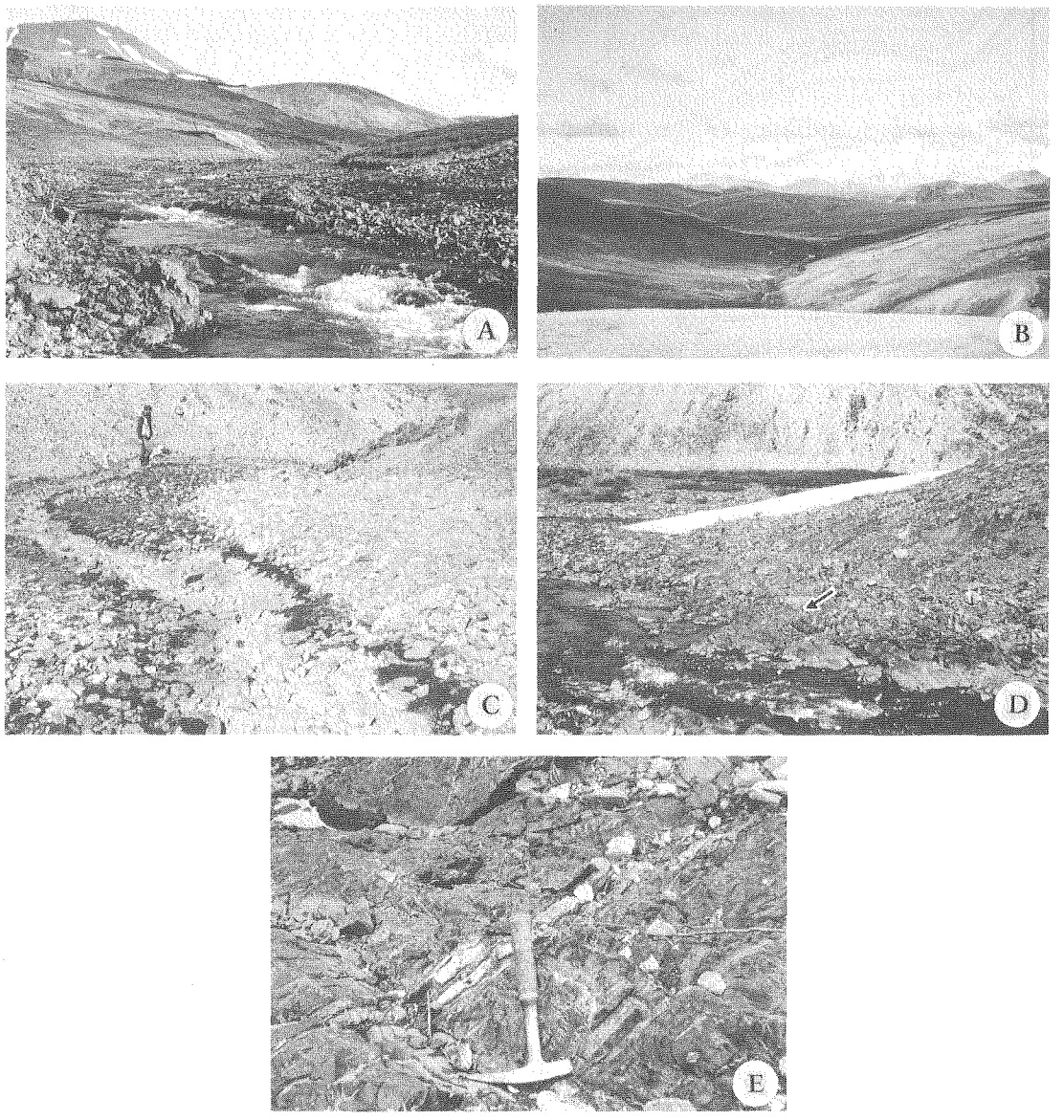


Figure 4. Terrain and outcrop photographs of the Red Dog Creek area: A, the creek viewed upstream (south); B, the valley viewed downstream (north) from the foot of Deadlock Mountain; kill zone to right, barite and quartz talus slope to left; C, dry iron-stained tributary entering Red Dog Creek main stem from west; D, typical black shale ore-bearing outcrop (black, arrow); E, sulfide-quartz veins in creek bottom.

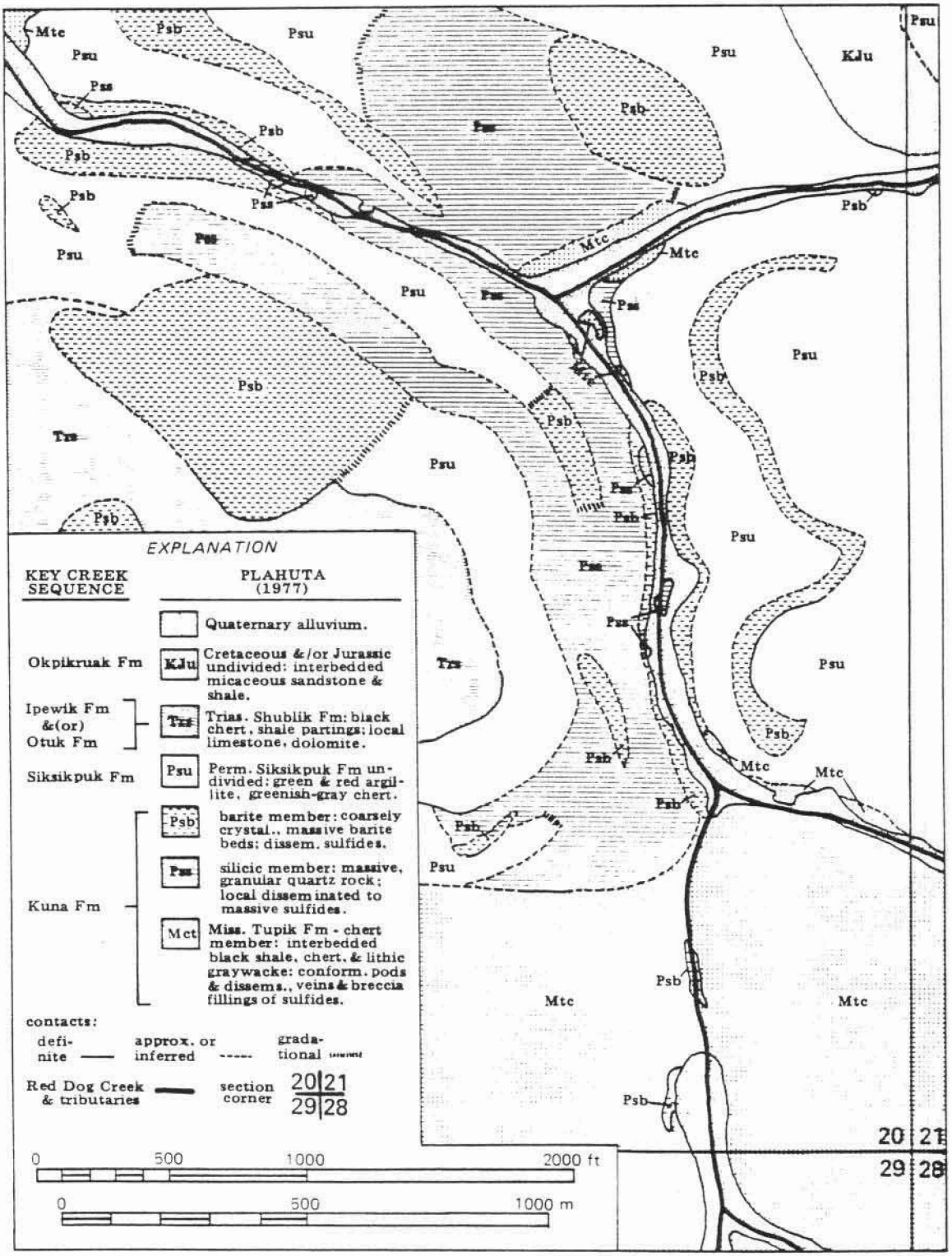


Figure 5. Geologic map of the Red Dog main deposit; simplified from part of map by Plahuta (1977). Column at far left shows a possible correlation of Plahuta's units with units of the Key Creek sequence.

was not apparent at the time of field work for the thesis. Barite has not been referred to as ore in publications but is present in quantity and may be valuable. Plans and negotiations are presently under way to begin mining the Red Dog deposit in the late 1980's.

Host rock is black shale, siltstone, and chert of the Early Mississippian to Early or Middle Pennsylvanian Kuna Formation (arrow, Figure 4D, and unit Mtc, Fig. 5). The ore takes several forms: sulfide disseminations in host rock; discordant quartz-rich sulfide veins and stockwork fillings (Fig. 4E); massive, fine-grained, conformable podiform bodies; and barite veins, some of which contain variable amounts of zinc, lead, and iron sulfides. Copper content of the deposit is low, and only very rare traces of chalcopyrite are seen in or between major minerals.

Overlying the mineralized horizon are rocks of the Pennsylvanian to Early Triassic Etivluk Group (unit Psu and possibly part of unit Trs, Fig. 5), which here consist mainly of unsilicified gray, green and red argillites interbedded with radiolarian cherts and thin barite layers of the Permian Siksikpuk formation. Rocks that form the gradational contact between the mineralized Kuna Formation and the overlying barren Etivluk Group rocks at Red Dog are probably Pennsylvanian in age; this part of the Key Creek sequence has so far been dated only by radiolaria, the study of which is not yet sufficiently refined for this region to distinguish narrow time intervals with certainty (I.F. Ellersieck, pers. comm., 1983). Only Permian radiolaria have been reported from the Etivluk Group in the study area (Mull and others, 1982). The transition between the mineralized Kuna Formation and the overlying barren Siksikpuk Formation is quite thin at Red Dog, on the order of a few tens of meters or less. Sulfide veins in the underlying Kuna Formation do not penetrate up into Etivluk group rocks. However, the fine-grained podiform ore and a fairly thick layer of barite occupy this interval (creek outcrops of unit Psb, Fig. 5).

A unit of carbonaceous granular quartz rock (unit Pss, Fig. 5) also occupies this transitional interval throughout much of the main ore zone. In outcrop this rock is often hard and blocky. In hand specimen it sometimes resembles metasandstone, including areas of recemented breccia, or highly pitted gossan. Locally it contains black carbonaceous material much like that in the Kuna Formation shale, which suggests that the quartz rock may have replaced some of the black shale and chert, or simply is intergrown with it. The quartz-rich rock in thin section does not resemble either metasandstone or any kind of volcanic rock. Instead, it is an aggregate of interlocking fine- to coarse-grained quartz crystals that sometimes exhibit concentric hexagonal growth bands. Spaces between quartz grains commonly contain up to several percent sulfide minerals and barite. Locally it contains more concentrated sulfides. This

granular quartz rock occurs in massive discontinuous layers up to several tens of meters thick. It has been referred to as a primary chemical precipitate (Lange and others, 1981).

A barite unit (exposures of unit Psb uphill away from the creek, Fig. 5) overlying the granular quartz unit is generally lighter in color than either the lower barite bed or the barite veins, and seems to contain fewer sulfides than either. Neither the quartz rock nor the barite is continuously exposed, so thicknesses and detailed relationships are difficult to determine. Barite-rich talus covers most of the hill.

Igneous rocks in the vicinity of Red Dog Creek only occur in two small exposures, one about 150 m long 1/2 km NE of the ore deposit, and one about 200 m long 1/2 km further NE. Ellersieck and others (1983) describe them as andesite or basalt composed of plagioclase, augite, biotite, apatite, and ilmenite(?) which is partly altered to chlorite, kaolinite, calcite, and leucoxene. These rocks are probably of Pennsylvanian or Mississippian age and appear to interfinger with the upper Kuna Formation (Ellersieck and others, 1983). Plahuta and others (1983) see no evidence of a genetic connection between Red Dog ore and these sparce, altered igneous rocks. Large gamma-ray anomalies found over the volcanic rocks and sulfide mineralization at Drenchwater Creek were not observed in a 1,753 m by 1,448 m study area directly over and around the Red Dog ore body (Metz and others, 1979a). Either there are no igneous rocks directly associated with ore at Red Dog or their type and/or depth prevent detection by gamma-ray spectrographic methods that were successful at Drenchwater.

No rocks older than those of the Carboniferous Kuna Formation are exposed in the immediate vicinity of Red Dog Creek. The informal Kivalina member of the Kuna Formation forms the stratigraphic footwall to mineralization, and underlying quartzose clastics containing diagenetic sphalerite, galena, and pyrite are a possible source of metals and silica (Plahuta and others, 1983). These authors present no further details on these metalliferous quartzose clastics, however, and express no opinion on their stratigraphic correlation.

## B. Outcrop and ore description

Most exposures of the ore at the Red Dog deposit occur in the stream bottoms or lower banks (Fig. 4D), where the host rock is a hard, highly silicified black shale and chert of the Kuna Formation. The most noticeable kind of ore readily found in outcrop is a zinc-quartz vein system that strikes generally northeast-southwest (Fig. 4E). Veining is locally very concentrated, with sufficient cross-cuttings and little enough host rock to be termed a stockwork or breccia (Fig. 6A and 6B). These veins are often many centimeters

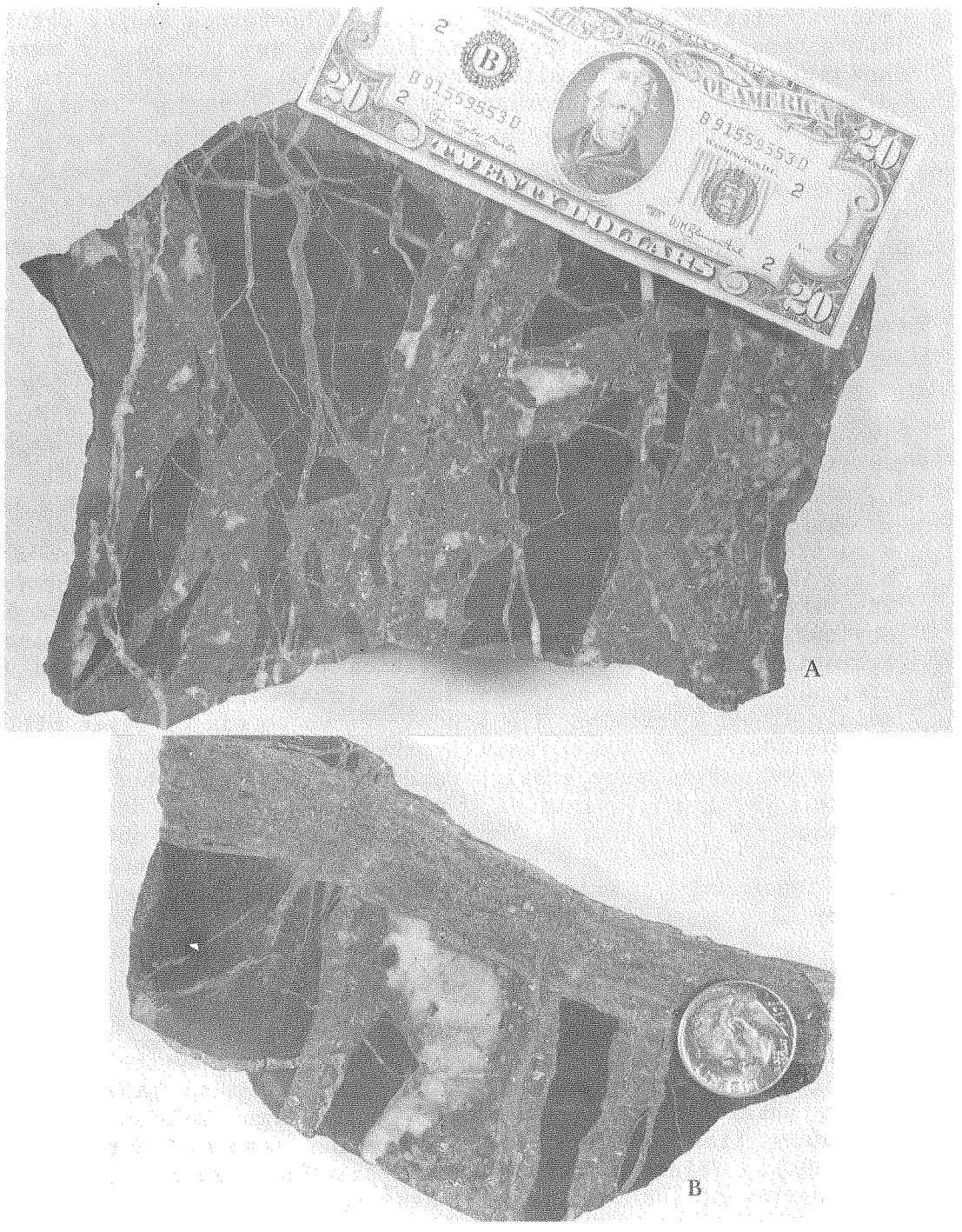


Figure 6. Slabbed Red Dog vein-type ore: A, mostly sphalerite (gray) with some white quartz and angular black host rock fragments; B, sulfide veins cross-cutting at right angles; dusty appearance of black fragment, left, caused by minute but closely spaced sphalerite disseminations. Note is 156 mm long, coin is 18 mm in diameter.

thick and nearly pure sphalerite (Fig. 7A), but sometimes they are microscopically thin, cutting both black host rock and/or earlier ore. Laminations of sphalerite, iron sulfides (pyrite and/or marcasite), and quartz frequently alternate (Fig. 7B). All sphalerite, whether disseminated or in discordant veins, is of varying shades of brown through reddish brown.

Sulfide ore also occurs as unlaminated breccia fillings adjacent to veins. This mineralization, besides containing abundant clasts of black shale and chert of all sizes (Fig. 7C), has a clastic-appearing texture itself and contains considerably more galena than do most of the sphalerite-pyrite-marcasite veins. This is suggestive of relatively late emplacement, since galena is, in general, paragenetically late at Red Dog. Thus although the breccia ore is spatially associated with veins, its internal structure and mineral content is more similar to that of some of the ore termed "podiform" (see below).

The vein and breccia ore styles are the most obvious in outcrop at Red Dog but another type of ore may be more abundant, namely, disseminated sphalerite with minor disseminated galena in the same black Kuna Formation rock. These disseminations can be seen in Figure 6B but are more distinct in Figures 8A and 8B. Figure 8A shows obvious layering of macroscopic sphalerite grains in black Kuna Formation rock. A possible variation of this disseminated type of ore, which was nicknamed "buckshot" in the field, is also composed mainly of sphalerite but the grains are up to six or seven millimeters in diameter (Fig. 8B). Locally these grains occur in concentrated masses of nearly pure sphalerite containing little host rock, though in thin section individual grains can still be distinguished by zonation and thin quartz rims. This ore type does not appear to be layered or laminated at this scale. Such disseminated ore could be very important at Red Dog because it is the dominant type at the nearby Lik deposit (Fig. 1), a subsurface ore body hosted in similar black Kuna Formation rocks and apparently lacking an underlying vein system (Harrover and others, 1982).

After the veins, breccia, and disseminated ore, the most abundant Red Dog mineralization is massive fine-grained pyrite and marcasite that contains variable amounts of sphalerite and galena. Like the major sphalerite mineralization, this iron sulfide varies from extremely fine veinlets to major veins several centimeters thick (Fig. 9A). Veins of this material are found mainly up the eastern tributaries of Red Dog Creek. Massive, fine-grained pyrite-marcasite also occurs as small pockets containing quartz and isolated black host rock clasts (Fig. 9B). In places, this material forms small outcrops composed almost entirely of anhedral iron sulfide grains (breccia?) cemented by late quartz (Fig. 10A). Other hand specimens of ore collected at Red Dog represent scarcer types; the sample in Figure 8C

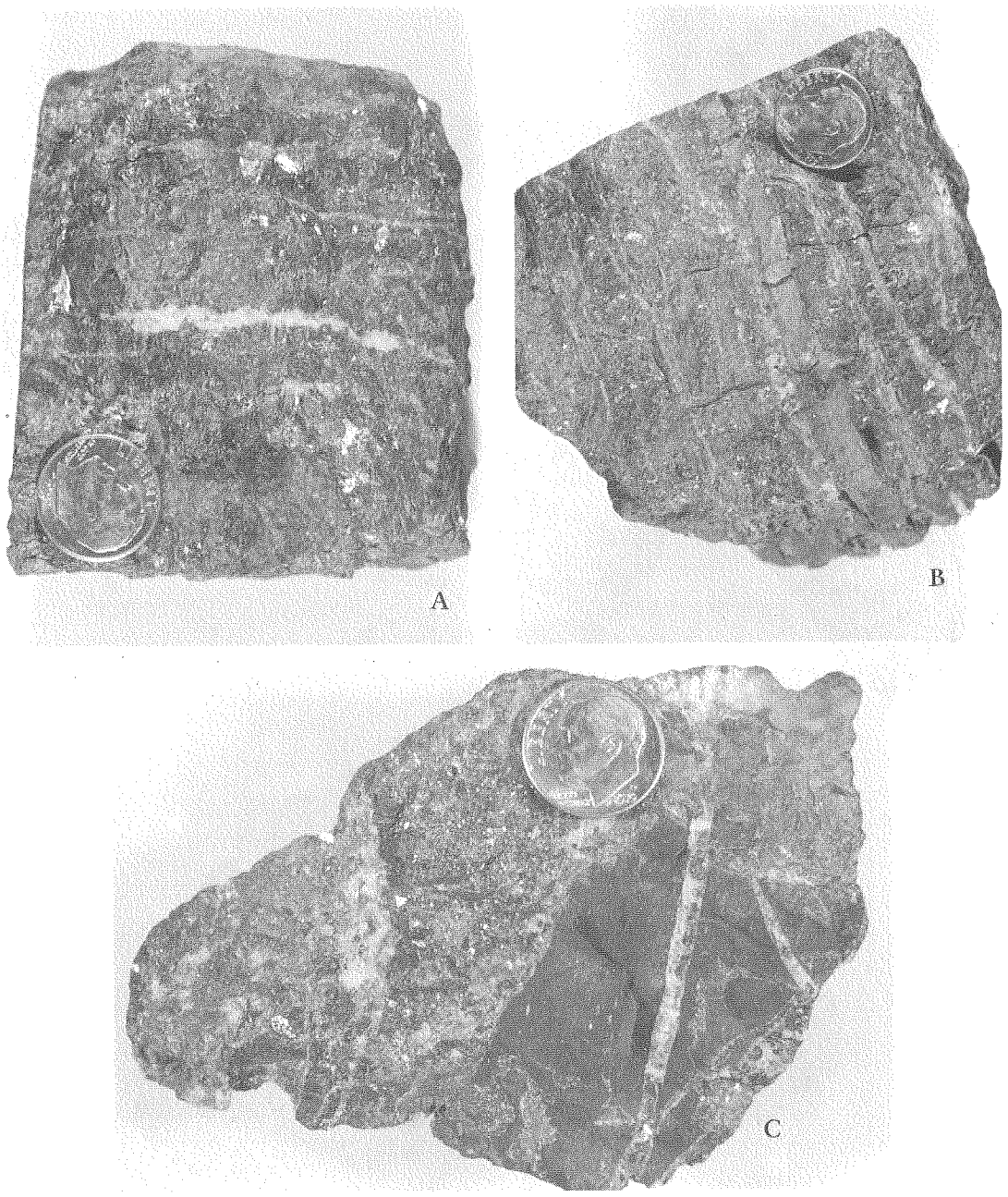


Figure 7. Vein ore: A, almost pure sphalerite showing color banding and symmetry with white quartz down center; B, banded sphalerite and iron sulfide; C, host rock fragment in unbanded ore, mostly sphalerite; earlier quartz veins in fragment. Coin is 18 mm in diameter.

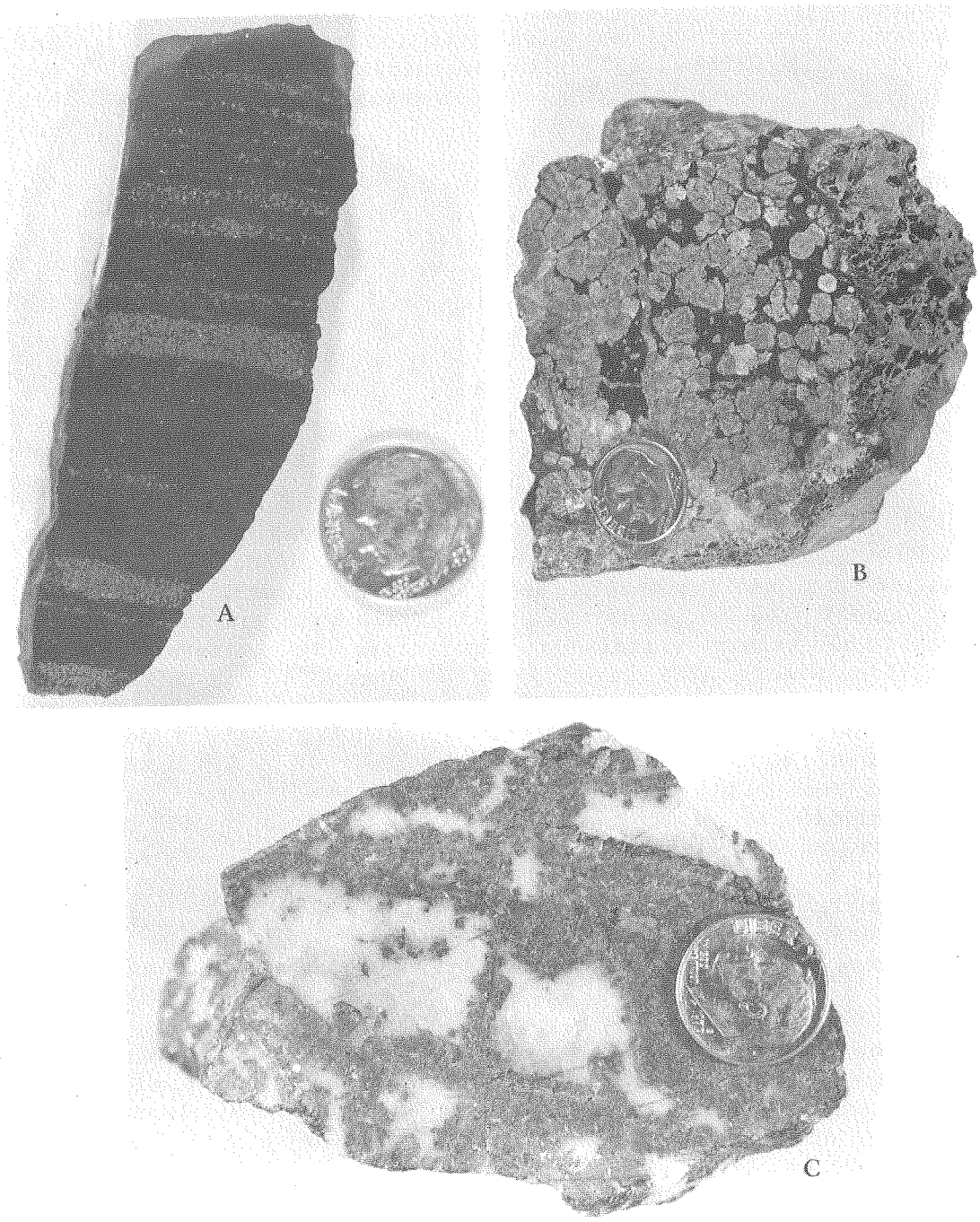


Figure 8. A, fine-grained disseminated sphalerite showing lamination; B, coarse-grained disseminated sphalerite, or "buckshot;" C, sphalerite veins intersecting in white quartz. Coin is 18 mm in diameter.

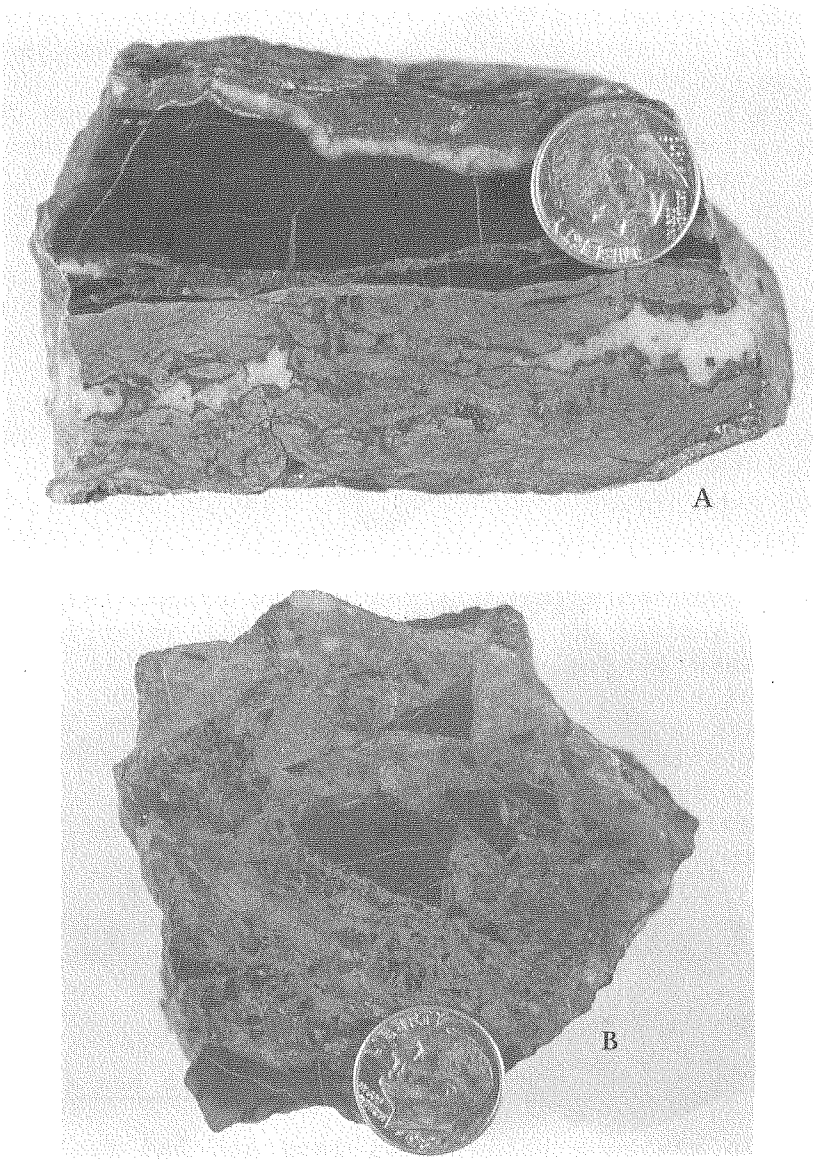


Figure 9. A, Iron sulfide-quartz veins with a wedge of host rock containing sphalerite veinlets; B, host rock-iron sulfide breccia cemented by colorless quartz. Coin is 18 mm in diameter.

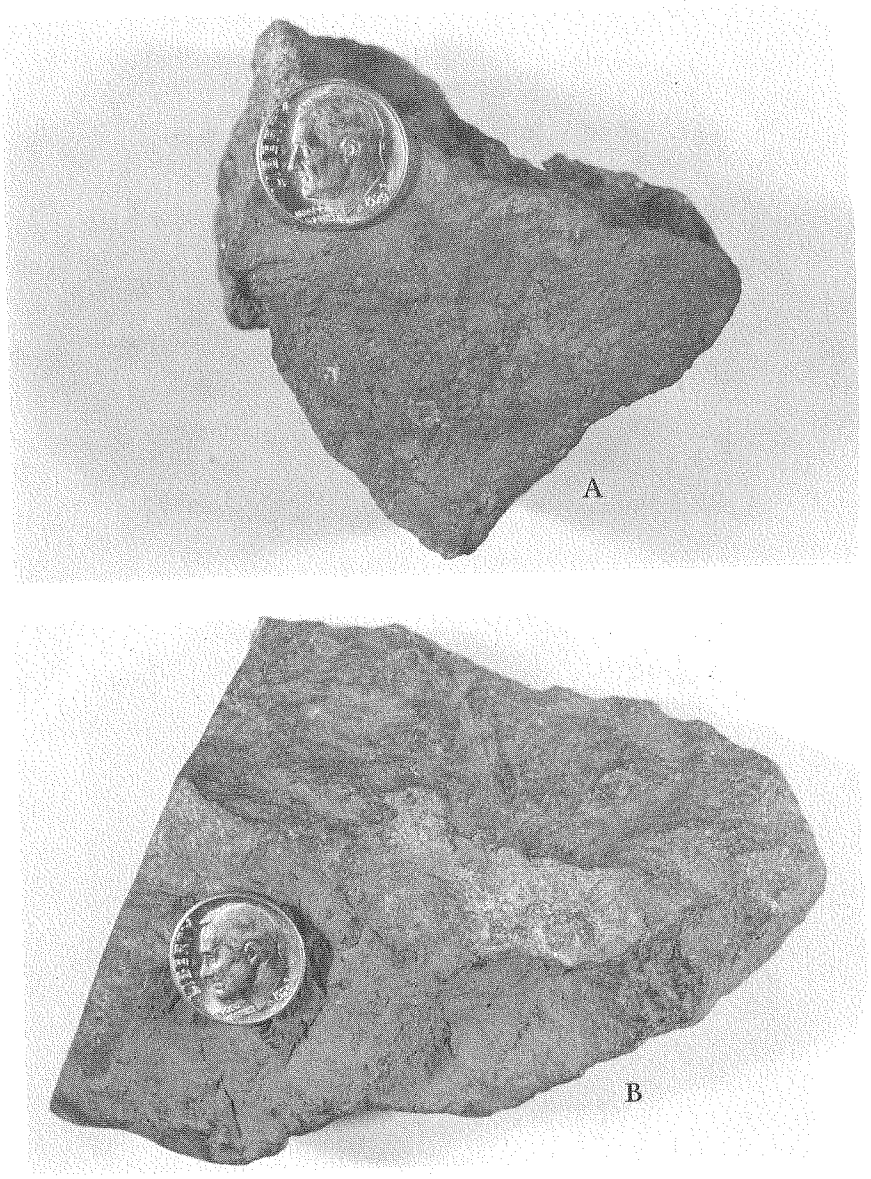


Figure 10. A, iron sulfide microbreccia cemented by colorless quartz; B, very fine-grained iron-lead ore of the podiform variety. Coin is 18 mm in diamter.

shows unusually concentrated sphalerite from the granular quartz rock (unit Pss) discussed above.

Red Dog "podiform" ore lies in discontinuous pockets at or near the top of the Kuna Formation. In its most easily distinguished form this podiform ore is a very fine-grained rock composed of iron sulfides and sphalerite in various proportions, often with a high galena content (Fig. 10B). Elsewhere it is coarser-grained, with an internally clastic texture that includes fragments of botryoidal pyrite, particles of black host rock, and megascopic white quartz. The latter variety is difficult to distinguish from the breccia ore (Fig. 7C and 9B). The two types may grade together.

Massive galena vein material was found as float in the main fork of Red Dog Creek near the southwest corner of the study area. The two float samples may have come from the hilltop deposit. Their rough, subhedral surface is much different from that of most Red Dog sulfide veins. This galena may therefore have formed by relatively free growth as a layer or vein in soft sediment rather than confined within a fracture.

Yellowish barite veins, containing laminations of sphalerite up to one centimeter thick and minor galena laminae up to about two millimeters thick, were dug out of the stream bank. Few of these veins were found, but they may represent conduits for solutions that formed some of the barite layers in overlying strata. They rise almost vertically through the black shale and chert of the Kuna Formation host rock with a NNE strike like that of the sulfide veins. Veins occur even more rarely as massive gray barite rock containing quartz but only very minor sulfides. Only two or three of these veins were found during field work but this type may be genetically connected to the massive barite layer in the Siksikpuk Formation overlying the main ore zone: the massive barite layer, like the veins, is gray, quartz-bearing, and relatively low in sphalerite and galena.

## C. Host rock and diagenesis

The black Red Dog host rock, which consists of both chert and shale, appears to have been well consolidated before the discordant mineralization was introduced. During diagenesis and/or later, an influx of silica saturated most of the shale in the mineralized area, giving it the hardness of chert, though not quite chert's brittleness or concoidol fracture. The shale and chert are therefore difficult to distinguish and undoubtedly grade together. With few exceptions, sharp boundaries between this rock and vein minerals are the norm at Red Dog (Fig. 11A). The rock varies from aphanitic to coarser material containing polycrystalline silica grains that could be recrystallized radiolaria (Fig. 11B). Often it displays a vague

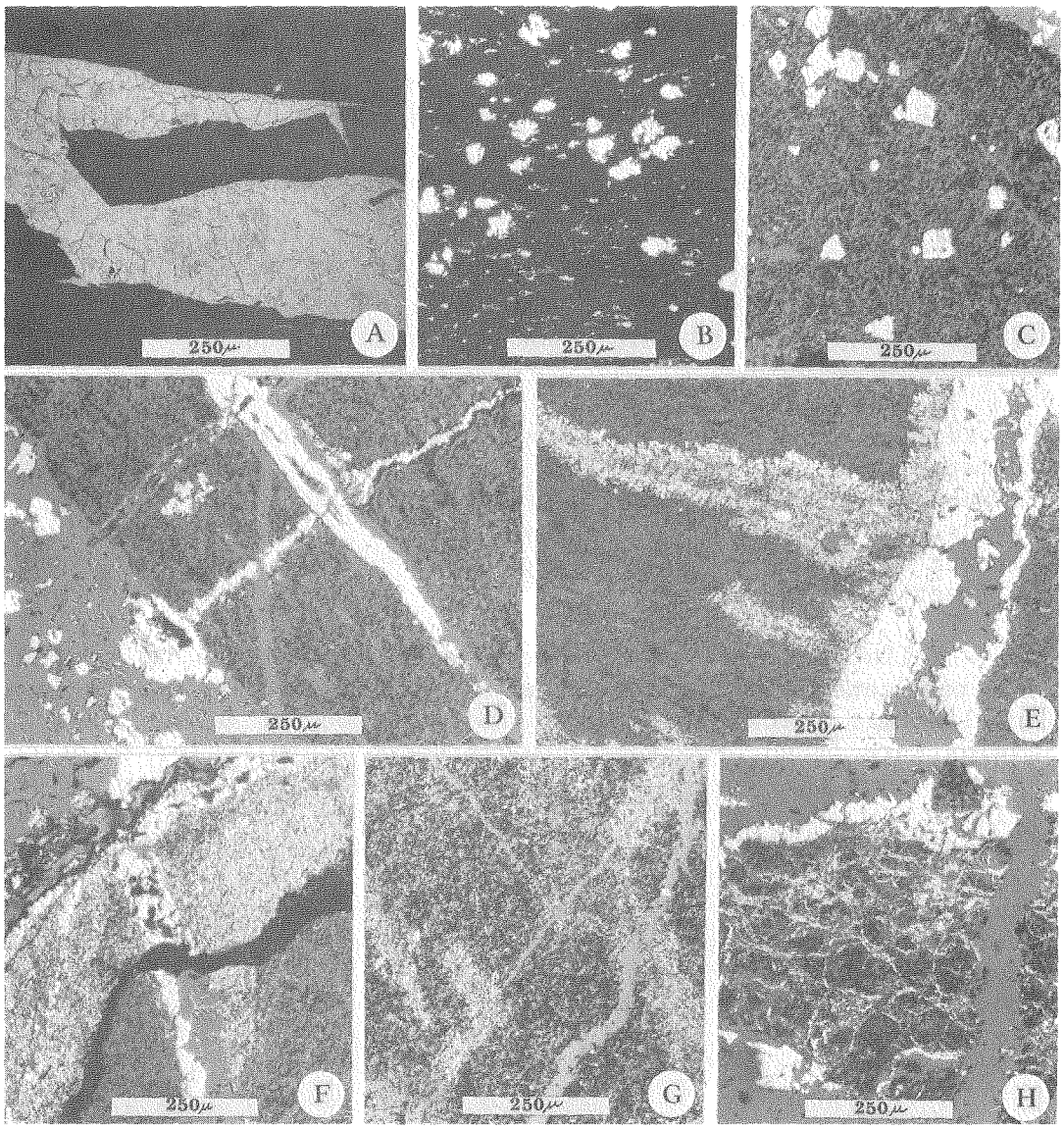


Figure 11. Host rock and replacement; A, thin section showing rock fragment trapped in quartz veinlet, and sharp contacts; B, thin section showing lamination and polycrystalline silica grains; C, common disseminated pyrite grains; D, host rock-quartz vein contact with iron sulfide stringers; E, host rock showing lamination and very fine-grained pyrite "wisp" material; iron sulfide-quartz veinlet, right; F, highly replaced host rock preserving part of a quartz-iron sulfide veinlet; G, rock fragment veined and partly replaced by sphalerite (medium gray); lightest mineral is very fine-grained "wisp" pyrite; H, host rock highly replaced by pyrite and silica.

lamination (Fig. 11D,E). A typical sharp edge is seen in Figure 11D, in this case between quartz and shale. Such fragments extend in size down to the lower limit of optical microscope magnification.

Traces of what appear to be chlorite can be seen in thin section in a matrix of black flaky carbonaceous material, silica grains, aphanitic silica, and sulfide grains. During field sampling for this thesis small amounts of sericite and clay minerals were found coating fracture surfaces in host rock. Lange and others (1981) report locally intense hydrothermal alteration of the chert and shale, with replacement by aggregates of kaolinite, montmorillonite, sericite, chlorite, calcite, and quartz. However, these authors do not report the size of these aggregates or their method of identification. Evidence for metamorphism is minimal at Red Dog and then only indicative of very-low-grade as defined by Winkler (1976).

Minute sulfide grains are ubiquitous in this black host rock. Aside from the macroscopic disseminated ore mentioned above (Figs. 6B, 8A, and 8B) and discussed further below, these particles are usually only at most a few microns in diameter (Fig. 11F, lower right) but sometimes coarser (Fig. 11C). They consist almost entirely of pyrite with an occasional sphalerite or galena speck. The pyrite grains are either anhedral or cubic; none of them appear to be marcasite and no other pyrite habits are observed in these diagenetic grains other than the relatively scarce framboid or pyritized microfossil.

"Wisps" (Fig. 11E) of iron sulfide too fine-grained to identify as pyrite or marcasite are common. These irregular concentrations often exist alone with no apparent connection to any discordant mineralization, but sometimes they connect with veinlets (Fig. 11E). Elsewhere they crosscut each other or intersect hairline fractures (Fig. 11D). Although these "wisps" may have no bearing on the lead-zinc mineralization, it is possible that they indicate "sweating out" of metals from the black Kuna Formation rock.

The host rock generally is in very sharp contact with the discordant quartz and sulfide mineralization at Red Dog on all scales. However, there is other evidence of minor replacement, on a microscopic scale, of host rock by sulfides and silica (Fig. 11F). Further examples of host rock replacement are shown in Figures 11G and 11H. A dark gray pitted material like that surrounding the black fragment in Figure 11H may represent host rock almost wholly replaced by silica. This quartz replacement occurred early in the sequence of post-diagenetic events at Red Dog. Replacement probably involved remobilization and redeposition of diagenetic iron sulfide, with possible introduction of additional iron sulfide at the same time. The main discordant mineralization may have contributed to this minor replacement and silicification.

Pyritized triaxon sponge spicules are found throughout the Red Dog host rock (Fig. 12A). They are found scattered randomly through the host rock or, more rarely, are concentrated in thin silica-rich layers (Fig. 12B). Fragments in all orientations are seen in polished section, from longitudinal (Fig. 12F) through various parabaloid or bullet-shaped sections (Fig. 12B), to hollow circles when a spine is cut perpendicular to its axis. Very rarely, remnants of what may be pyritized spicule fragments are also found within grains of other sulfide minerals (Fig. 12C,D,E). No unreplaced silica spicule fragments have been observed in Red Dog samples. Shales hosting sedimentary exhalative ore deposits commonly contain pyritized fossils that indicate the chemically reducing environment in which the stratiform sulfides remain stable (Large, 1983).

These triaxon spicules belong to the class Hyalospongea, or Hexactinelidae (depending on the taxonomic system used), of Devonian to Recent occurrence; further refinement of identification is not possible, both because the species or genus of a sponge can rarely be determined on the basis of spicules alone, and because imperfect pyrite replacement of the original opaline material may have obscured details of the spicules (R.C. Allison, pers. comm., 1980). Such sponges live at depths of between 500 m and 1,000 m, and require fairly clean water to keep their feeding-breathing (dermal) pores clear (Moore and others, 1952). Thus the depth of deposition of the Red Dog host rock is presumably constrained to 500 m or greater.

Pyrite framboids from Red Dog ore and host rock (Fig. 13) range from less than 5 microns to over 20 microns in diameter, though much larger ones have been found in sediments elsewhere (Sweeney and Kaplan, 1973), and each is composed of discrete pyrite microcrysts (Fig. 13E,F). Once thought to represent mineralized bacteria, framboids have now been synthesized in the laboratory by chemical reactions, not involving fossilization, that could easily occur in nature under a variety of circumstances (Berner, 1969; Farrand, 1970). Special conditions are required for pyrite to grow into and be preserved as framboids (Rickard, 1970). Probably the most common process involves the initial coalescence of organic globules, or droplets, which are held in a spherical shape by surface tension. Iron and sulfur then diffuse into these globules from the surrounding solution and pyrite crystallizes into microcrysts within the globules at many small nucleation centers. Continued pyrite precipitation eventually replaces most of the organic material, forming a spherical framboid. A membrane of hardened organic maceral matter remains around each framboid, isolating it after formation from its precipitating solution. Without this protection, continued reaction between framboid and solution very quickly alters the microcrysts and the spherical shape into other forms (Farrand, 1970).

The conditions for framboid formation are most often found in

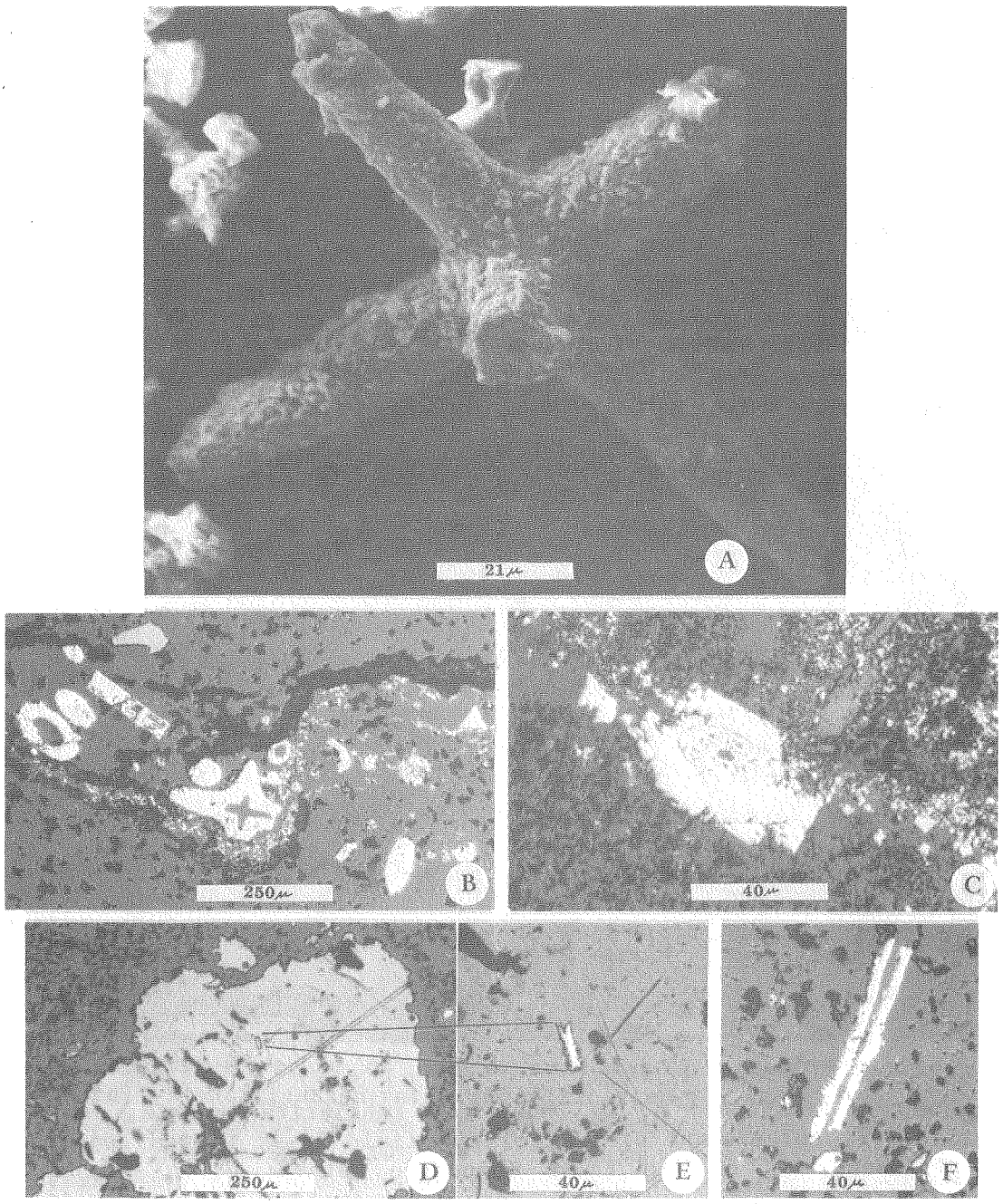


Figure 12. Pyritized sponge spicules: A, scanning electron microscope (SEM) photo of triaxon spicule showing the six spines at mutual right angles and hollow axis; B, part of a thin layer of spicule fragments in black host rock; center, oblique section through a spicule hub; C, oblique spine section in subhedral pyrite grain; D,E, probable spicule spine in a disseminated sphalerite grain; F, longitudinal section of spine in host rock.

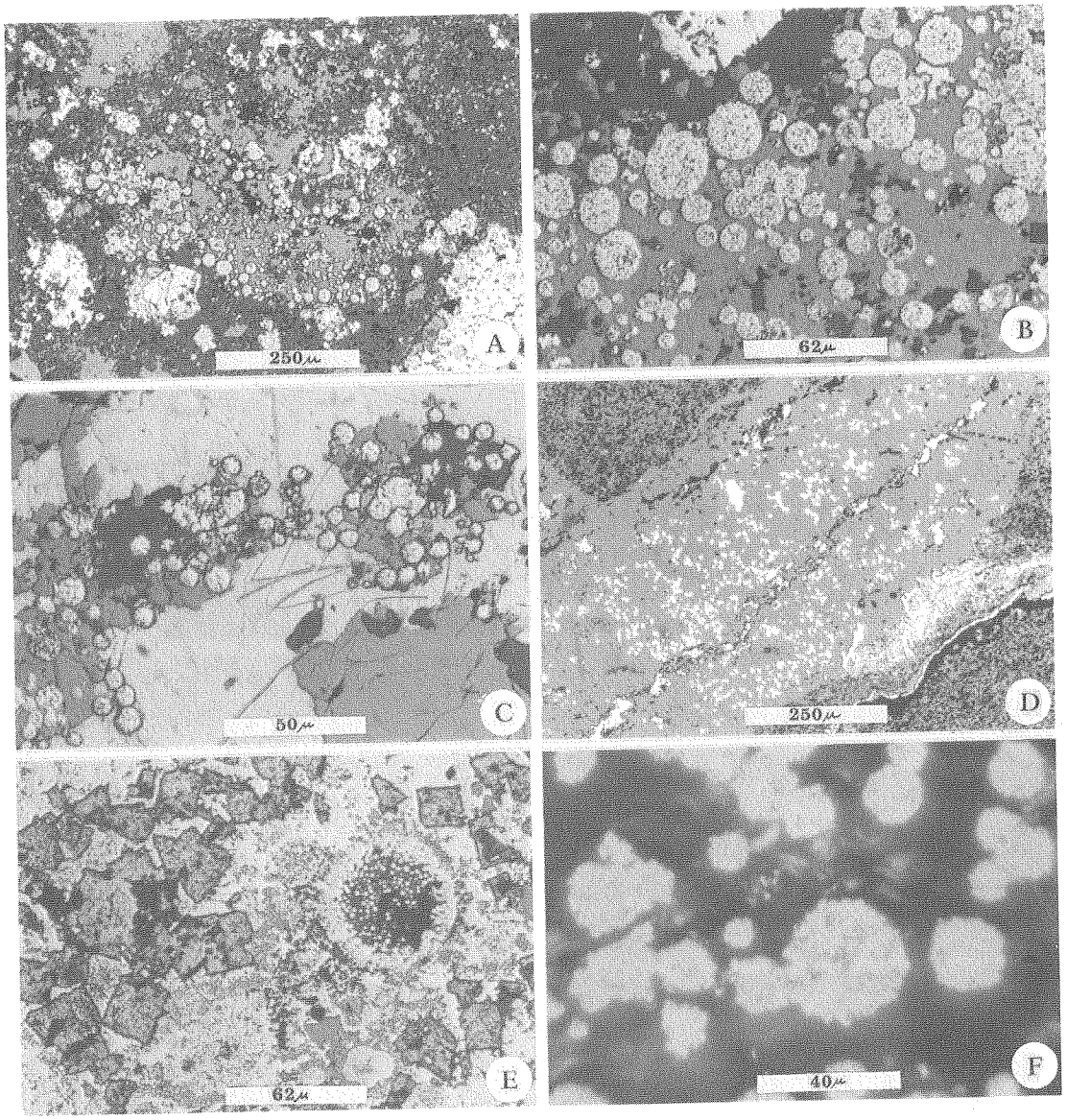


Figure 13. Framboids: A, in intergrown sphalerite, quartz, and iron sulfide; B, enlargement of part of the field in A; pitted appearance of framboids is due to their composite nature; C, in galena and sphalerite with minor quartz; D, high concentration in quartz veinlet; E, large framboid showing constituent crystallites, overgrown by pyrite and minor sphalerite; gray cubes are galena; F, framboids of quartz veinlet in D under higher magnification and oil immersion.

anoxic muds rich in decomposing organic material, especially near the sediment-water interface (Farrand, 1970). Some framboids that may have formed in such mud are found randomly distributed through the Red Dog carbonaceous shale and chert. However, at Red Dog framboids are found much more commonly in veinlets where they are trapped in quartz and other sulfides (Fig. 13). Rickard (pers. comm., 1979) says that it is not unusual for framboids to occur in hydrothermal veins, that it merely is not often reported. He suggests that framboids and quartz (Fig. 13D) can be precipitated simultaneously at less than 200°C as $SiO_2$ + $FeS(Fe_3S_4)$ (greigite) from a solution containing small amounts of leached Fe and $S^{2-}$ and saturated with quartz.

Larter and others (1981) describe framboid-filled pyrite tubes from the Ballynoe barite deposit, which is also closely associated with the large Mogul zinc-lead mine. These authors regard the tubes and their contents, including minor sphalerite, to be part of the preserved submarine chimney system of a "black smoker" that once fed the pyritic part of this deposit.

Framboids are also found in empty worm tubes from a base-metal sulfide deposit on the Juan de Fuca Ridge (Koski and others, 1984). This implies that hydrothermal fluids expelled via these tubes through the walls of a smoker chimney probably contained some portion of hydrocarbons (c.f. organic globules, above). Sediment cores collected in the Guaymas Basin smelled strongly like diesel fuel and sediment sampling equipment repeatedly became clogged with waxy material (Edmond and Von Damm, 1983). These authors attribute the hydrocarbons to hydrothermal "cracking" of the abundant planktonic carbon in the Guaymas silts. That framboids are found in probable exhalative tubes in Ireland (Larter and others, 1981), in undisputed worm tubes through modern smoker chimney walls (Koski and others, 1984), and in Red Dog veinlets suggests a link between Red Dog and other sedimentary exhalative deposits.

## D. Sulfide micromineralogy

Microscope study of Red Dog ore was directed primarily toward mineral identification and classification of textures. Although sphalerite, galena, pyrite, and barite are the main minerals, others have been mentioned in the literature (bornite: Plahuta, 1978; pyrrhotite: Metz and others, 1979a), and in informal discussion with other geologists (e.g. greenockite). It was wished, therefore, to make a complete inventory of sulfide and gangue minerals from Red Dog ore, principally because any mineral or texture present (or conspicuous by its absence) could have an important bearing on the origin of the deposit. On a microscopic scale, abundant exceptions and reversals can be found to qualify any overall genetic or paragenetic scheme proposed for Red Dog, but it is hoped that what

follows is a fair summary of the most important features of the Red Dog ore.

Cominco Alaska reports a zinc:lead ratio of about 3.4:1 for the Red Dog deposit (Jones, 1982). A preponderance of sphalerite over galena is readily apparent in hand specimen and under the microscope. Iron sulfides fall somewhere between the two in abundance. Only trace amounts of other sulfides have been identified during thesis work.

Sphalerites at Red Dog group approximately according to the styles of ore in outcrop: disseminated, vein, breccia (which may form a continuum with the veins), and podiform. Sphalerite in the first two categories is relatively free of other minerals and texturally simple, while sphalerite in the breccia and podiform ores is fine grained and intimately involved with other minerals.

Disseminated sphalerite occurs in two subtypes: fine-grained laminated (Fig. 8A) and coarse-grained unlaminated (Fig. 8B). In thin section the laminated form is seen to consist of small subangular to subrounded grains of sphalerite in relatively quartz-rich layers, alternating with layers of finely laminated carbonaceous shale in which polycrystalline quartz grains take the place of sphalerite (Fig. 14A). The nature of these compound quartz grains is not clear, though some of them resemble what Nokleberg and Winkler (1982) call recrystallized radiolaria in sphalerite-bearing black cherts from Drenchwater. The coarse-grained disseminated sphalerite (Fig. 14B) does not differ greatly from the other sub-type except for the lack of layering. Sphalerite grains of both sub-types are concentrically zoned with no sign of nuclei at the centers of zoning; many contain fine silica inclusions, which might suggest replacement of the polycrystalline quartz grains; both are associated with subordinate small galena grains both internal and external to the sphalerite (Fig. 14C); and both usually have thin silica rims (Fig. 14B,D). The carbonaceous matrix material of the coarse-grained sphalerite (Fig. 14E) also contains abundant pyrite.

Laminations could be mainly controlled by sediment influx, much as varves are, with a constant supply of ZnS being periodically dominated by extra sediments. Alternatively, the input of zinc may have fluctuated rhythmically while sedimentation remained more or less constant. Finlow-Bates (1980) cites symmetrical cycles of sulfide and interbedded dolomite in the Mt. Isa deposit as a probable example of the latter case. Sibson and others (1975) propose what they call "seismic pumping," or the dilatancy/fluid-diffusion mechanism, to explain episodic ejection of large volumes of hydrothermal fluids along fault traces during shallow earthquakes. Generation of a graben like that in which the Kuna Formation was probably deposited might be expected to produce frequent earthquakes. Rhythmic magma injection at depth could also account for periodic expulsion of ore-bearing fluids,

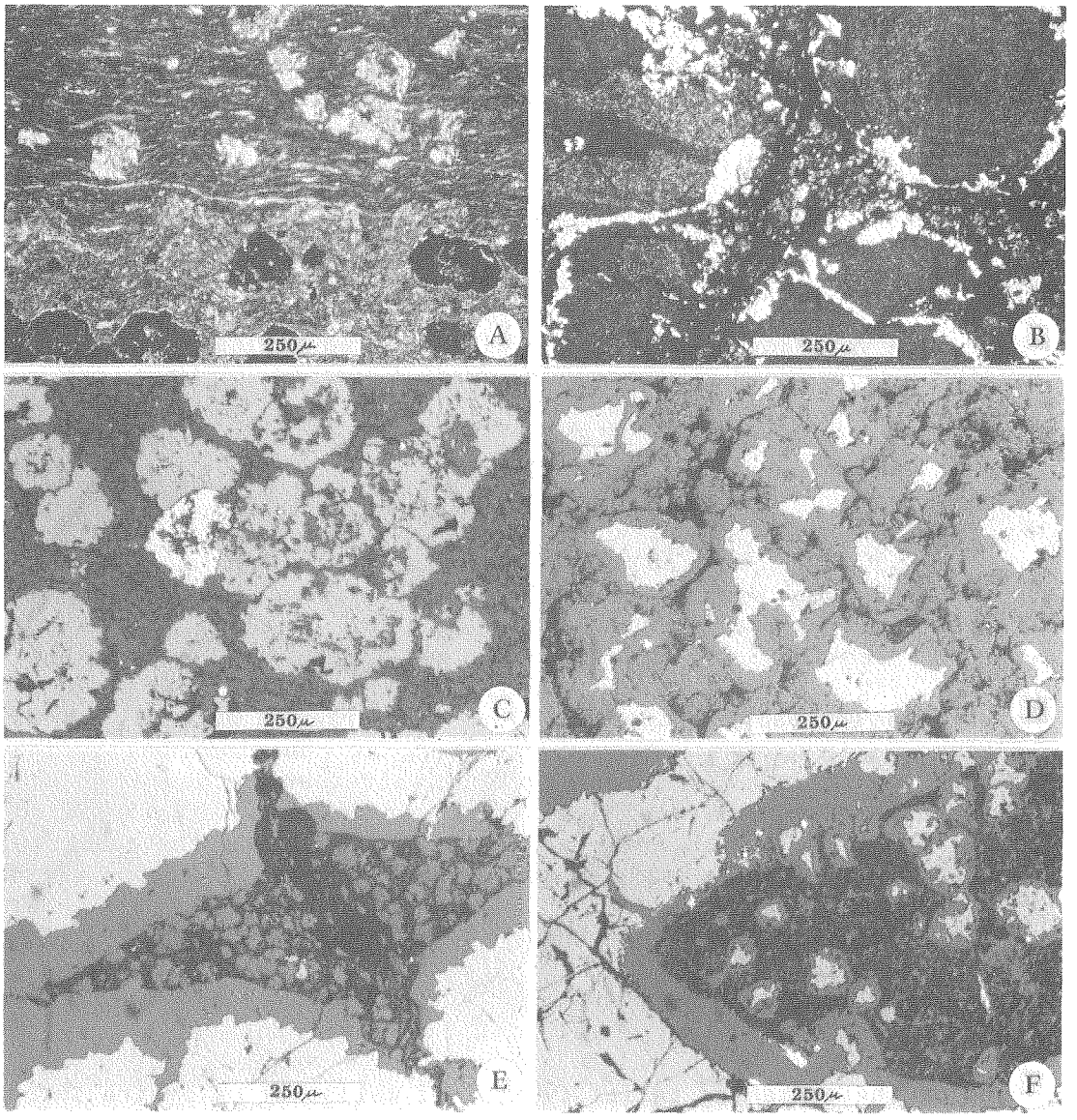


Figure 14. Disseminated sphalerite: A, thin section of hand specimen in figure 7A; upper half dark, well laminated, with polycrystalline quartz grains; lower half light, contorted, with sphalerite grains; B, thin section of "buckshot" sphalerite ore from hand specimen of figure 8B, shows zoning and thin quartz rims; C, sphalerite grains and one galena grain in host rock; D, sphalerite disseminations in coarse host rock; E, junction of four sphalerite grains; F, sphalerite-quartz disseminations in host rock fragment rimmed by quartz, sphalerite.

especially if this were accompanied by thermal dewatering of sediments containing adsorbed metal ions. Given the right composition and density, these metal-rich fluids could spread out along the ocean floor through unconsolidated sediments to react with organically produced sulfide ion at or near the sediment-sea water interface, leading to syngenetic sulfide growth.

Quartz rims on the disseminated sphalerite grains of both types are one hint that the pervasive silicification of shales in the Red Dog ore zone may have occurred penecontemporaneously with disseminated sphalerite-(galena)-(pyrite) emplacement. Silicification could not have been very advanced when the disseminated grains formed, since the latter appear to have grown in soft sediment. On the other hand, fragments of fully silicified disseminated ore are found in larger veins and breccias (Fig. 14F). It is suggested that shale silicification took place simultaneously with and/or after the disseminated mineralization, but before the onset of veining.

A polished section of typical Red Dog vein sphalerite shows nothing but an expanse of medium gray color with or a few pits, fractures, tiny pyrite or galena grains, and hairline quartz veinlets. In thin section this massive vein sphalerite is rhythmically color zoned (Fig. 15A). It is seen to contain abundant dusty black particles (probably opaque sulfides and organic matter), as well as larger pyrite grains. Nearly as often, it contains small patches of clear quartz in interlocking grains; alternating bands of (usually colloform) iron sulfides (Fig. 15B); and clasts of silicified host rock (Fig. 15C). Euhedral sphalerite terminations are common on the inward side of sphalerite bands in the symmetrical sphalerite-iron sulfide vein ore (Fig. 15B). Cross-cutting veinlets of quartz and later sphalerite are very common. No open spaces or vugs remain.

Occasional small patches (on the order of 5 mm in diameter) of sphalerite in the massive vein ore are found in polished section to contain abundant pale yellowish inclusions or exsolutions that show none of the polishing relief typical of marcasite or pyrite in contact with sphalerite. These grains are anhedral, on the order of 1-2 microns wide by a few microns long, and most are aligned with sphalerite crystal planes (Fig. 15F), though some are more equant and not aligned. Their small size renders microhardness testing and reflectance measurements unreliable. Although they are locally quite concentrated (Fig. 15F), X-ray diffraction of sphalerite samples supposedly rich in the unidentified particles disclosed no mineral other than sphalerite or quartz. In this method, any mineral phase comprising 5% or more of the sample by volume should have given identifiable peaks (N.C. Veach, pers. comm., 1980). Yet these grains are sufficiently common in the vein sphalerite to be of potential importance. They appear too pale in color to be chalcopyrite, nor is copper at all abundant at Red Dog (section G, below). But color is

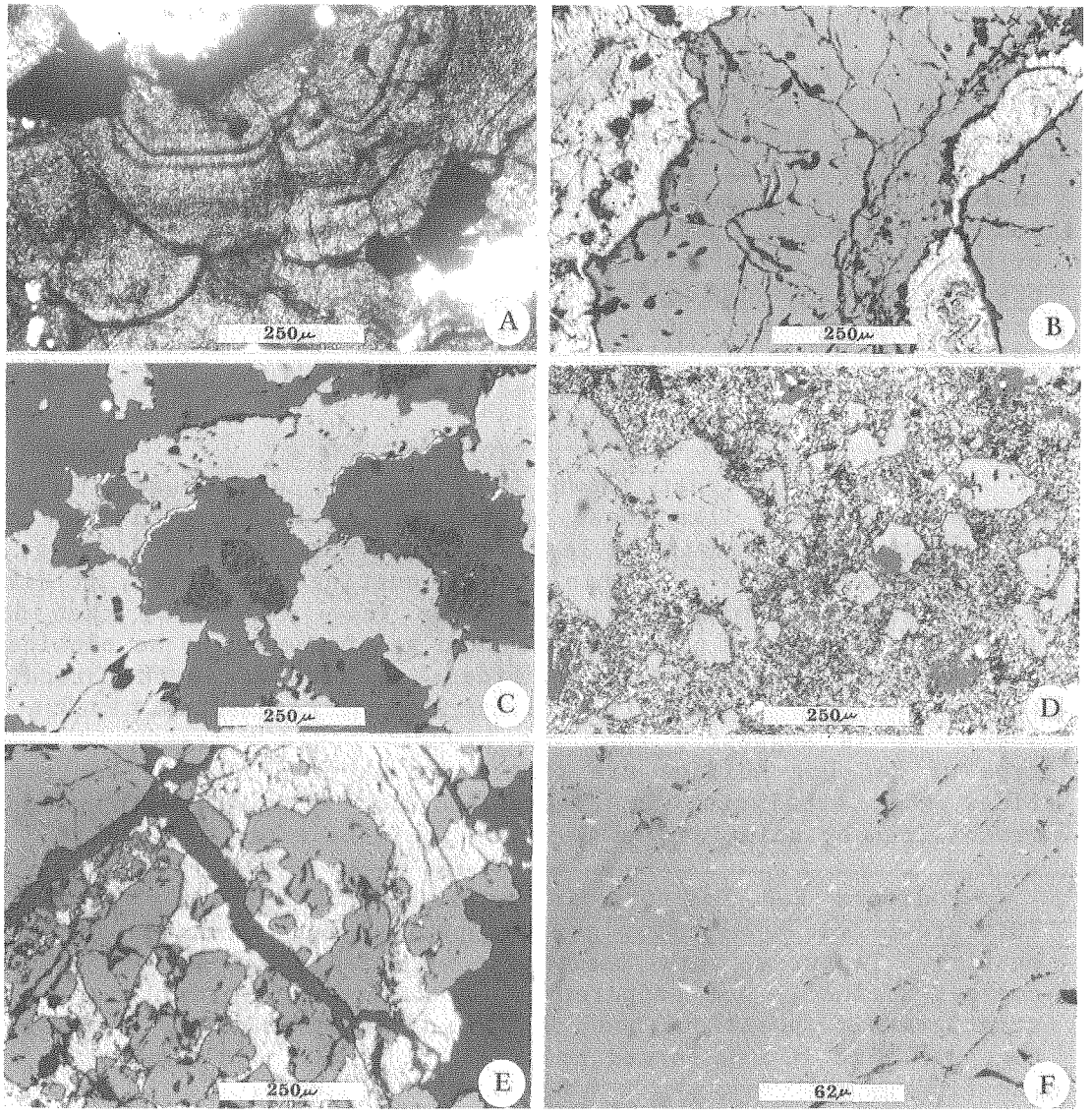


Figure 15. Sphalerite: A, thin section of vein sphalerite showing growth zones; B, laminated sphalerite-iron sulfide vein ore from hand specimen in figure 7B; sphalerite termination far right; C, irregularly intergrown sphalerite and quartz; note small host rock fragments, center, and asymmetric pyrite rind between quartz and sphalerite; D, anhedral sphalerite grains (light gray) in mass of fine-grained pyrite and quartz; E, intergrowth of sphalerite and marcasite, fractures cemented by quartz; F, massive sphalerite; contains pale yellow exsolutions or inclusions of pyrrhotite or chalcopyrite.

not the most reliable indicator in reflected light microscopy, and very small local concentrations of copper in sphalerite would have been diluted by the emission spectroscopy sample preparation process. The other most likely identity of the unknown mineral is pyrrhotite, which is the proper shade of very pale yellow and commonly forms crystallographically aligned lath-like inclusions in sphalerite exactly like the Red Dog ones (Williams, 1974, Fig. 5c). Although the unknown particles from Red Dog do not clearly exhibit the anisotropy or birefringence characteristic of pyrrhotite in polished section, the presence of pyrrhotite in significant quantity at Red Dog might account for the moderately strong magnetic signature of the deposit reported by Metz and others (1979a). The presence of pyrrhotite in equilibrium with sphalerite at Red Dog also seems to be called for on theoretical grounds (see below).

Breccias like that shown in Figure 7C are found at Red Dog adjacent to veins like those in Figure 6. This breccia may merely represent a finer-grained, less orderly type of vein filling, or a chaotic intersection of multiple cross-cuttings. However, it displays a much greater complexity of textures (e.g. Fig. 15D) than do the massive sphalerite ± pyrite veins, and galena seems to be considerably more abundant in the breccia sulfides. Sphalerite in the breccia ore tends, like the other minerals, to have a fragmental texture (Fig. 15D). It is suggested that the breccia could represent a separate type of Red Dog sulfide ore that combines fragments of earlier sulfides (the sphalerite in Figure 15D for example) with components remobilized by solution and redeposition (the extra galena).

Podiform Red Dog ore is generally an extremely fine-grained intergrowth of sphalerite, galena, pyrite, and marcasite in a quartz matrix. Textures vary somewhat, especially from very fine- to coarser-grained, but apparently not in any orderly way. The stratigraphic position and fabric of the podiform ore strongly suggests that it was formed by exhalation and rapid deposition on the sea floor.

Sphalerites from four samples of Red Dog ore, one of each type discussed above, were analyzed by electron microprobe for S, Mn, Fe, Zn, and Cd. Results of these analyses are given in Table 1. The main reason for this work was to accurately determine the iron content of the sphalerites, an important indicator of physical and chemical conditions attending ore formation. Manganese and cadmium were determined principally because they are common impurities in natural sphalerites and serve as a check on the precision of the Zn and Fe determinations.

Iron content of the Red Dog sphalerites by atom percent is displayed graphically in Figure 16A, following the example of Nokleberg and Winkler (1982, Fig. 13A). The anlyses plot in a roughly

Table 1. Electron microprobe analyses of sphalerite from the Red Dog deposit.[a]

| Sample[b] | LL 26-7 (disseminated) | | | | |
|---|---|---|---|---|---|
| Analysis | 1 | 2 | 3[c] | 4[d] | 5[d] |
| | Major elements (weight percent) | | | | |
| S | 33.029 | 32.890 | 33.064 | 32.910 | 32.622 |
| Mn | 0.048 | 0.044 | 0.061 | 0.055 | 0.049 |
| Fe | 0.674 | 1.572 | 4.379 | 1.947 | 0.438 |
| Zn | 66.318 | 65.578 | 62.066 | 65.161 | 66.401 |
| Cd | 0.001 | 0.002 | 0.005 | 0.002 | 0.002 |
| Total | 100.070 | 100.085 | 99.576 | 100.074 | 99.512 |
| mole % FeS | 1.2 | 2.7 | 7.6 | 3.4 | 0.8 |
| | Structural formulas (atom percent) | | | | |
| S | 50.067 | 49.848 | 50.056 | 49.851 | 49.829 |
| Mn | 0.042 | 0.039 | 0.054 | 0.048 | 0.043 |
| Fe | 0.586 | 1.368 | 3.806 | 1.693 | 0.384 |
| Zn | 49.304 | 48.745 | 46.083 | 48.408 | 49.743 |
| Cd | 0.000 | 0.001 | 0.002 | 0.001 | 0.001 |

| Sample[b] | LL 26-8 (vein) | | | | |
|---|---|---|---|---|---|
| Analysis | 1[e] | 2[f] | 3 | 4 | 5 |
| | Major elements (weight percent) | | | | |
| S | 32.374 | 32.997 | 32.945 | 33.081 | 33.037 |
| Mn | 0.054 | 0.038 | 0.042 | 0.049 | 0.052 |
| Fe | 3.843 | 2.494 | 7.803 | 4.663 | 8.074 |
| Zn | 61.765 | 64.404 | 58.791 | 61.117 | 58.369 |
| Cd | 0.006 | 0.002 | 0.002 | 0.001 | 0.002 |
| Total | 98.041 | 99.935 | 99.583 | 98.911 | 99.535 |
| mole % FeS | 6.8 | 4.3 | 13.4 | 8.2 | 13.9 |
| | Structural formulas (atom percent) | | | | |
| S | 49.879 | 49.966 | 49.703 | 50.304 | 49.808 |
| Mn | 0.048 | 0.034 | 0.037 | 0.044 | 0.046 |
| Fe | 3.399 | 2.168 | 6.758 | 4.071 | 6.988 |
| Zn | 46.671 | 47.831 | 43.501 | 45.581 | 43.158 |
| Cd | 0.003 | 0.001 | 0.001 | 0.001 | 0.001 |

Table 1. continued

| Sample[b] | LL 26-25 (vein/breccia) | | | | | |
|---|---|---|---|---|---|---|
| Analysis | 1[g] | 2 | 3[h] | 4[i] | 5 | 6 |
| | Major elements (weight percent) | | | | | |
| S | 33.109 | 32.411 | 32.685 | 32.477 | 33.035 | 33.321 |
| Mn | 0.033 | 0.047 | 0.037 | 0.061 | 0.034 | 0.045 |
| Fe | 8.635 | 4.495 | 5.661 | 0.412 | 5.937 | 5.773 |
| Zn | 58.231 | 62.593 | 61.144 | 66.303 | 61.288 | 61.109 |
| Cd | 0.001 | 0.002 | 0.002 | 0.002 | 0.002 | 0.001 |
| Total | 100.009 | 99.548 | 99.529 | 99.254 | 100.297 | 100.249 |
| mole % FeS | 14.8 | 7.7 | 9.8 | 0.7 | 10.1 | 9.9 |
| | Structural formulas (atom percent) | | | | | |
| S | 49.680 | 49.319 | 49.565 | 49.760 | 49.660 | 50.008 |
| Mn | 0.029 | 0.041 | 0.033 | 0.054 | 0.030 | 0.039 |
| Fe | 7.437 | 3.926 | 4.928 | 0.362 | 5.123 | 4.974 |
| Zn | 42.853 | 46.712 | 45.474 | 49.822 | 45.185 | 44.979 |
| Cd | 0.000 | 0.001 | 0.001 | 0.001 | 0.001 | 0.001 |

| Sample[b] | LL 3-9A (podiform) | | | | |
|---|---|---|---|---|---|
| Analysis | 1 | 2 | 3 | 4 | 5 |
| | Major elements (weight percent) | | | | |
| S | 33.372 | 33.180 | 33.036 | 33.184 | 32.792 |
| Mn | 0.062 | 0.048 | 0.049 | 0.057 | 0.063 |
| Fe | 3.023 | 1.012 | 2.229 | 2.024 | 1.610 |
| Zn | 63.533 | 66.559 | 64.982 | 65.857 | 65.221 |
| Cd | 0.007 | 0.003 | 0.003 | 0.003 | 0.004 |
| Total | 99.998 | 100.802 | 100.125 | 101.125 | 99.690 |
| mole % FeS | 5.3 | 1.7 | 5.9 | 3.5 | 2.8 |
| | Structural formulas (atom percent) | | | | |
| S | 50.332 | 49.944 | 49.892 | 49.767 | 49.881 |
| Mn | 0.055 | 0.042 | 0.043 | 0.050 | 0.056 |
| Fe | 2.617 | 0.875 | 1.933 | 1.742 | 1.406 |
| Zn | 46.994 | 49.137 | 48.131 | 48.439 | 48.656 |
| Cd | 0.003 | 0.001 | 0.001 | 0.001 | 0.002 |

a. Analyst: W.J. Nokleberg; b. Samples analyzed are: LL26-7, "buckshot" sphalerite ore, ; LL26-8, vein ore from sample in Figure 6B; LL26-25, vein ore from an area with high Pb, Zn, Cu, Hg, and Mo values in soil samples (Metz and others, 1979a); LL3-9A, podiform ore very similar to that shown in Figure 10B, from the same location. c. Dark grain core; d. Light grain rim; e. Dark red core; f. Light rim; g. Dark red; h. Dark core; i. Light rim.

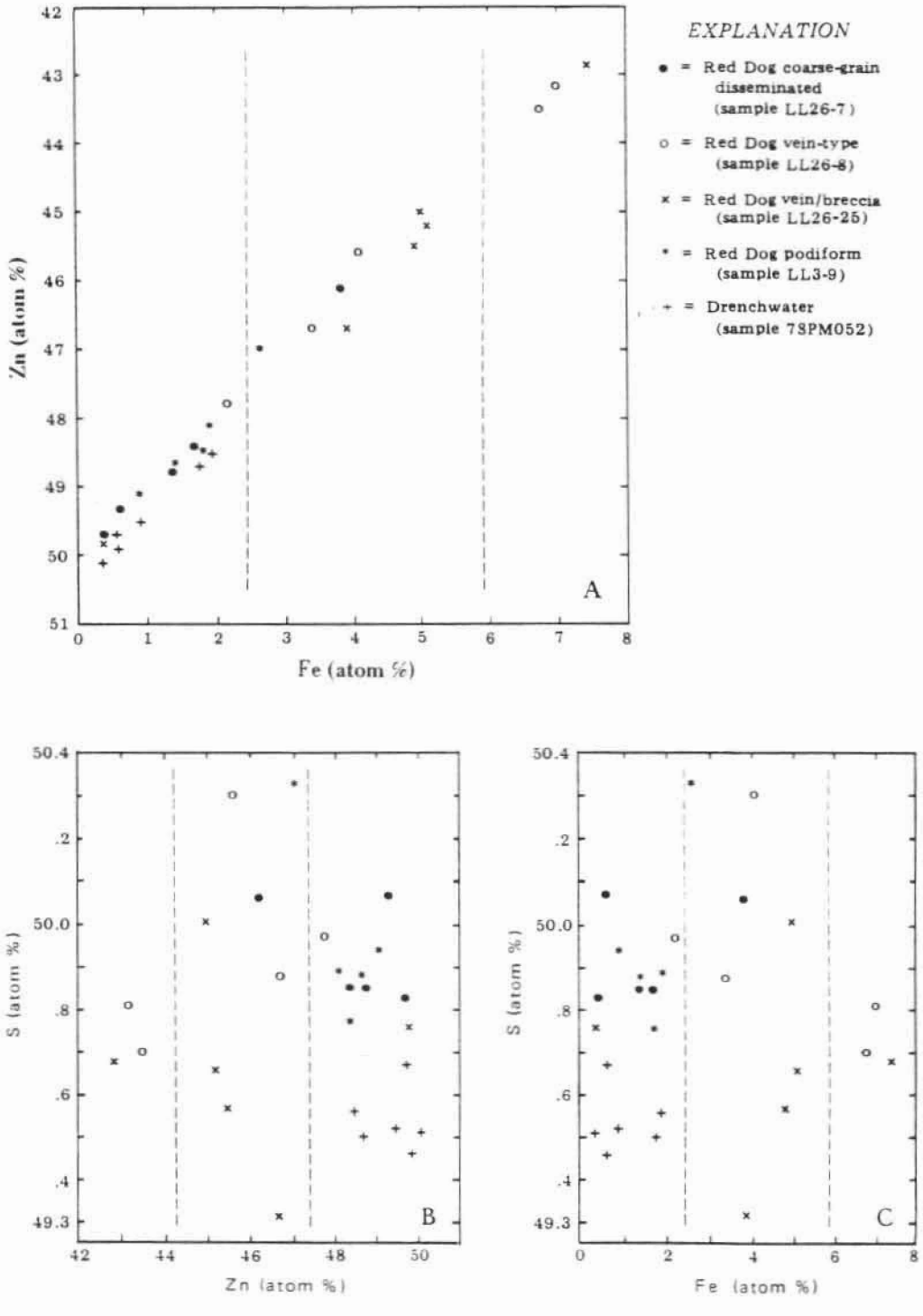


Figure 16. Electron microprobe analyses of Red Dog and Drenchwater sphalerites: A, variation of atom % Zn with atom % Fe; B, variation of atom % S with atom % Zn; C, variation of atom % S with atom % Fe. Data from Table 1 and from Table 3 (Chapter V).

linear trend with Zn decreasing as Fe increases, since these are by far the major cation constituents of sphalerite; departures from linearity are due either to minor element content (mainly Mn and Cd) or to error in the analyses.

Variations along this linear trend do not appear to be random. Iron contents of the sphalerites, except for one value from podiform ore (#1), are seen to fall in three fairly distinct groups of low, medium, and high Fe (Fig. 16A). Analyses from the vein-type and breccia ores, with one exception each, fall in the two highest-Fe groups and, with the exception of one disseminated ore analysis, only vein and breccia sphalerites fall in these two higher groups. Disseminated and podiform Red Dog sphalerites, together with all the Drenchwater analyses, occupy the lower end of the iron-content continuum. Red Dog podiform analysis #1 is grouped with the mid-range sphalerites because of its sulfur content; Figures 16B and 16C show that sphalerites in the middle group of iron contents in Figure 16A have the largest spread of sulfur contents.

A more common and useful way of reporting iron content of sphalerite is in terms of mole percent FeS. This parameter has been calculated from the raw microprobe data, listed in Table 1, and plotted against mole percent ZnS in Figure 17A. In this figure most of the deviation from a straight line (Fig. 16A) disappears since, to three significant figures, mole percent CdS is zero and mole percent MnS is 0.1 in each analysis. The data points retain the same order with respect to each other, although the original three groups are no longer so distinct. The ranges of mole percent FeS for Red Dog sphalerite samples are: disseminated, 0.8-7.6; vein, 4.3-13.9; vein/breccia, 0.7-14.8; and podiform, 1.7-5.3. By comparison, Sims and Barton (1961) and Deere and others (1966) put the upper limit of iron content in sphalerite, at elevated temperature, at around 40 mole percent FeS. Brown and Lovering (1973) report a range of 0.4-22.9 mole percent FeS for sphalerites from the Broadlands geothermal field, New Zealand. Koski and others (1984) report an even wider range of 0.2-32.3 mole percent FeS in sphalerites from the Juan de Fuca Ridge off the coast of Oregon. Urabe and Sato (1978) report a very narrow, low range of less than 5 mole percent FeS for sphalerites from several Japanese Kuroko deposits; of 41 analyses from the Uchinotai-nishi deposit, only two were slightly above 1 mole percent FeS.

In a general way, the FeS content of sphalerite varies directly with temperature, and inversely with $fS_2$ and $fO_2$ (Urabe and Sato, 1978; Finlow-Bates, 1980; Haymon, 1983; Koski and others, 1984; Zierenberg and others, 1984). These qualitative trends are labeled in Figure 17A. Given precise knowledge of iron sulfide phases in equilibrium with sphalerite, it is often possible to use mole percent FeS to put semi-quantitative constraints on temperature, though there is still rather wide latitude within the stability fields of sphalerite

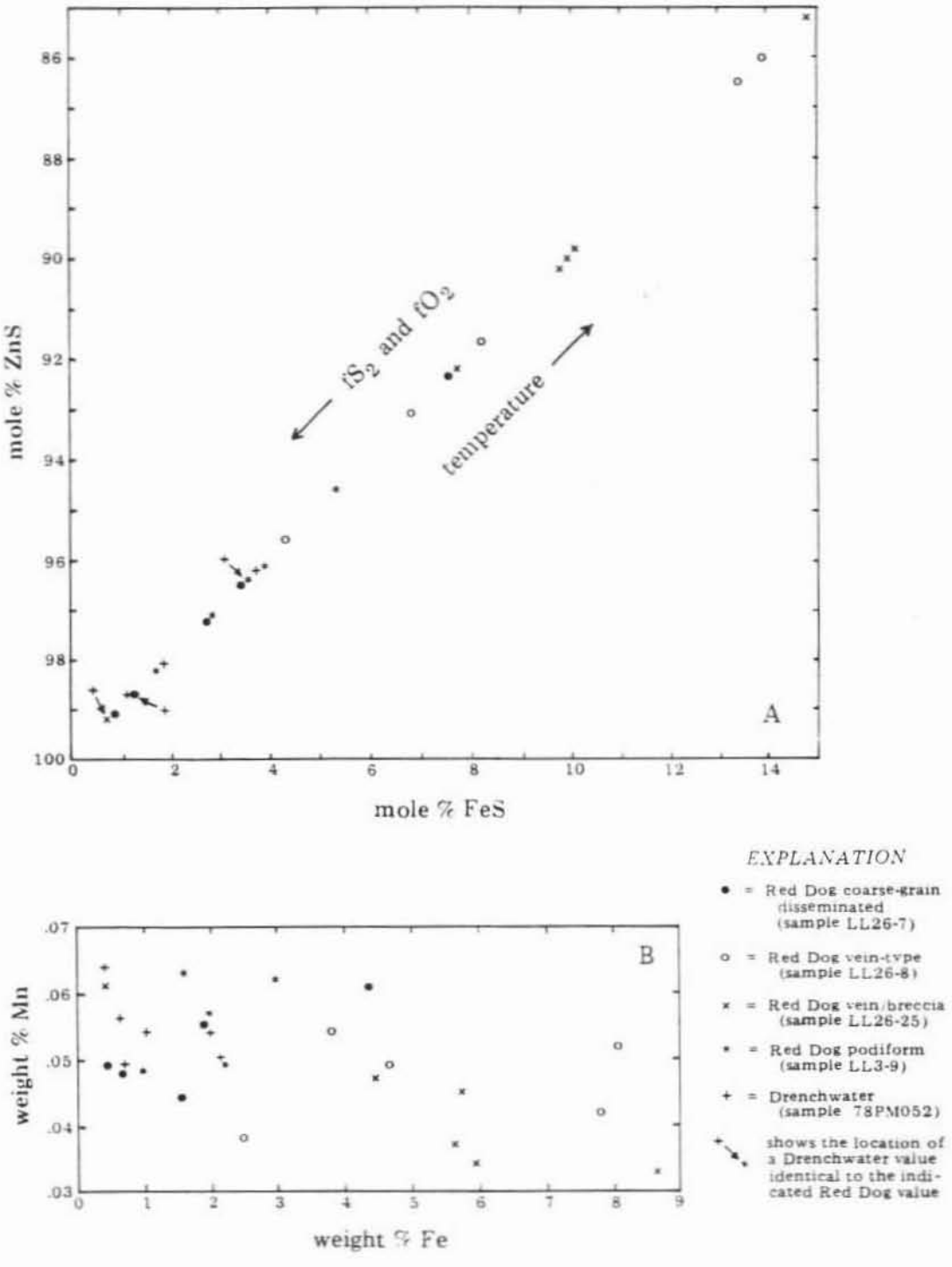


Figure 17. Electron microprobe analyses of Red Dog and Drenchwater sphalerites: A, variation of mole % FeS with mole % Zns; B, variation of weight % Mn with weight % Fe. Data from Table 1 and from Table 3 (Chapter V).

plus one iron sulfide. Most precise, of course, are compositions falling along univariant curves between iron sulfide stability fields, though several prominent investigators differ significantly in their placement of these phase boundaries in the system Fe-Zn-S, especially below about 300°C (Sims and Barton, 1961; Barton and Toulmin, 1966; Campbell and Williams, 1968; Scott and Kissin, 1973; Brown and Lovering, 1973; Barton and Skinner, 1979). The univariant curve of greatest interest to this study, that of sphalerite + pyrrhotite + pyrite, falls at anywhere from about 6 mole percent FeS to 11 or 12 mole percent FeS at 200°C, depending on the phase diagram consulted. This is too great a variation to be very useful here, given the narrow spread of low mole percent FeS values observed in Red Dog sphalerites. Scott and Barnes (1971) conclude that FeS content of sphalerite, even in equilibrium with pyrrhotite, is not useful in quantitative geothermometry without data on $fS_2$ at the time of deposition.

Furthermore, as noted above, no pyrrhotite has been definitely identified in Red Dog ores, despite several dozen tests of reflectance versus Vickers microhardness performed on anisotropic iron sulfide grains; each of these grains proved to be marcasite. Therefore the univariant curve sphalerite + pyrrhotite + pyrite cannot be applied here in any event. On the other hand, most authors agree that, below about 250°C, pyrrhotite should be present in sphalerite when the FeS content reaches about 11-12 mole percent or more. It therefore seems very likely that at least some of the yellowish, lath-shaped "exsolutions" mentioned above are indeed pyrrhotite. Unfortunately, it is not known whether any of the sphalerite grains analyzed by microprobe contained these particles.

Several tentative conclusions can be drawn about the data in Figure 17A, however. First, the FeS contents of the vein and most breccia analyses group together at greater than 4 mole percent. Likewise the disseminated and podiform sphalerites group together at less than about 4 mole percent FeS. Therefore, even in the absence of recognized pyrrhotite, and despite some overlap, it can be said that the veins and breccia ores formed at somewhat higher temperatures and/or somewhat lower sulfur fugacities than did the disseminated and podiform sulfides. This difference could be due to fluctuations in the temperature and/or chemical content of the hydrothermal fluid. As stated above, the veins and breccia ores appear to have been emplaced later than the disseminated sulfides, so there may have been time in between for a rise in temperature of the hydrothermal source. Sealing of the source by silicification, by dewatering of sediments, and by minerals clogging interstitial pores may have contributed to this temperature increase by insulating the heat source and hindering convection (Facca and Tonani, 1967; Hodgson and Lydon, 1977; Einsele and others, 1980; Lonsdale and Lawver, 1980). Conversely, Zierenberg and others (1984), studying a hydrothermal system on the East Pacific

Rise, concluded that the ore-forming fluid in this sytem, presumably of constant composition at the source, evolved to higher fS during sulfide deposition due to mixing with ambient sea water. This hypothesis also makes more sense for Red Dog if it is assumed that the podiform ore (high $fS_2$) was precipitated from hydrothermal solutions emerging from the veins and breccias (low $fS_2$) onto the sea floor. Similarly, the disseminated sulfides, if indeed they are diagenetic, also would have formed in an environment more open to the chemical and cooling influences of ambient sea water than did the confined vein and breccia ores. Thus it may not be necessary to call on any difference in the original ore-forming solutions at the source to account for observed FeS variations between the ore types.

Sphalerites from the breccia ore contain both the highest and lowest FeS analyses in the whole Red Dog suite (Fig. 17A). FeS contents of the breccia sphalerites are the highest of any of the four ore samples, averaging 10.46 if the lowest value is omitted. This one low value is a very distinct anomaly which, however, is easily explained if it is assumed that the breccia ore includes clasts of earlier-formed, low-FeS sphalerite. This possibility is consistent with the fine-grained, partly fragmental-appearing texture of some of the breccia ore (Fig. 15D). Alternatively, the breccia ore could contain sphalerite from both main-stage, relatively high-T hydrothermal activity (higher FeS), and sphalerites deposited later after the whole system had cooled down (lower FeS).

Manganese contents of Red Dog and Drenchwater sphalerites are plotted against iron content in Figure 17B. These analyses, with a total range of 0.033-0.064 weight percent Mn, are moderately low for natural sphalerites. Sims and Barton (1961) report that Mn content of sphalerite from 38 mines in the Central City district, Colorado varies widely from 0.0007 to 0.28 weight percent. Cadmium content of the Red Dog sphalerites varies only from 0.001 to 0.007 weight percent, while 17 of the Central City sphalerites range from 0.20 to 0.64 weight percent Cd. As much as 4 to 5 percent Cd and Mn in sphalerite has been reported worldwide (Deere and others, 1966). Sims and Barton (1961) predict, because of similar geochemical behavior of the two metals, that Mn content of sphalerite should correlate with Fe content, that the two should increase or decrease together. The Central City manganese/iron data points have a slope of about 0.017 and a correlation coefficient of 0.817 ($r^2 = 0.67$). The Red Dog data points have a slope of -0.002, with a correlation coefficient of only -0.484 ($r^2 = .23$). The slopes of the lines of best fit for both sets of data are near zero. A negative slope for the Red Dog points could as well mean that iron and manganese substitute together for zinc in sphalerite. Increased manganese content would mean slightly less iron content. Probably the manganese versus iron content of sphalerite is close to arbitrtary, depending upon the porportions of the two elements in the ore-forming solution; there seems to be no definite

chemical partitioning.

Euhedral galena occurs only rarely at Red Dog (Fig. 13E and 18A,D). Typically it is seen intergrown with quartz in a vaguely colloform way (Fig. 18B), or even more often as a completely shapeless matrix cementing grains of other minerals (Fig. 18C). It is a subordinate mineral in the disseminated Red Dog ore (Fig. 14C) and is a major, very fine-grained component in the ground mass of much of the podiform ore (Fig. 10B). Perhaps most commonly of all, galena occurs as small anhedral specks, coatings, and infillings within and between grains of all the other minerals. In cases where it is possible to decide with reasonable certainty, galena is usually seen to embay, replace, or overgrow sphalerite rather than the reverse; replacement of pyrite and marcasite seems to be far less common.

The overall impression from study of many polished sections is that galena at Red Dog is usually late and not as abundant as the other sulfides. This impression is further supported by the presence of galena laminations within barite veins that appear to be relatively late (see below). In addition, several pieces of solid, coarse-grained vein (?) galena free of cross-cutting veinlets were found in float that probably came from the hilltop part of the deposit. Given the pervasiveness of cross-cutting relationships in Red Dog ore, any vein material not so affected must be assumed to have formed late in the sequence of mineralizing events. The relative abundance of galena in the breccia ore compared to the massive veins is the main reason for believing that the breccia sulfides might constitute a separate class of ore, one formed under rather different conditions than the veins and possibly more closely related to the podiform ore.

In a few polished sections, Red Dog galena contains small, shapeless inclusions or exsolutions so similar in color and reflectance to the host galena that they could not be satisfactorily photographed in reflected light. These mineral blebs do not show any alignment. They are distinct under half-crossed nicols since they are quite anisotropic, unlike galena. The particles were not distinguished by X-ray diffraction of galena samples containing them so, as with the inclusions or "exsolutions" in sphalerite, these grains must comprise less than 5% of the galena even when they are most abundant. So far these grains in Red Dog galena remain unidentified. However, the sulfosalts boulangerite ($Pb_5Sb_4S_{11}$) and bournonite ($PbCuSbS_3$) have been identified as exsolution blebs in galena from the nereby Lik deposit (Sterne and others, 1984). These two minerals have optical properties similar to those of the unidentified particles in Red Dog galena.

Pyrite accounts for all of the identifiable iron sulfide disseminations in the Red Dog host rock, where it appears as both

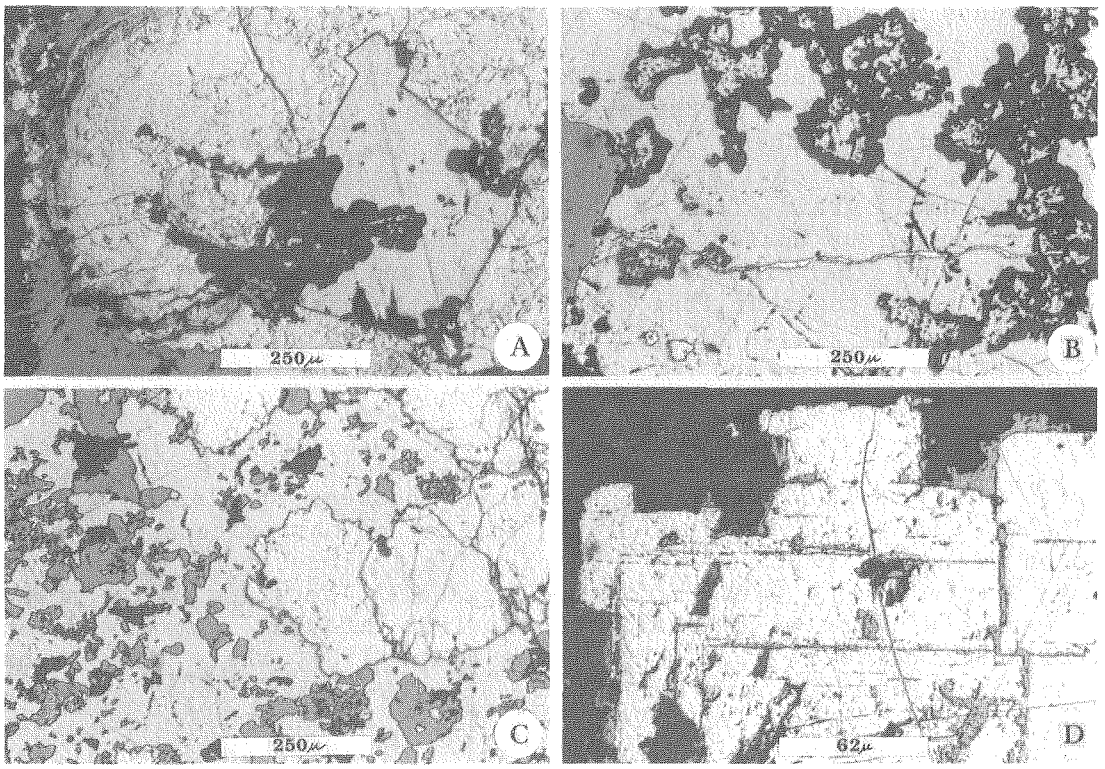


Figure 18. Galena: A, euhedral galena grain intergrown with quartz and surrounded by botryoidal mass of iron sulfide; B, fairly common rounded intergrowth of galena and quartz; marcasite veinlet horizontal, stops at sphalerite, left; C, pyrite and quartz in a matrix of anhedral galena (light gray); D, euhedral galena coated and slightly replaced by scarce unidentified mineral (darker gray) in quartz (black).

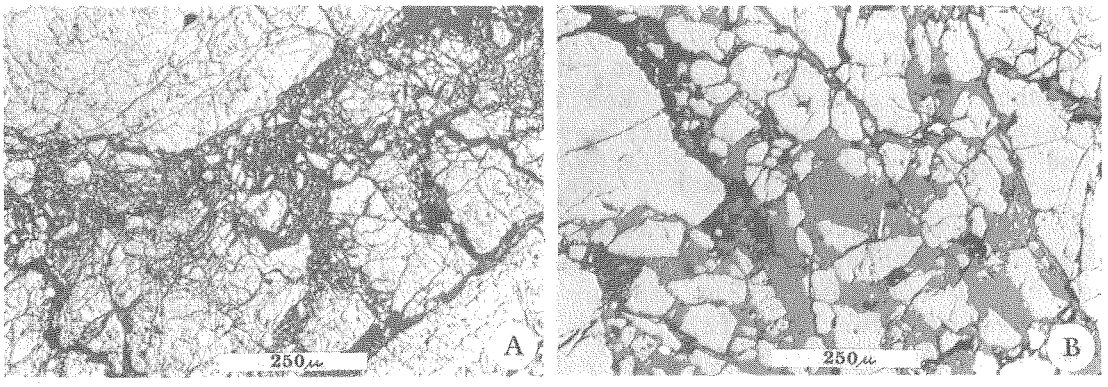


Figure 19. Microbreccia: A, pyrite in quartz; B, sphalerite in quartz.

cubic and anhedral grains (Fig. 11C). Many botryoidal and other fragments contained in later vein mineralization are also composed mainly of pyrite (Fig. 18A,C). After these early stages pyrite is usually accompanied by marcasite, either in alternating overgrowths or in randomly interlocking grains. The only characteristic that clearly distinguishes the two minerals in polished section is the anisotropy of marcasite; but even this distinction is often defeated by very small grain size, by tarnish and weathering on grain surfaces, and by anomalous anisotropy in pyrite that can be caused by polishing relief and other factors. Therefore, and since the two minerals usually occur together, the effort to distinguish them was made mainly during initial stages of microscope study, and only in selected cases thereafter. Pyrite and marcasite are often referred to together here as "iron sulfide."

Deposition of hydrothermal iron sulfide at Red Dog probably began with the formation of pyrite particles between sphalerite grains in the disseminated ore. Thereafter, pyrite and marcasite appear to have been deposited continuously or episodically throughout the period of ore emplacement, with marcasite gradually becoming more abundant toward the close of mineralization. Iron sulfides commonly occur as colloform bands in sphalerite veins (Fig. 15B), where they probably record periods of lower temperature (Finlow-Bates, 1980); overgrowths on other minerals (Fig. 12C, 13E, 18A); abundant veinlets cutting across almost any other texture (Fig. 11D, 18B); an anhedral matrix binding other mineral grains (Fig. 15E); anhedral and botryoidal clasts within ground masses of other minerals (Fig. 18C); microbreccias with quartz cement (Fig. 19A), especially in pyrite-rich veins periferal to the ore zone; and in very fine-grained form in breccia ore (Fig. 15D) and podiform ore. Marcasite often forms euhedral terminations on anhedral pyrite grains and euhedral crystals in quartz veinlets.

The occurrence of marcasite together with pyrite is very common in sulfide deposits and does not say a great deal about conditions of mineralization (Krauskopf, 1967). The solution acidity required for marcasite precipitation might, however, help to explain the virtual absence of calcite in the Red Dog ore zone; most $CaCO_3$ originally present in the host sediments may have been dissolved and flushed from the system by the weakly acid hydrothermal fluids.

Chalcopyrite is very rare at Red Dog. Only a few tiny, anhedral specks have been found in two of the polished sections during thesis work. These few grains appear to fill voids and/or replace tiny patches of other minerals. The largest chalcopyrite particle found (about 130 x 190 microns) appears to have replaced pyrite or sphalerite jointly with an adjacent anhedral galena grain of the same size. Some of the unidentified yellowish inclusions or exsolutions in sphalerite (see above) could be chalcopyrite, especially since some of

them are randomly situated blebs rather than aligned lath-shaped particles (Sims and Barton, 1961; Ramdohr, 1969). No other copper minerals have been identified in Red Dog ore during this study. This lack of Cu minerals in exposed Red Dog ore could be the result of zoning common in sediment-hosted stratiform deposits (Finlow-Bates, 1980; Large, 1983), that is, more copper could be present at depth. However, no such hidden copper mineralization has been reported from drilling (Jones, 1982; Plahuta and others, 1983).

Frequent changes in the composition and/or temperature of hydrothermal fluids depositing the Red Dog sulfide mineralization are indicated by color banding and pyrite laminations in the massive veins, and by variations in the FeS content of sphalerites throughout the deposit (see above). Local physico-chemical changes are also abundantly illustrated on the microscopic scale by all sorts of replacement and overgrowth structures that occur in almost every direction with respect to the overall paragenetic sequence of the deposit (see section F, below). Such paragenetic reversals and the resulting replacement textures are found mostly in the breccia and podiform ores.

Although pyrrhotite may exist in very fine-grained or otherwise unidentified form in Red Dog ore, it is possible that much pyrrhotite was already replaced by other minerals, generally pyrite and marcasite, while the deposit was still evolving to its final form (Haymon, 1983; Zierenberg and others, 1984). Direct evidence for this replacement is mostly lacking but elongated crystals replaced by pyrite in Red Dog ore (Fig. 20A) closely resemble pseudomorphs after pyrrhotite reported by Zierenberg and others (1984).

Pyrite and marcasite are not often replaced except by each other. When replacement of iron sulfides does occur, it is most often by galena (specks in Fig. 20A; intergrowth in Fig. 20B could be depositional), but replacement by sphalerite is seen occasionally (Fig. 20C,D). As stated above, galena is usually a final phase embaying sphalerite, filling voids between other minerals (Fig. 18C, 20C,D), or invading grain boundaries (Fig. 20E).

In spite of this widespread, small-scale replacement, many delicate depositional features are preserved in Red Dog ore. Such features as botryoidal (colloform) growths and fine shell structures are typical of open-space fillings, as in fractures and breccias. At Red Dog, although small clumps of botryoidal pyrite are frequently found in sphalerite veins, such features as those shown in Figures 20F through 21 are far more common in the breccia and podiform ores, locally comprising a majority of the sulfide material. Much of this colloform mineralization is seen in polished section to consist of mottled, dusty-appearing iron sulfide (Fig. 20F). Elsewhere, it seems to be more solid, though with very closely-spaced centers of nuclea-

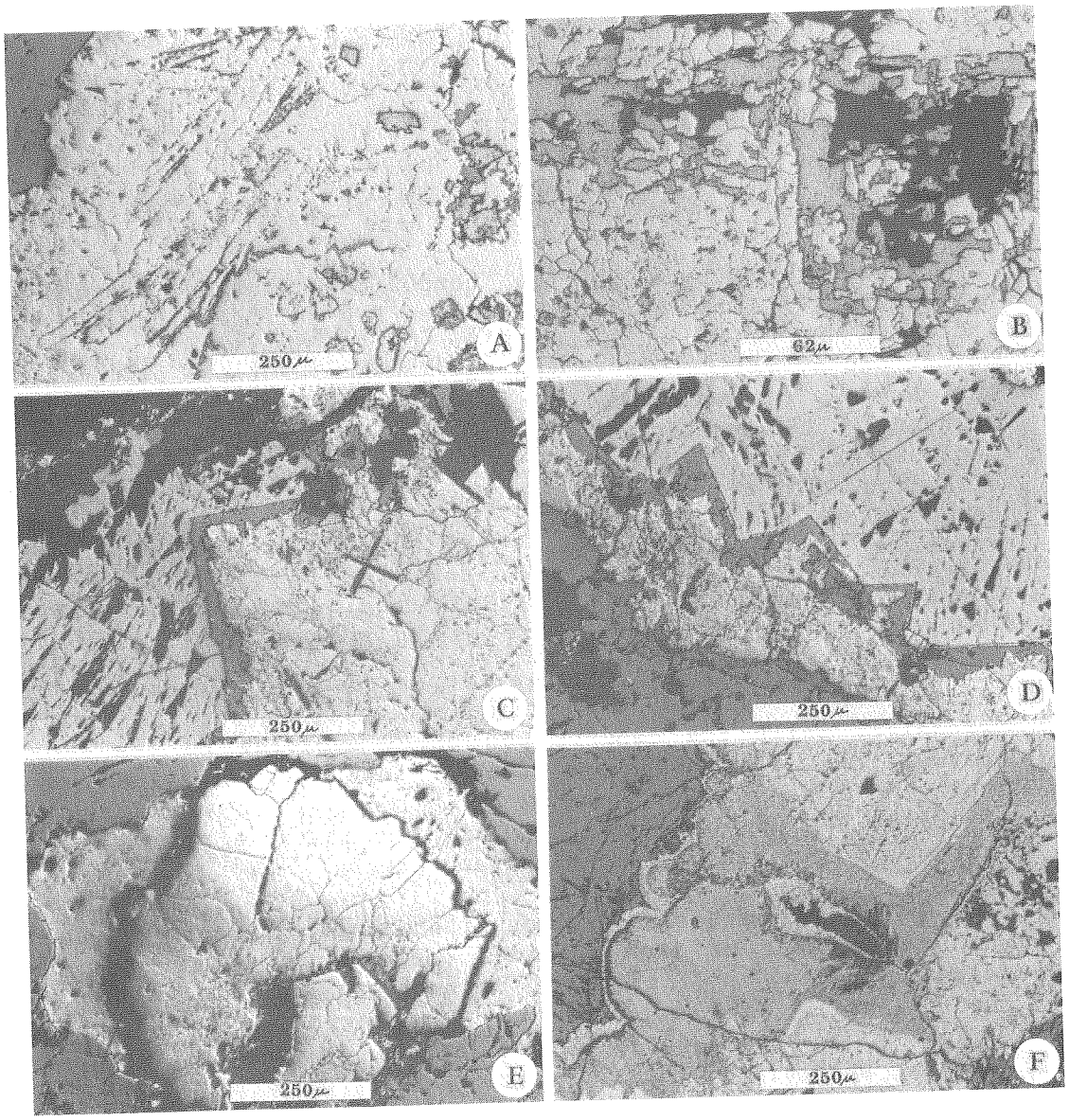


Figure 20. Sulfide replacement, overgrowth, and infilling: A, bladed pyrite overgrown by additional pyrite; subhedral galena grains (light gray, right); B, subhedral galena in pyrite-marcasite intergrowth; black is quartz; C, iron sulfide, right, overgrown by thin layer of sphalerite (dark gray), then galena pitted light gray, left; cross is composed of silica, origin unknown; D, more extensive replacement of iron sulfide; colors as in C; E, pyrite grain overgrown by galena (lighter gray, right and left), then sphalerite; F, poorly crystalline pyrite intergrown with pyrite-marcasite (above and below), and coated with botryoidal pyrite (left).

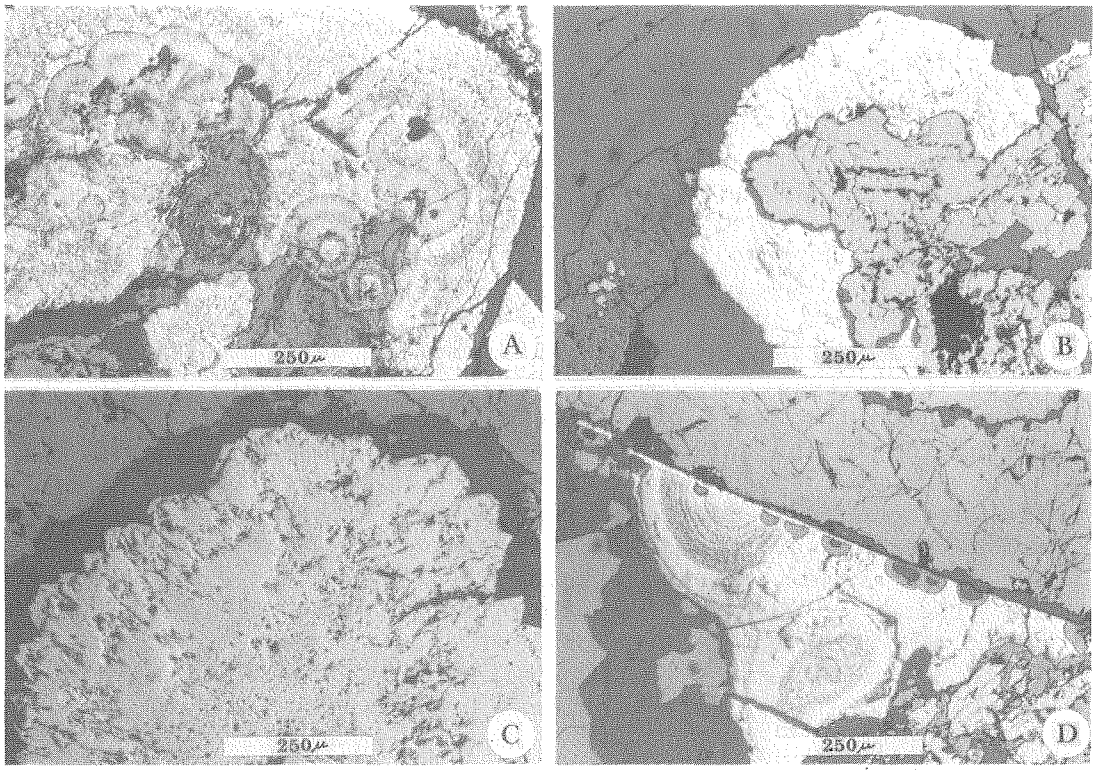


Figure 21. Botryoidal fragments; A, multi-centered iron sulfide growth; sphalerite middle and bottom middle; B, sphalerite (lighter gray) with thin quartz rim overgrown by marcasite; trace of galena (lightest gray) in sphalerite; C, pyrite with marcasite terminations, rimmed by quartz (dark gray), then sphalerite (medium gray); D, small quartz-cored sphalerite growths in larger iron sulfide growth; sphalerite, top.

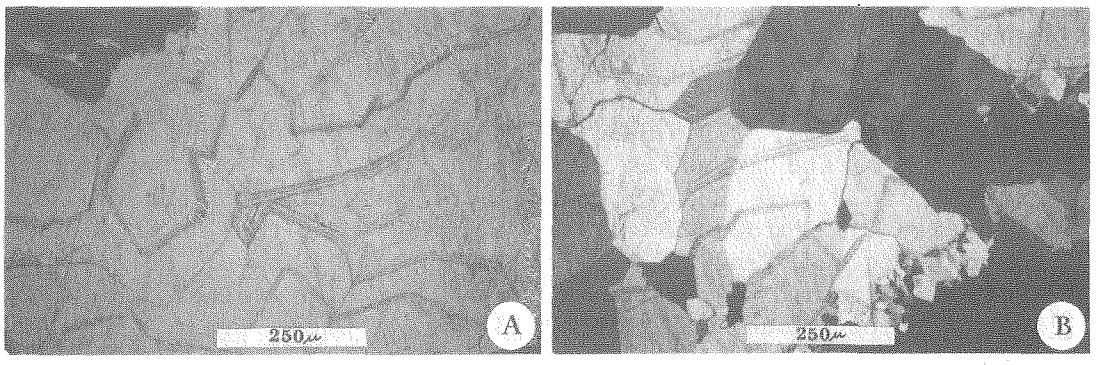


Figure 22. Thin sections showing the same euhedral vein quartz; A, plain light; dusty outlines appear to be very fine-grained sphalerite in part; B, crossed nicols; extinction boundaries cross growth zones.

tion (Fig. 21A). Less often, but still commonly, botryoidal sphalerite is also intimately intergrown in these fragile textures (Fig. 21B). Usually, though outlines are well preserved, evidence of minor to fairly extensive recrystallization and/or pore filling and overgrowth is present (Fig. 21C,D), blurring fine detail. As noted above, virtually no open space remains in any of the Red Dog ore, so it is not surprising that continued mineralization has cemented and recrystallized what may once have been quite open structures composed of fine colloform sulfide minerals.

The common preservation of such frail textures might not be expected if post-depositional metamorphism were important at Red Dog. Aside from relatively minor replacement already noted and rare shearing on the scale of a single grain or two, the only evidence of disruption in the deposit is the pervasive fracturing that appears to have occurred throughout all stages of mineralization. Fracturing includes multiple cross-cutting relationships among veins, abundant fragmentary mineral grains, and the common occurrence of iron sulfide and, to a lesser extent, sphalerite microbreccia (Fig. 19). Plahuta and others (1983) point out that high-angle vein systems at Red Dog are consistent with a tensional environment like that in a back-arc basin or aulacogen. The internal fabric of the veins and breccias themselves reflects this tensional regime.

All fractures are filled, if not with sulfides or sulfides plus quartz, then with quartz alone. Quartz is the only gangue mineral found in sulfide ore at Red Dog. Barite veins and lenses contain minor sulfides but virtually no barite has been observed in any of the four main types of sulfide ore. Quartz gangue occurs mainly as vein fillings and as a ground mass, or cement, between mineral grains. In either of these forms it usually consists of very fine- to medium-grained polycrystalline intergrowths of anhedral grains. The lamination common in sphalerite is absent in quartz gangue, though quartz zoning is occassionally seen in ore (Fig. 22) and is common in the granular quartz rock (unit Pss, section A above).

## E. Barite

Figures 23A, 23D, and 23F illustrate hand specimens of three types of barite found at Red Dog. The light colored barite vein material in Figure 23A is composed of subhedral to euhedral crystals of barite intergrown to varying degrees with the sulfides and minor quartz (Fig. 23B and 23C). Barite appears dark in polished section because of its low reflectance; it has high relief and a distinct brown color under reflected light. Once again the euhedral crystalline habit indicates that open space was still forming, or at least unfilled, during emplacement. No veins or veinlets of any kind were found to cross-cut the barite veins. Although only about five

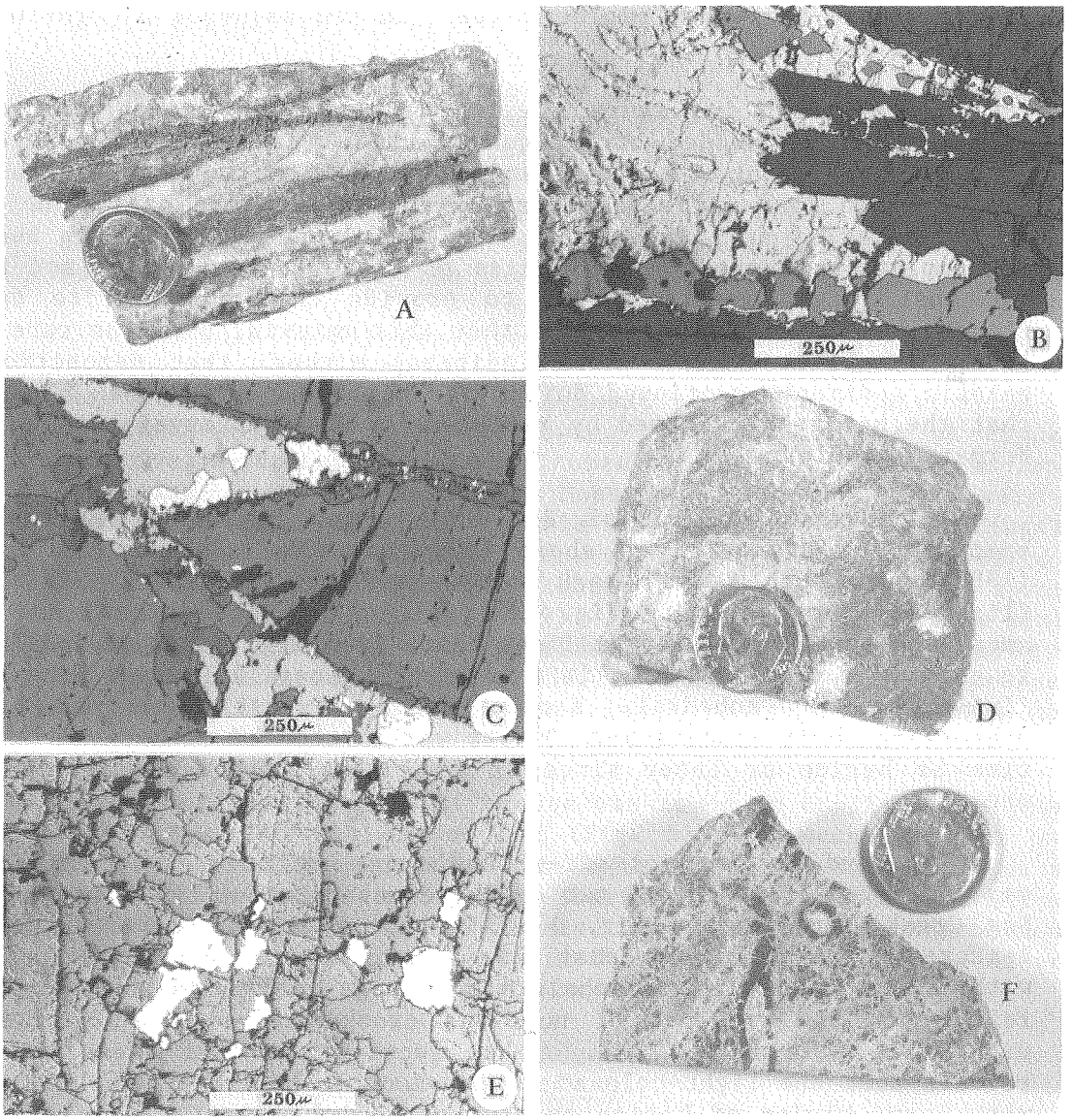


Figure 23. Red Dog barite: A, vein barite containing layers and crystals of sphalerite (dark) and thin laminations of galena (not visible in photograph); B, euhedral barite crystals (dark gray), with sphalerite (medium gray) and iron sulfides; from vein barite of A; C, barite crystal termination in sphalerite with minor pyrite and galena; darkest gray, including thin rims on barite, is quartz; D, sample of massive gray barite-quartz of stratigraphically highest barite unit; E, subhedral barite grains (rough gray) and sphalerite (almost white) in quartz (smooth gray); from hand specimen similar to that in D; F, massive barite-quartz rock containing possible fossil worm tubes (black). Coin is 18 mm in diameter.

barite veins were found and sampled, this lack of cross-cutting suggests that they were emplaced late in the sequence of ore-forming events at Red Dog.

The specimen in Figure 23D is a light gray fragment of rubble from the uphill bedded barite-quartz unit. Talus of this material forms a slope about 500 m long and 100 m high on the west bank of the Red Dog main fork and also occurs extensively on the east side (Fig. 5, exposures of unit Psb uphill away from creek). Barite in bedrock is completely covered, so thickness of this barite unit is not known but must be at least 10-20 m to provide this much barite talus. Plahuta and others (1983) report that this material contains rare thin layers of black chert, which indicates either that deposition of pelagic sediments continued during its formation on the sea floor, or that the barite cap formed by replacement of an interval of Siksikpuk Formation shale.

A polished section of Red Dog bedded barite like the hand specimen in Figure 23D is shown in Figure 23E. Plahuta and others (1983) report that this rock type commonly contains 10-20% quartz (lighter, smooth gray in Fig. 23E), with 5% being minimum, and that among the scarce included sulfides there is a high ratio of sphalerite to galena. Sulfide grains in this barite generally appear like this, fine-grained and anhedral. Barite grains are mostly anhedral, though preserving their elongation. Quartz was introduced either at the same time as barite or later since it is almost never euhedral in this material.

The hand specimen of off-white barite-quartz rock in Figure 23F was collected from bedrock two or three meters above the bottom of Red Dog Creek (Appendix A, Fig. 1). This rock has a variable, complex texture, and contains at least three parts barite to one part silica, with minor interstitial sphalerite and galena. Its most striking feature is the presence of numerous crooked tube-shaped structures with dark walls (Fig. 23F). Thin section study of these features reveals that the light-colored interior of each tube is filled mostly with large blades of barite transverse to tube length; space between barite crystals is filled with aggregates of very small quartz grains. The dark tube walls are composed mainly of very fine silica grains with a few of barite. Under plain light this wall material is greenish brown to tan, dusty-looking, and peppered with minute black specks. Except for some indistinct, resealed cracks perpendicular to the tube length, this very fine-grained wall material exhibits no discernible internal structure. The groundmass outside the tubes consists in part of fine barite grains intergrown with very fine-grained, equant, subrounded quartz grains, and in part of light greenish or brownish colloform clumps of very fine quartz crystals. Very fine-grained sphalerite is commonly scattered throughout between barite and quartz grains. Galena forms somewhat larger clumps with

signs of replacement like embayments in, and inclusions of, quartz and barite grains.

These tubular structures may not be fossils, and they may have originated in some other sediment type that has subsequently been replaced by the barite-quartz rock. However, replacement of sediment does not account well for the large difference in crystal size, habit, and composition between the tube interiors, the walls, and the ground mass. Few remnants of other rock types have been observed within the barite-quartz rock of this lower barite unit.

Lonsdale (1979) describes living vestimentiferan tube worms of the species Lamellibrachia barhami that were recently sampled in the San Clemente fault zone off the coast of southern California. These creatures are described as growing in dense tangles of crooked to relatively straight chitinous tubes, some more than 1 m long and averaging 1 cm in diameter. Most significantly, they were found growing on piles of pure, friable exhalation barite accreting around active submarine hot springs. The only known close relatives of these worms are the Vestimentiferae clustered around some thermal springs on mid-ocean ridges (Lonsdale, 1979). Fossilization of similar creatures at Red Dog during the Carboniferous period could account for the tubular structures in Figure 23F, as well as for their presence in barite-rich rock associated with other rocks of possible submarine exhalative origin.

One other interval of barite was found in unsilicified lowermost Etivluk Group rocks at Red Dog (Fig. 5). It occurs mostly as very thin, conformable laminations in light tan shale, but one layer almost 15 cm thick was found. This barite layer contains considerable disseminated fine-grained sulfides, mostly galena, in the bottom 5 cm (sample LL4-27, Table 1, Appendix B). No veins were found associated with this barite.

## F. Summary of Red Dog mineralization

Figure 24 is a very general and schematic summary of mineralizing events at the Red Dog main deposit. Time may be read from left to right as long as allowance is made for much overlap in events and for temporary, local reversals in order. Chalcopyrite has been omitted from the figure because of its extreme scarcity in this deposit. Breccia ore has not been listed as a separate category of Red Dog mineralization but is probably an intermediate type between vein and podiform ore.

Pyrite and sphalerite undoubtedly formed first, beginning during sedimentation and diagenesis. Pyrite appears throughout the black host rock as tiny grains, framboids, and not uncommon fragments of

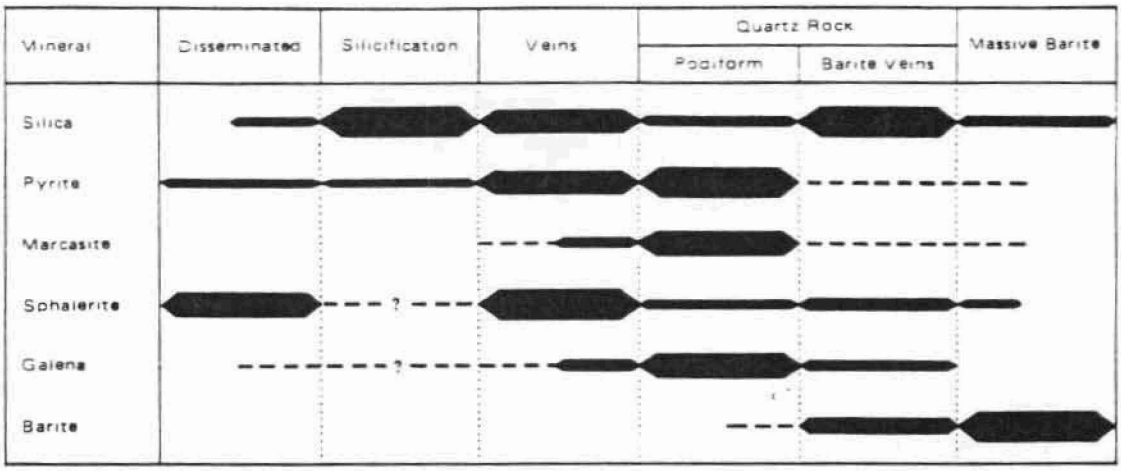


Figure 24. Inferred sequence of Carboniferous mineral deposition at Red Dog Creek. Time to the right. Quartz rock is meant to be approximately contemporaneous with both podiform sulfide ore and barite veins. See text for explanation and discussion.

replaced sponge spicules. Sphalerite disseminations are also abundant and are generally much larger than the disseminated pyrite, sometimes incorporating the latter. Zoning in these sphalerite grains and in associated quartz indicates free growth, probably in soft sediments. A few galena specks associated with these diagenetic sphalerite grains are indicated by the dashed line for this mineral under Disseminated in Figure 24. Although these disseminated sulfides appear to be the earliest forms of mineralization, it is not necessary to assume that their formation had ceased before the onset of veining. Some sphalerite disseminations are closely associated with veins and the samples reported here were collected near the top of the Kuna Formation, so dissemination may have continued until near the close of hydrothermal activity.

The widespread silicification of black Kuna Formation shale in the Red Dog ore zone could have begun at the same time as the disseminated sphalerite but probably not much before; the sediments had to be soft and permeable to allow free growth of the zoned sphalerite grains. Silicification was probably well under way, if not complete, before veining; sharp vein-wall rock contacts show no systematic relationship to directions of shale particle lamination. Rather, mineralized fractures occur at random as in a very isotropic medium. Introduction of silica continued throughout the stage of vein filling, into the formation of the granular quartz rock that appears to overlie the main ore horizon, and beyond, forming a sizeable proportion of the massive barite rock. Conceivably, deposition of the granular quartz rock began only after most porosity in the shale had been plugged by silicification forcing silica-saturated solutions to

the surface. Likewise with the sulfide veins and podiform ore. Ongoing silica emplacement probably continued to affect host rock and sediments whose deposition may also have continued after the onset of veining. However, overlying cherts and unsilicified shales of the Permian Siksikpuk Formation are not veined.

Sphalerite and quartz form the bulk of vein ore in the Red Dog main deposit, with pyrite and marcasite also very abundant; iron sulfides frequently form laminations and other growths within the sphalerite-quartz. Toward the periphery of exposed mineralization, especially up the eastern tributaries of Red Dog Creek, the proportion of iron sulfide in veins increases, while veins become smaller. This may in fact be the edge of the deposit; Finlow-Bates (1980) notes that iron sulfides often form a separate facies at the margins of submarine exhalative ore bodies. Galena is not as abundant as sphalerite, iron sulfide, or quartz in surface samples of vein ore. Most often it appears to be late, replacing or overgrowing earlier minerals, though in places it forms somewhat larger concentrations. Cross-cutting of veins is very prominent, and clasts of host rock within vein mineralization are common.

Although the podiform ore at the top of the black shale horizon may have formed at the same time as the veins, it is shown later than the veins in Figure 24 because of its higher galena content, galena being paragenetically late at Red Dog. Alternatively, the higher galena concentration in the podiform ore could be due to differences in the environment of deposition of this ore from that in the vein system, and therefore may represent a kind of zoning. Interfingering with the granular quartz rock, the podiform ore probably formed from exhalative activity at about the same time as the latter.

Sulfide breccia fillings adjacent to both veins and podiform ore may represent an intermediate type of mineralization. The breccia ores are coarser grained than much of the podiform sulfides, contain abundant host rock fragments, and sometimes appear to grade laterally through stockwork to individual veins. On the other hand, their semi-clastic ore texture and higher galena content relate the breccia sulfides more closely to the podiform ore, into which the breccia fillings also appear to grade. FeS content of sphalerite in the breccias overlaps the corresponding ranges for vein and podiform sphalerites, which are fairly distinct from each other in FeS contents.

Both macroscopic and microscopic ore textures in veins and breccias provide pervasive evidence of open space filling. These include botryoidal growths, especially of iron sulfide; zoned crystals of sphalerite, quartz, and iron sulfide; euhedral crystals of each mineral; fragments of early ore contained in larger masses of later ore; clasts of host rock that are loose rather than crushed; and so

on. This textural evidence agrees with the view of Plahuta and others (1983) that the environment at Red Dog was tensional during ore emplacement, as in a back-arc basin or aulacogen. However, vugs are almost wholly lacking, all open spaces have been filled with quartz and sulfides during the waning stages of hydrothermal activity.

Barite-rich veins are relatively rare at Red Dog. That they contain sulfide minerals, often in substantial quantities, is taken as evidence that they are transitional between the massive sulfides and massive barite, which is poor in sulfides and overlies the ore zone. That the barite veins are of a different generation than the sulfide-quartz veins is shown by the fact that the latter contain virtually no barite, while the former contain little quartz, no fragments of pre-existing ore, and are not cross-cut by other veins. However, the barite veins also show ample evidence, from megascopic lamination to microscopic euhedral crystals, of open space filling.

The thick barite unit in the Permian Siksikpuk Formation overlying the deposit may have been fed by veins within the main ore zone. But if so, these must be quite scarce since the massive barite contains only sparse sulfide minerals, and few sulfide-poor barite veins were found in outcrop.

Other than the minerals mentioned above, only small amounts of possible pyrrhotite in sphalerite, and unidentified inclusions or exsolutions in galena were found by this study in Red Dog ore. Calcite, fluorite, and other gangue minerals besides quartz, if present, must occur in very small amounts and very small grains; none were found in microscope study for this thesis. Silicification and small amounts of chlorite and sericite are the only common indications of metamorphism at Red Dog.

## G. Geochemistry

To study the chemical composition of Red Dog ore and country rock, 61 mineral and rock samples were semiquantitatively analyzed by the author using DC-arc emission spectroscopy. There were several reasons for this work. First, to see whether there were any obvious trace element differences between Red Dog ore, host rock, and gangue. The source of the sulfide mineralization is a tantalizing question that cannot be answered by a semiquantitative reconnaissance study of trace elements, but it is hoped that publication of the data may suggest some avenues for further research. A second goal was to determine definitely the silver-bearing phase. High silver values were reported from Red Dog (Plahuta, 1978) and most geologists assumed that silver must be in galena; however, cases have been reported in which high-silver sphalerite is closely associated with virtually silver-free galena (for example, Taylor and Radtke, 1969). The third

intention was to obtain a spectrum of trace element contents of minerals at Red Dog that could be compared with trace elements found in other deposits, especially those in the DeLong Mountains.

Aside from sample contamination by mineral inclusions, emission spectroscopic results can be affected by several other sources of error: (1) contamination during sample preparation; this is minimized by careful handling of samples and equipment; (2) voltage fluctuation or maladjustment of the Spectro Varisource, resulting in a hotter or colder "burn" than standard; (3) matrix effects caused by a preponderance of major mineral in the sample; varies with major mineral and other factors; (4) contamination of chemicals and/or imperfect temperature control during film developing can cause spectral lines to be lighter or darker than they should be across the whole film; (5) interelement wavelength interference; can largely be prevented by chosing the optimum line for each element as determined by theory and experience; (6) subjective component in comparing lines from the sample film with lines on the standard film; for most lines and concentrations this is not a severe problem but it can be a source of error in determination of elements for which large differences in concentration cause only small differences in line density, for instance Cd; (7) accuracy of the technique varies between elements as concentration approaches the upper or lower analytic limit; in general, accuracy is best in the mid-range for a given element. The quantitative effect of any one or a combination of these errors on a given reading is difficult to state with any certainty. However, with proper precautions, results should be within about ±30% of true values overall (P.D. Rao, pers. comm., 1981).

Results of the analyses are summarized in Table 2. Eight elements were selected for the table: Ag primarily to determine the main silver-bearing phase at Red Dog; Cd, Cu, and Fe because these are important trace elements in sphalerite; Sb because stibnite is often an important accessory mineral in galena; As because very high arsenic content might indicate the presence of arsenopyrite, which was not identified in polished section; Pb, Zn, and Fe to check on cross-contamination between sphalerite, galena, and Fe-sulfide, as well as to determine the abundance of these elements in the host rock. Appendix B, Table 1, reports seven additional elements, Sn, Co, Mn, Mo, Ni, Ti, and Cr, for each sample. No data were determined for host rock Sb or As because that portion of the host rock sample film was marred during developing. Field locations of samples are given in Appendix A, Figure 2. The analyses in Table 2 are compared graphically with similar analyses from other Key Creek sequence deposits in Figure 25. No statistical analysis of the data is attempted here because of the wide error limits and the uneven availability of sample material from the various ore types and deposits. A few general observations on the Red Dog trace element results follow but these comments are made only qualitatively and

Table 2. Summary of emission spectrographic[a] analyses of Red Dog minerals and host rock.

| Sample[b] type (no.) | Element[c] range (approximate mean in parentheses) | | | | | | | |
|---|---|---|---|---|---|---|---|---|
| | Ag | Cd | Cu | Sb | As | Pb | Zn | Fe |
| Sphalerite (15) | 35-500 (180) | 500->500 (>500) | 150-1,000 (690) | 100-2,000 (900) | 200-3,500 (1,000) | 750-15,000 (3,600) | - | .3-7 (2.9) |
| Fe sulfide (10) | 20-1,000 (350) | <100-100 (<100) | 35-500 (280) | 3,500-10,000 (4,900) | 5,000->10,000 ( >8,300) | <20->20,000 (>10,000) | 750->10,000 (>7,400) | - |
| Galena (9) | 1,000->5,000 (>3,000) | <100-500 (<180) | 35-350 (130) | 20-1,000 (240) | <200-1,000 (<320) | - | 2,000->10,000 (>10,000) | <.1-7 (<1.3) |
| Barite (7) | 2-750 (140) | <100->500[d] (?) | 1-100 (32) | 50-750 (260) | <200-750 (<310)[e] | 750->20,000 (>10,000) | 750-10,000 (3,400) | .1-5 (1.9) |
| Host rock (14) | <1-750 (79) | <100-500 (<140) | 5-750 (180) | n.d. | n.d. | <20->20,000 (>5,300) | 750->10,000 (>4,600) | .5-10 (3.7) |
| Quartz-ba rock (6) | 35-150 (81) | <100-100 (<100) | 15-500 (190) | 150-500 (280) | <200-500 (<260) | 1,500-20,000 (9,400) | 500->10,000 (>5,400) | .2-5 (1.3) |

a. All analyses performed by the author according to the procedure described by Stevens (1971) b. Sample locations are given in Appendix A, Figure 2. c. Analytical range: Ag 1-5,000 ppm; Cd 100-500 ppm; Cu 1-20,000 ppm; Sb 20-10,000 ppm; As 200-10,000 ppm; Pb 20-20,000 ppm; Zn 200-10,000 ppm; Fe 0.1-20%; n.d. = no data. More complete analyses are given by sample number and type in Appendix B, Table 1. d. All but one analysis of 500 ppm were 100 ppm. e. Average of five analyses, no data for two.

should be evaluated as such.

Differences, if any, between ore and host rock at Red Dog are not very striking. Fourteen samples of this rock average higher than iron sulfide in Ti and Ni (Appendix B). If significant, high Ti and Ni must be a primary characteristic of the rock itself because no amount of contamination by disseminations of sulfides lower in these elements could raise Ti and Ni in host rock analyses to the observed levels. However, host rock burns were recorded on a separate film. Unknown matrix effects could also enter into the host rock analyses. For these two reasons, the high Ti and Ni might not be significant.

High content of iron, lead, and zinc in host rock may in many cases be due simply to very fine disseminated pyrite, galena, and sphalerite. These were in some cases visible in the crushed rock

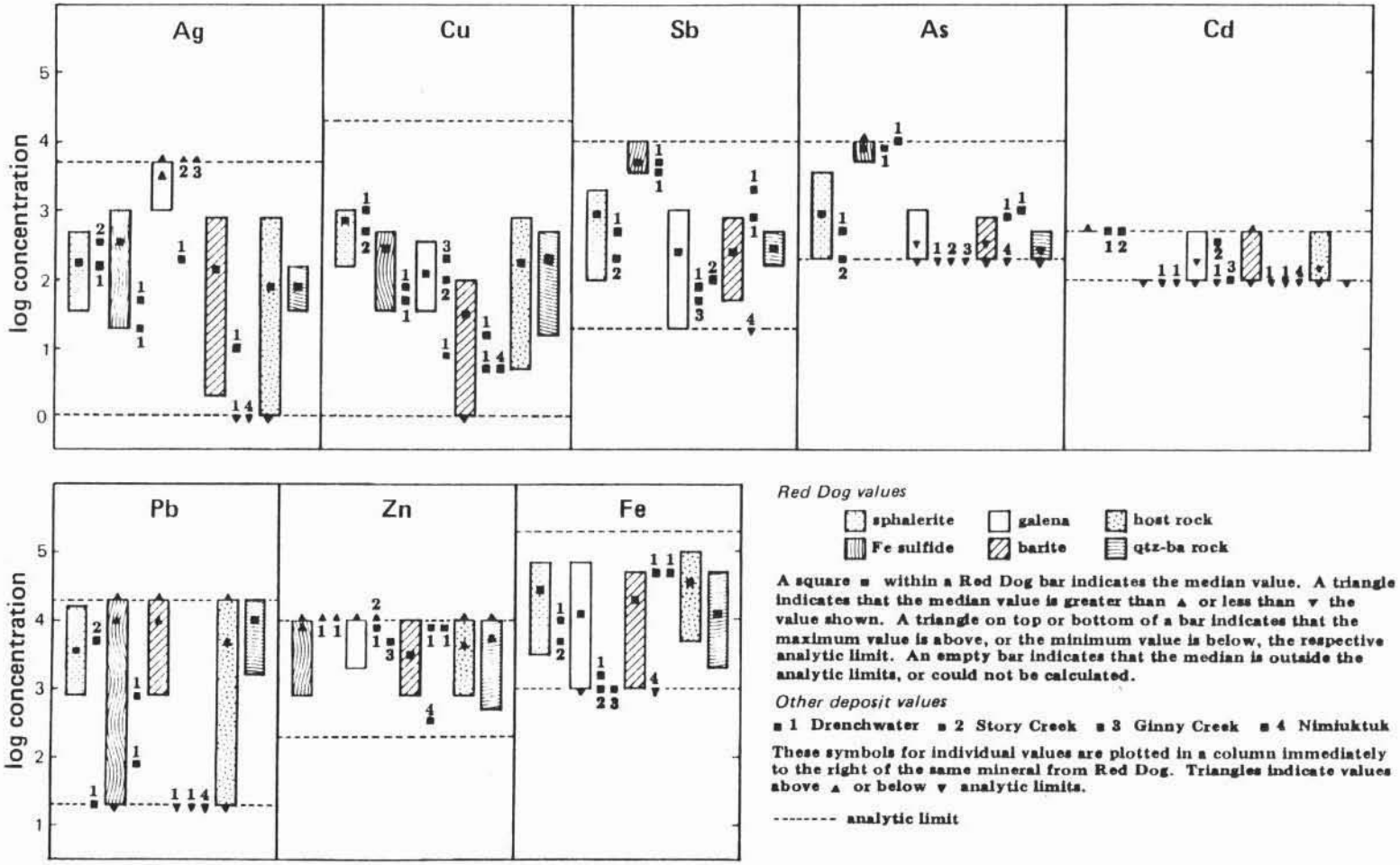


Figure 25. Comparison of emission spectrographic trace element analyses from Red Dog, Drenchwater, Story Creek, Ginny Creek, and Nimiuktuk. Data from Tables 2, 4, and 5.

material during grinding despite precautions against them. However, one sample of host rock thought to be from outside the ore zone (LL3-15, Appendix B) and showing a mere trace of pyrite under the microscope, differs from other samples of black rock only in its somewhat elevated Ni and Co, and low Zn and Pb. If this is taken to be a sample of pre-mineralization host rock, which is not certain, it does not differ very markedly from host rock sampled well within the ore zone.

Similarity in trace element contents between ore and country rock at Red Dog does not in itself provide much insight into ore formation or emplacement. The trace element data includes no compelling evidence against the possibility that Kuna Formation cherts and shales provided some cations by during ore formation; chemical partitioning of trace elements between sulfide minerals and enclosing black shales during diagenesis is well documented (Raiswell and Plant, 1980), though the degree of this effect doubtless varies between deposits. Equally possible is that the mineralizing event itself mobilized metal ions into the country rock at Red Dog from an outside source; no black Kuna Formation shale clearly unaffected by the Red Dog mineralization was available for spectrochemical analysis. A third possibility, of course, is that ore-bearing fluids and country rock had no effect on each other during the mineralizing event. This seems unlikely, given the existence of important disseminated sphalerite-(galena) within the host rock, and some dissolution and replacement of host rock on a microscopic scale.

Table 2 shows clearly that galena contains an order of magnitude more silver than does sphalerite. On the other hand, if sphalerite is said to be high in silver, iron sulfide contains still more. Even if the highest silver value for iron sulfide is omitted, nine samples of the mineral still average 280 ppm silver. So, while other minerals and even host rock and gangue contain silver, it can be said with some confidence that the main silver-bearing mineral at Red Dog is galena.

In Table 2, it is seen that scarce copper at Red Dog shows some preference for sphalerite, as does cadmium. All but one of the cadmium values for sphalerite were above the maximum detection level of the technique, so its actual range is unknown but could be very high. High cadmium values have been reported from the waters of Red Dog Creek (Watts, Griffis and McOuat (WGM) field staff, pers. comm., 1978). Antimony and arsenic are both strongly concentrated in iron sulfide at Red Dog, with perhaps surprisingly little in galena and somewhat more in sphalerite. This is approximately the same relationship seen in Drenchwater Creek analyses (Chapter V, Table 4). The high range of As values for iron sulfide suggests that arsenopyrite may be present in Red Dog ore even though this mineral was not positively identified in polished section. It is also striking that iron sulfide contains so much more lead than sphalerite

does. The difference is even true for two samples from which both iron sulfide and sphalerite were separated for analysis. Only one sample (LL 26-7, Appendix B) of disseminated sphalerite was analysed due to the lack of additional specimens. There is nothing striking about this analysis compared to those of other Red Dog sphalerites, although it has the second highest Pb content.

Red Dog barite has its own trace element signature, although it is not remarkable compared to other minerals from the same deposit. The high lead and zinc content could be due to galena and sphalerite contamination, though barite from the hand specimen with the highest visible amounts of these minerals, LL4-13, analyzed lowest for Pb and second lowest for Zn (Appendix B). Sample LL4-27 (Appendix B) is from a layer of barite rich in disseminated galena found within the gray to tan unsilicified shales of the Permian Siksikpuk Formation away from the main ore zone (Fig. 5). Compared to other Red Dog barites, LL4-27 is high in Ag, Cu, Mo, Mn, Ni, and Co. A different source may be indicated for this occurrence of barite, though it is here represented by only one sample.

# V. DRENCHWATER CREEK

## A. Background

Drenchwater Creek flows northwest from the crest of the Brooks Range to the Kiligwa River, a tributary of the Colville River (Fig. 1). Topography in the mineralized area is even more subdued than that around Red Dog. None but very small intermittent tributaries enter Drenchwater Creek in the study area.

The Drenchwater Creek mineralized area is located in T10S, R1E, Umiat Meridian in the Howard Pass quadrangle. During field work in 1950-53, 1976, and 1977, I.L. Tailleur observed iron staining from sulfide weathering in dark-gray shale and chert along Drenchwater Creek (Tailleur and others, 1977). The study area is conspicuous anyway because of large kill zones which generally are due to the weathering of pyrite and marcasite in chert, shale, and tuff.

The Drenchwater Creek mineralization contains the best exposed and most abundant zinc-lead sulfide and barite discovered within the National Petroleum Reserve Alaska (NPRA) up to 1977. The U.S. Geological Survey studied the area intensely that summer as part of their mineral resource-assessment of the Reserve (Churkin and others, 1978). A resulting report by Nokleberg and Winkler (1982) on Drenchwater is the most complete yet published on any deposit discussed in this thesis.

## B. General deposit description

Mineralization at Drenchwater Creek, as at Red Dog, consists of sphalerite, galena, pyrite, marcasite, and minor barite. It is found in an irregular zone about 6 to 45 m wide that extends at least 1,830 m eastward from the creek. Country rock in the area is what Nokleberg and Winkler (1982) call a tectonic breccia, meaning a series of relatively thin, discontinuous lenses of different rock types randomly thrust together along numerous low- to high-angle faults with considerable repetition. These authors group the many thrust slices into five plates, each defined by certain proportions of various rock types and by distinct structural domains. Of these, the Drenchwater thrust plate is marked by a high proportion of sphalerite- and galena-bearing igneous rocks, and hosts the main mineralized zone.

Figure 26 reproduces, with some modification, that part of the geologic map of Nokleberg and Winkler (1982, Plate 1) that shows most areas of sulfide and barite exposure at Drenchwater Creek. Contacts, units and faults remain exactly as in Nokleberg and Winkler (1982), although several units which occur elsewhere on their larger map but not in the thesis study area have been omitted from the explanation.

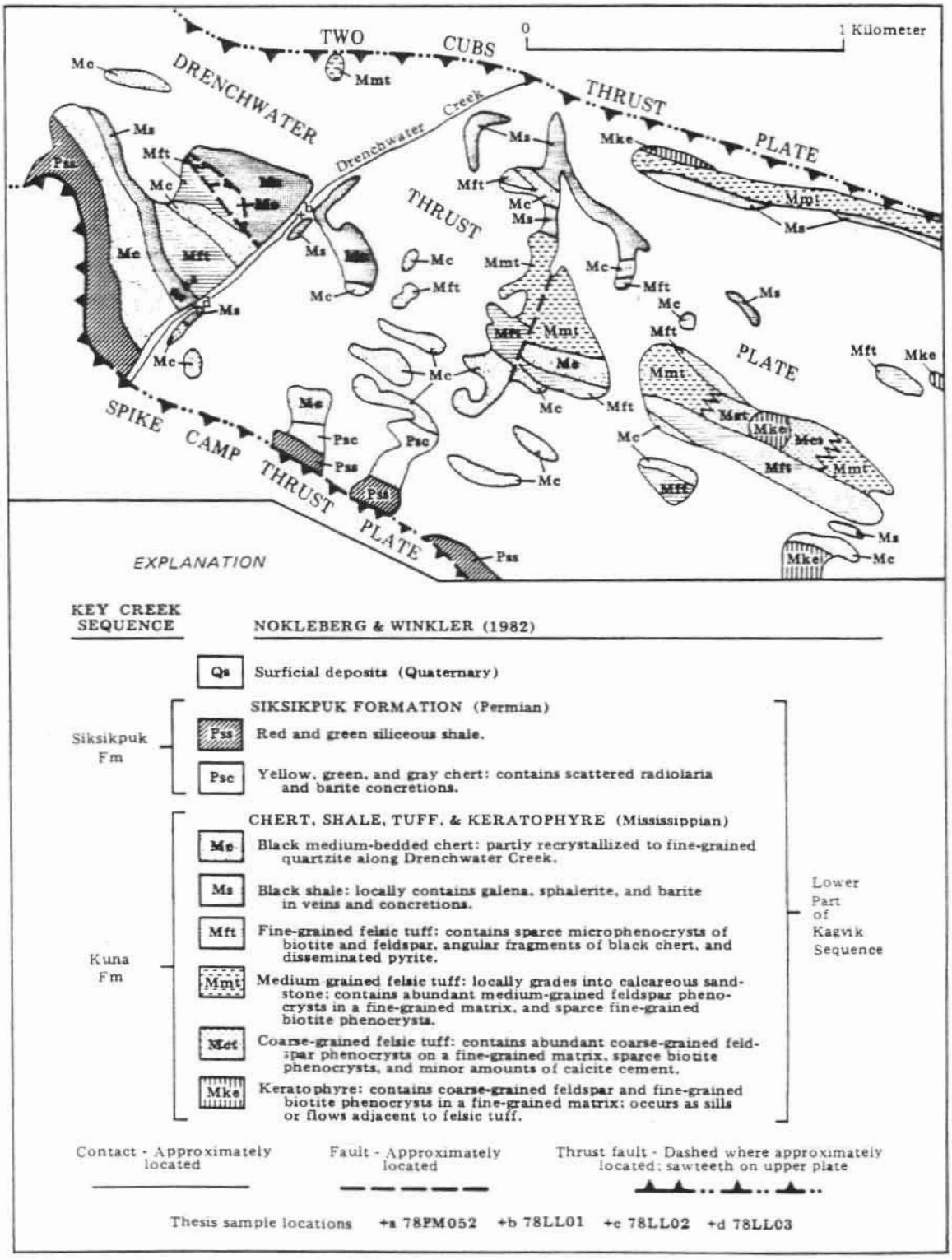


Figure 26. Geologic map of the Drenchwater thrust plate; modified from Nokleberg and Winkler (1982). Column at far left shows a possible correlation of map units with units of the Key Creek sequence.

The correlation of Key Creek nomenclature with the units of Nokleberg and Winkler (1982) is solely my suggestion.

The Drenchwater sulfides occur mostly in Mississippian-age dark-gray chert and shale adjacent to tuff, tuffaceous sandstone, and a few keratophyre and andesite flows and sills (units Mc and Ms, Fig. 26). Both cherts and shales also contain moderate to large proportions of fine volcanic debris such as glass shards, feldspar crystals, lapilli, and tiny rock fragments. Fossils, stratigraphic associations, and K/Ar age dates all indicate the Mississippian age (Nokleberg and Winkler, 1982). Although the extreme degree of thrusting at Drenchwater has obscured internal stratigraphic order, their age and geographic location place all these rocks within the Kuna Formation of the Key Creek sequence. The sulfides occur mostly within dark cherts and shales adjacent to volcanic and volcaniclastic rocks but also, more sparcely, within the volcanics themselves.

Hydrothermal replacement of fine-grained feldspar, pumice lapilli, and mafic volcanic rocks in the chert and shale is common at Drenchwater; replacement minerals include kaolinite, montmorillonite, sericite, chlorite, actinolite, barite, quartz, calcite, fluorite, and prehnite (Nokleberg and Winkler, 1982). Shale hardening due to silicification is common, though not as extensive as at Red Dog, and locally the chert is altered to siliceous medium-grained metaquartzite; most sulfide minerals typically are found in such altered chert and shale (Nokleberg and Winkler, 1982).

Barite occurs very sparcely as fine disseminations between, or as tiny inclusions within, grains of sphalerite and galena in the Mississippian-aged rocks just discussed. It also forms its own segregations within Mississippian shale unit Ms (Fig. 26). Barite sample 78LL02 was found in place in shale just west of Drenchwater Creek, about 10 meters up the hill. Here coarse-grained barite occurs in a conformable layer up to about 3 cm thick. The hand specimen was thought too delicate to section but, judging from its dark gray color, the shale probably belongs to the Kuna Formation rather than to a younger unit. Cherts and shales of the overlying Permian Siksikpuk Formation (unit Pss and Psc, Fig. 26), which are generally very thinly laminated and much lighter colored on weathered surfaces, also locally contain barite (Nokleberg and Winkler, 1982).

## C. Sulfide and barite mineralization

Ore-bearing outcrops at Drenchwater are few and unspectacular compared to those at Red Dog. A typical hand specimen of one ore type looks like a medium- to dark-gray mudstone containing abundant extremely fine-grained pyrite, marcasite, sphalerite, and galena, all with a marbled appearance reminiscent of soft-sediment deformation.

Some larger grains are also found, as well as rare thin quartz-sulfide veins up to about 2 cm thick that crosscut cleavage. Under reflected light this material is seen to contain areas where fine-grained sphalerite and pyrite are segregated into separate masses in a quartz matrix. Much larger, often euhedral grains of galena and pyrite-marcasite are also found in the same quartz matrix, indicating that free crystal growth was sometimes possible (though this part of the sample could be a vein filling).

Another type of disseminated ore is a very hard silicified rock (probably what Nokleberg and Winkler, 1982, call black chert) containing abundant sphalerite grains and a few disseminated galena grains, as well as sparse very fine pyrite throughout. The angularity of the sphalerite grains suggests a microbreccia with a high amount of quartz, rather than truly disseminated sphalerite like that at Red Dog. No chalcopyrite was found during thesis study, nor do Nokleberg and Winkler (1982) report any copper mineralization other than a small amount of malachite staining. These investigators infer from microprobe scans the presence in galena of inclusions of an unidentified sulfosault containing abundant antimony with lesser arsenic and silver.

Table 3 lists six electron microprobe analyses of sphalerite from

Table 3. Electron microprobe analyses of sphalerite from the Drenchwater Creek deposit.[a]

| Sample[b] | 78PM052 | | | | | |
|---|---|---|---|---|---|---|
| Analysis | 1 | 2 | 3 | 4 | 5 | 6 |
| | Major elements (weight percent) | | | | | |
| S | 32.224 | 32.586 | 32.483 | 32.361 | 32.307 | 32.238 |
| Mn | 0.054 | 0.050 | 0.049 | 0.054 | 0.064 | 0.056 |
| Fe | 1.991 | 2.159 | 0.709 | 1.028 | 0.390 | 0.647 |
| Zn | 64.642 | 65,039 | 66,781 | 65.981 | 66.638 | 65.784 |
| Cd | 0.005 | 0.005 | 0.006 | 0.004 | 0.003 | 0.004 |
| Total | 98.916 | 99.837 | 100.028 | 99.429 | 99.402 | 98.730 |
| mole % FeS | 3.5 | 3.8 | 1.2 | 1.8 | 0.7 | 1.1 |
| | Structural formulas (atom percent) | | | | | |
| S | 49.497 | 49.558 | 49.462 | 49.524 | 49.512 | 49.668 |
| Mn | 0.048 | 0.044 | 0.043 | 0.049 | 0.057 | 0.050 |
| Fe | 1.755 | 1.884 | 0.620 | 0.903 | 0.343 | 0.573 |
| Zn | 48.697 | 48.511 | 49.872 | 49.522 | 50.087 | 49.707 |
| Cd | 0.002 | 0.002 | 0.003 | 0.002 | 0.001 | 0.002 |

a. Analyst: W.J. Nokleberg; b. Sample location shown in Figure 26.

Drenchwater ore sample 78PM052. Experimental conditions were the same as for the Red Dog microprobe analyses (Chapter IV).

In terms of atom percent Fe and mole percent FeS, the six analyses from Table 3 plot together with sphalerites from Red Dog disseminated and podiform ore (Fig. 16 and 17, Chapter IV). All six analyses have less than 4 mole percent FeS, as do all but three of the analyses reported by Nokleberg and Winkler (1982) from five Drenchwater sphalerite samples. This is a narrow range of sphalerite FeS compared to Red Dog and other reported analyses (see discussion of FeS content in sphalerite, Chapter IV).

Given that several variables are involved in interpreting FeS content of sphalerites - temperature, pressure, $fS_2$, $fO_2$, among others - it is illogical to draw too close a comparison between deposits on the basis of this one parameter. General conditions of T, P, and oxygen and sulfur fugacities may vary significantly between deposits. Low FeS in Drenchwater sphalerites may not mean the same thing as low FeS content of some Red Dog sphalerites. No pyrrhotite was identified in polished sections of Drenchwater ore during thesis work, nor is any reported by Nokleberg and Winkler (1982). This is in agreement with the mole percent FeS data; there should not be pyrrhotite in equilibrium with sphalerite at such low values of mole percent FeS (Scott and Kissin, 1973, Fig. 2).

Independent evidence indicates a wide range of temperatures for mineralization at Drenchwater. Lange and others (1981) report depositional temperatures from sulfur isotope data of 115° to 305°C (though this estimate is largely extrapolated from Red Dog sulfur data). Nokleberg and Winkler (1982) report a fluid inclusion temperature of only 100°C for Drenchwater mineralization, which is low indeed compared to temperatures reported from Kuroko ores (Lambert and Sato, 1974; Urabe and Sato, 1978; Solomon and Walshe, 1979), where direct volcanogenesis of sulfides is usually demonstrable; 100°C is even moderate for submarine sulfide-depositing hot springs, where temperatures of up to 380°C have been directly measured (Larter and others, 1981; Haymon, 1983; Zierenberg and others, 1984). 100°C is almost certainly too low an emplacement temperature for Drenchwater sulfides if it is supposed that these were deposited directly from igneous rocks with which they are spacially associated in outcrop. It seems more likely that the actual source of mineralization lies at considerable depth below the surface. This hypothesis is in agreement with lead isotope evidence for a mixed, not wholly juvenile, source for lead at Drenchwater (Chapter VII), and with the negligible Cu content of the deposit (see below). Exposed intrusive and extrusive rocks may belong to a post-ore event.

Manganese content of the six microprobe analyses in Table 3 (Fig. 17B) are moderately low for natural sphalerites in general (see

discussion of Mn in sphalerite, Chapter IV, section D). Cadmium contents of Drenchwater sphalerites, especially those reported by Nokleberg and Winkler (1982), may be a little higher than those from Red Dog. This difference, if significant, is probably due to a small difference in the source of mineralizing fluids rather than to conditions of deposition, since cadmium follows zinc chemically during mineralization (Simms and Barton, 1961).

## D. Geochemistry

Table 4 presents selected emission spectrographic analyses of minerals from the Drenchwater Creek occurrence. Results are compared graphically to those from other deposits in Figure 25, Chapter IV. All trace element values listed for Drenchwater sphalerite in Table 4 are within the ranges of values for Red Dog sphalerite given in Table 2 except Pb, which is remarkably low. Ni (determined but not listed in Table 4) which, at about 10 ppm, is slightly higher in Ni than the highest value for this element in Red Dog sphalerite.

Table 4. Selected emission spectrographic analyses of minerals from the Drenchwater Creek deposit.[a]

| Mineral | Element[b] | | | | | | | |
|---|---|---|---|---|---|---|---|---|
| | Ag | Cd | Cu | Sb | As | Pb | Zn | Fe |
| Sphalerite[c] | 150 | >500 | 1,000 | 500 | 500 | <20 | - | 1 |
| Fe sulfide[d] (medium grained) | 50 | <100 | 75 | 3,500 | 7,500 | 75 | >10,000 | - |
| Fe sulfide[d] (very fine grained) | 20 | <100 | 50 | 5,000 | 10,000 | 750 | >10,000 | - |
| Galena[d] | 200 | <100 | 7.5 | 75 | <200 | - | 7,500 | .15 |
| Barite[e] | 10 | <100 | 15 | 750 | 750 | <20 | 7,500 | 5 |
| Barite[f] | <1 | <100 | 5 | 2,000 | 1,000 | <20 | 7,500 | 5 |

a. All analyses performed by the author according to the procedure described by Stevens (1971); b. Analytical range: Ag 1-5,000 pp m; Cd 100-500 ppm; Cu 1-20,000 ppm; Sb 20-10,000 ppm; As 200-10,000 ppm; Pb 20-20,000 ppm; Zn 200-10,000 ppm; Fe 0.1-20%; c. Sample number LL7801; contains some quartz and trace iron sulfide, no visible galena; d. Sample number 78PM052, a dense breccia-like material composed mostly of sulfides; the two forms of iron sulfide are quite distinct and easily separated; e. sample number 78LL02; f. sample number 78LL03, white to yellowish or gray barite vein material from a stream cobble of very hard black chert or silicified shale.

With two exceptions, all trace element analyses of Drenchwater iron sulfides fall within the ranges of Red Dog iron sulfides. Those two exceptions (determined but not listed in Table 4) are Mo 150 ppm, somewhat higher, and Ti less than 50 ppm, somewhat lower than the upper and lower Red Dog values, respectively. A partitioning of a number of elements between the medium-grained and very fine-grained forms is apparent. These differences may indicate somewhat different generations, or may be completely random, given only one sample of each.

The one Drenchwater galena sample is low in Ag and Cu compared to the Red Dog analyses; all other elements fall within the corresponding ranges for Red Dog galena. However, looking at all mineral the analyses together, it is seen that the Drenchwater deposit as a whole may be lower in silver than Red Dog. The one Drenchwater galena sample is far below the silver average for Red Dog galenas. Every other Drenchwater mineral likewise analyzed below the average for Ag in its Red Dog counterpart.

The two Drenchwater barite samples differ quite markedly in some elements, both from each other and from the Red Dog barite. Silver is very low compared to Red Dog barite analyses, as is lead. Sb, As, and Mn in Drenchwater barite are all far above the highest analyses for Red Dog barite (Mn concentrations, not listed in Table 4, are: 78LL02 = 5,000 ppm and 78LL03 = greater than 5,000 ppm).

Thus, although there are some differences in trace element contents between the Red Dog and Drenchwater deposits, barite is the only mineral that could perhaps be identified on the basis of trace elements as coming from one or the other, provided the analyses in Table 4 are typical of Drenchwater minerals. On the whole, the two deposits appear to be quite similar in trace element content.

## VI. OTHER RELATED DEPOSITS

Several other sulfide and barite deposits are known to be hosted in rocks of the Brooks Range allochthon's Key Creek sequence (Fig. 2). Although they have been studied and reported in much less detail than either Red Dog or Drenchwater, the Ginny Creek and Story Creek occurrences share with these first two deposits major sulfide mineralogy, host rock sequence, and lead isotope ratios. There may be important differences in emplacement mechanism, however.

The Ginny Creek deposit (T33N, 11W, Kateel River Meridian, Misheguk Mountain quadrangle) consists of a 900 m by 600 m zone of sphalerite, galena, pyrite, and rare chalcopyrite in a rubbly mixture of gossan and partly limonite-stained sandstone (Mayfield and others, 1979). Much of the staining comes from weathering of intergranular siderite, which is abundant in this area but not in other deposit areas discussed in this thesis. Mineralization occurs mainly as minute intergranular disseminations within a sandstone believed to be the Upper Devonian through Lower Mississippian Noatak Sandstone. This formation includes some siltstone and shale and is thought to be a lateral equivalent of the Kanayut Conglomerate (Fig. 3). Thin quartz veins, most lacking sulfides, cut the sedimentary beds. C.F. Mayfield suggests that the Ginny Creek deposit may have been "formed in the Carboniferous as metal-bearing hydrothermal solutions percolated through this Late Devonian to Early Mississippian sandstone aquifer" (pers. comm., 1980).

The Nimiuktuk barite deposit (T12S, R34W, Umiat Meridian, Misheguk Mountain quadrangle) occurs as a small hill about 2.5 km west of the confluence of Klim Creek with the Nimiuktuk River (Mayfield and others, 1979; Barnes and others, 1982). Nearest bedrock, 500 m to the northeast, is a series of rubbly outcrops of Upper Mississippian black chert and shale. Outcrops of Upper Mississippian volcanic rocks and Lower Mississippian sandy limestone occur some 600 m southwest of the deposit. Intervening are only flatlands of tundra, though C.F. Mayfield reports that a small amount of black chert or shale float was found by D.F. Barnes on the barite rubble pile (pers. comm., 1980). The volcanic rock, possibly originally an andesite or a latite, has been dated by K/Ar at 333 ± 17 m.y., an age very similar to that of the quartz latite from Drenchwater (Mayfield and others, 1979). Barnes and others (1982) estimate the deposit to contain more than 1.5 million metric tons of high-grade barite with much larger tonnages probably concealed. The sample of barite from Nimiuktuk examined under the microscope during thesis work revealed little quartz and almost no sulfides in the homogeneous fine-grained barite matrix. Nimiuktuk is included with the other deposits discussed in this thesis because it is probably hosted by the Kuna Formation of the Key Creek Sequence.

Jansons and Parke (1981) and Ellersieck and others (1981) have described the Story Creek lead-zinc-silver occurrence (T12S, R26W, Umiat Meridian, Howard Pass quadrangle). Three styles of mineralization are present here: banded massive sphalerite and galena; brecciated sphalerite with a galena matrix; and quartz, sphalerite, and galena cementing black shale chips. Ellersieck and others (1981) report that the deposit is hosted an unnamed "siltstone" unit (Fig. 3), a layer of shale, silty shale, and sandstone that is transitional between the Upper Devonian to Lower Mississippian Kanayut Conglomerate and the Lower Mississippian Kayak Shale. The deposit does not appear to be stratiform, but rather occupies an almost straight N65°E-trending fracture zone that has been traced for 3 km along strike. Bedding is tightly folded and thrust faulted. The host rock is in thrust contact above typical Brooks Range allochthon sedimentary rocks (Ellersieck and others, 1981). Mineralization of the nearby Whoopee Creek occurrence, located in T33N, R5E, Kateel River Meridian, Howard Pass quadrangle, is very similar to that at Story Creek.

Table 5 presents selected emission spectrographic analyses of minerals from the few Ginny Creek, Nimiuktuk, and Story Creek hand

Table 5. Selected emission spectrographic analyses of minerals from the Ginny Creek, Nimiuktuk, and Story Creek deposits.[a]

| Deposit and Mineral | Element[b] | | | | | | | |
|---|---|---|---|---|---|---|---|---|
| | Ag | Cd | Cu | Sb | As | Pb | Zn | Fe |
| Ginny Creek galena | ≥5,000 | 100 | 200 | 50 | <200 | - | 5,000 | .1 |
| Ginny Creek unseparated[c] | 35 | <100 | 75 | 3,500 | 5,000 | 5,000 | >10,000 | 15 |
| Nimiuktuk barite | <1 | <100 | 5 | <20 | <200 | <20 | 350 | <.1 |
| Story Creek sphalerite | 350 | 500 | 500 | 200 | 200 | 5,000 | - | .5 |
| Story Creek galena | ≥5,000 | 350 | 100 | 100 | <200 | - | >10,000 | .1 |

a. All analyses performed by the author according to the procedure described by Stevens (1971); b. Analytical range: Ag 1-5,000 ppm; Cd 100-500 ppm; Cu 1-20,000 ppm; Sb 20-10,000 ppm; As 200-10,000 ppm; Pb 20-20,000 ppm; Zn 200-10,000 ppm; Fe 0.1-20%. c. From a hand specimen of silicic very fine-grained rock containing intergrown galena, sphalerite, and Fe sulfide.

specimens. Conditions and procedures are the same as for Red Dog and Drenchwater emission spectrographic analyses in preceding chapters.

Two Ginny Creek samples were analyzed. The galena comes from a large galena grain embedded in a small lump of gossan, while the second analysis is of a hard, silicic material composed mainly of sphalerite, iron sulfides, and galena too fine grained to be separated. The galena sample analyzed very high in silver, but only low to medium for the other elements checked when compared to Red Dog, Drenchwater, and Story Creek. The unseparated Ginny Creek ore is low in silver, which may reflect low galena content in the sample; but at greater than 5000 ppm its Mn content is much higher even than any Red Dog iron sulfide analysis and is equalled only by the Drenchwater barite. This sample is also high in Ti (750 ppm) and Ni (200 ppm), though Mo (less than 10 ppm) was below detection. High As and Sb undoubtedly reflect high pyrite content.

Emission spectrographic analysis of the one sample of Nimiuktuk barite (Table 5) shows all elements other than Zn and Ti (500 ppm) to be near or below their detection limits and even these two are low. Lead and iron are below detection and zinc is lower than any other analysis done for this thesis except for two Drenchwater barite samples. Barnes and others (1982) speculate that a sulfide deposit might occur at depth at Nimiuktuk, or that such a deposit might be displaced some distance by thrust faulting. A thorough examination of one small sample from the barite deposit, however, does not support this possibility.

The Story Creek sphalerite and galena samples are both taken from the same hand specimen. As at Red Dog, Ag is seen (Table 5) to be preferentially contained in galena. Microscope study of Story Creek polished sections revealed no discreet Ag phases. A high-grade sample of banded sulfide ore collected by Ellersieck and others (1981) contained 4,300 ppm Cu, which is quite high compared to other deposits reported in this thesis, next highest being certain sphalerite samples from Red Dog and Drenchwater at 1,000 ppm each. Copper analysis of the Story Creek sphalerite sample in Table 5, at only 500 ppm, is considerably lower. However, this is not from the same style of ore as that reported by Ellersieck and others.

# VII. LEAD ISOTOPE RATIOS FROM THE DELONG MOUNTAINS DEPOSITS

## A. Introduction

Two galena samples from Red Dog and one from Drenchwater were submitted to a commercial laboratory for lead isotope analysis in hopes of obtaining mineralization ages. The ratios from this analysis could not be interpreted by accepted calculations or growth curves. Not only were they anomalous, giving "future" ages of a sort, but they did not even seem to belong to any recognized anomalous type (see Appendix C). These problems proved to result from significant error in the $^{204}Pb$ determinations. This isotope, primordial and nonradiogenic, forms a very small proportion of any naturally occurring lead sample, never more than two percent, so its accurate determination is more difficult than that of the other lead isotopes. $^{204}Pb$ error causes points plotted from the ratios to fall off the growth curve on a straight line through the origin of the curve (Kanasewich, 1968), so the error is fairly simple to recognize. Nevertheless, it cannot be corrected for and invalidates the data.

The same three samples were therefore submitted to another laboratory, which produced results that appear to be accurate. These ratios (Lueck, 1980) are listed in Table 6. Lange and others (1981) report two additional lead analyses from Red Dog and one from Drenchwater (Table 6). Both of these studies derived lead model ages of about 170-200 m.y., using the Stacey and Kramers (1975) lead growth model (Appendix C). These Triassic to Jurassic lead model ages conflict with the fact that the host rocks are known to be Carboniferous while the mineralization is thought to be syngenetic.

The data in this chapter also includes new analyses from the Red Dog, Story Creek, and Ginny Creek deposits (Table 6). The close similarity of the new ratios to the previously published ones greatly increases confidence that the samples have not been fortuitously chosen from a heterogeneous population. At the same time, the publication of the new theory or model of plumbotectonics allows for a different, better interpretation of the lead data (Doe and Zartman, 1979; Zartman and Doe, 1981). A summary of lead isotope theory, including plumbotectonics, is given in Appendix C.

## B. Data

The data from Table 6 are plotted in Figure 27, A and B, a pair of diagrams showing lead growth curves plotted from Zartman and Doe's (1981) table of theoretical values for lead evolution in the four plumbotectonics environments: A. mantle; B. orogene; C. upper crust; D. lower crust. The superimposed ovals, also from Zartman and Doe

Table 6. Lead isotope data from four base-metal sulfide deposits, DeLong Mountains, Alaska

| Deposit | Sample no. | Sample type | $\frac{206}{204}$ | $\frac{207}{204}$ | $\frac{208}{204}$ |
|---|---|---|---|---|---|
| 1. Red Dog[a] | LL26-18 | coarse-grained galena vein (float) | 18.404 | 15.590 | 38.228 |
| 2. Red Dog[a] | LL4-14 | galena lamination in barite-sulfide vein | 18.413 | 15.604 | 38.197 |
| 3. Red Dog[b] | 78ARD-1 | vein galena | 18.414 | 15.602 | 38.254 |
| 4. Red Dog[b] | RD-63B | disseminated galena | 18.409 | 15.598 | 38.238 |
| 5. Red Dog[c] | LL26-6B | galena from sp-py-ga-qtz vein/ breccia ore | 18.403 | 15.602 | 38.254 |
| 6. Drenchwater[a] | 78PM052 | disseminated galena | 18.406 | 15.592 | 38.270 |
| 7. Drenchwater[b] | 77ANK-13H | disseminated galena | 18.428 | 15.609 | 38.351 |
| 8. Story Creek[c] | 79Md194B | galena from brecciated massive sp-ga ore | 18.404 | 15.595 | 38.224 |
| 9. Ginny Creek[c] | 78Ek127A | coarse galena crystal from sphalerite ore | 18.395 | 15.592 | 38.236 |

Note: Locations of Red Dog hand specimens for analyses 1, 2, and 5 are given in Appendix A, Figure 2.

[a]Analyses from Lueck, 1980.
[b]Analyses from Lange and others, 1981.
[c]New analyses for this report.

(1981) represent fields of actual lead isotope ratios from around the world attributed by the model to the four environments and are included for comparison. The solid-line oval marked 'Island arc' goes with curve B for the orogene, and includes 80% of reported values for that curve. The dashed-line ovals enclose more restricted groups of analyses and are meant to more closely approximate average values for the other three environments. Points marked X indicate theoretical present values for each growth curve, meaning that lead-bearing deposits forming in any one of these environments today should have lead isotope ratios similar to that of the X point for the corresponding growth curve. Two figures are needed because there is no good way to show all three ratios on one; ternary diagrams force $^{207}Pb$ into an apparent decrease in relative abundance even though it actually increases with time along with the other radiogenic lead isotopes. Finally, tic marks on the curves are in units of 400 m.y. before present.

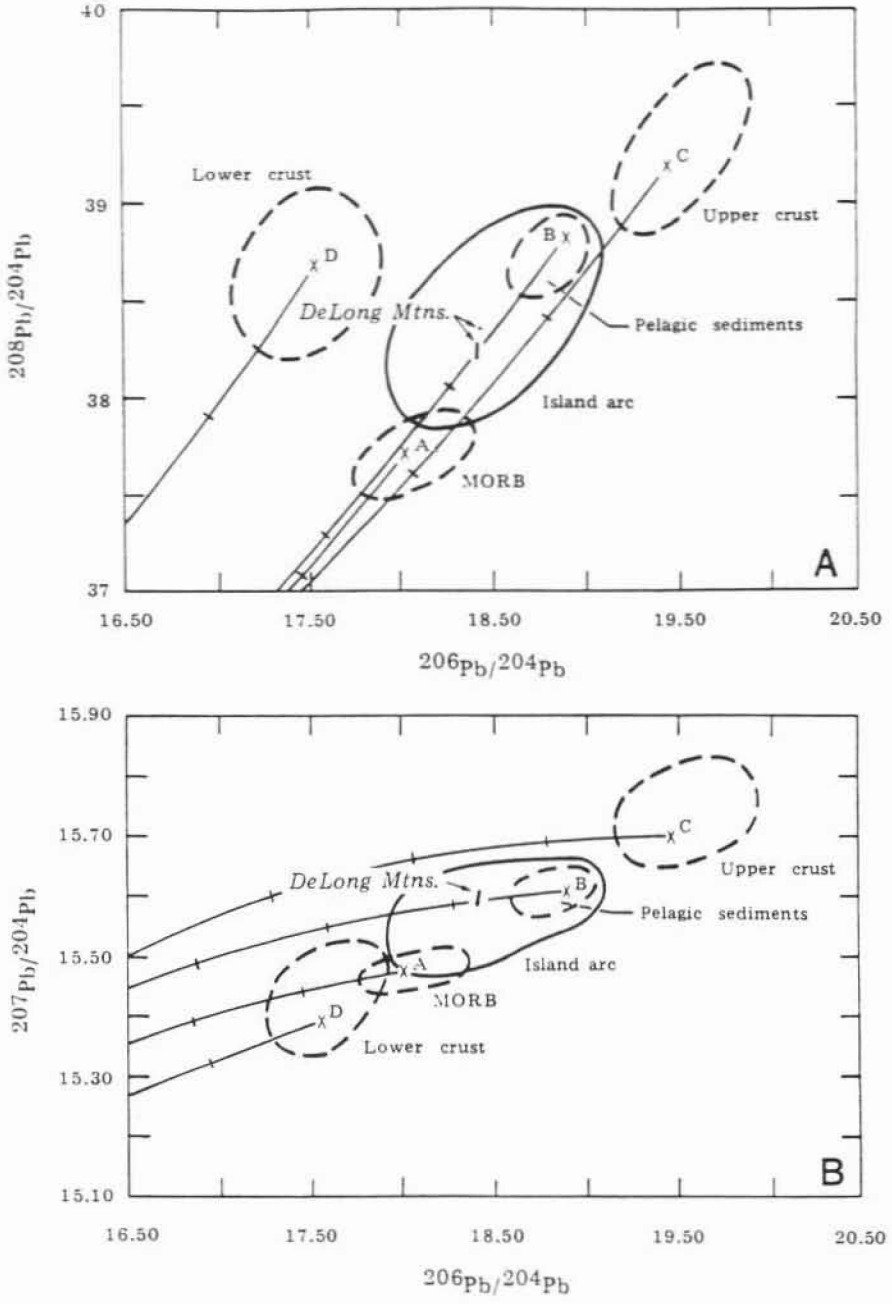


Figure 27. DeLong Mountains lead isotope ratios plotted on lead-lead diagrams modified from Zartman and Doe (1981). See text for explanation.

That analysis no. 7, Table 6, from Drenchwater Creek, has the highest value for each of the three lead isotope ratios may be significant in some way but the difference between these ratios and the others in the table is so small that it is difficult to evaluate. High $^{207}Pb/^{204}Pb$ usually indicates a greater than average continental lead contribution to the isotope composition (R.E. Zartman, pers. comm., 1981). This is an anomalous fact if it is taken for granted that galena at Drenchwater was generated directly from the exposed igneous rocks with which it is now associated.

All the DeLong Mountains analyses fall on or extremely close to curve B (Fig. 27), that for the worldwide orogene lead-mixing environment. The orogene is a broad term for geologic environments in which rocks of the mantle, the lower crust, and the upper crust are tectonically mixed together in various proportions, often with significant additions of unconsolidated sediments. Each of these components contains lead with a certain isotope content. Mixing them gives rise to a new and distinct average lead isotope composition curve (curve B in Fig. 27).

Even more importantly, all nine sets of ratios in Table 6 are so similar to each other that they cannot be plotted as separate points on Figure 27. Although further analyses from the Key Creek sequence could introduce variations, the close similarity of the nine sets of ratios reported here makes this group of values quite atypical of lead isotope suites from such a broad area. Clusters of deposits within the Selwyn Basin, Yukon Territory and northern British Columbia, a geological environment similar in many respects to the Key Creek sequence of Alaska, have lead isotope ratios that group as closely as those found anywhere (Godwin and Sinclair, 1982). Yet even these groups of lead ratios show considerably more variation than do those from the DeLong Mountains, especially over comparable distances.

## C. Interpretation

A lead model age for the DeLong Mountains deposits of approximately 310-320 m.y., late Mississippian and/or early Pennsylvanian, is indicated by the plot in Figure 27 (tic mark nearest the data point stands for 400 m.y.b.p.) and, more precisely, by interpolation of the ratios from Table 6 into the table of theoretical values for the orogene in Zartman and Doe (1981). The close grouping of the data on both graphs of Figure 27 indicates that all four deposits formed contemporaneously in an orogene environment where juvenile and continental lead were mixed. Neither oceanic igneous rocks nor pelagic sediments of Carboniferous age could alone have generated the observed lead isotope ratios, a thorough mixing of leads from both, and perhaps other sources, was required. The model age is compatible with a syngenetic origin for at least part of the sulfide

mineralization at Red Dog and Drenchwater Creek where the host rock is of Carboniferous age.

Of possible subcategories of orogene environment in which the DeLong Mountains mineralization may have been emplaced, several are mentioned in the literature: Lange and others (1981) suggest for Red Dog and Drenchwater a mature arc setting, more specifically like that of Tertiary Japanese Kuroko deposits, or in an Andean-type arc setting; Metz and others (1979b; 1982) postulate a failed rift arm, or aulacogen, extending from the Chukchi Sea to a hypothetical hot-spot triple junction in the Romonzoff Mountains near the Canadian Border. A third possibility is raised by comparing DeLong Mountains ratios with a field for ratios from the European Kupferschiefer presented in plumbotectonics. Such a comparison shows a strong similarity between lead isotopes from these two areas. The DeLong Mountains lead isotope data by themselves do not strongly favor any one of these three settings over the other two, nor does this list necessarily exhaust the possibilities. What is clearly ruled out by the available lead isotope data is an origin for the lead in the deposits in a purely oceanic setting (G.L. Cumming, pers. comm., 1979).

The extreme similarity between their lead isotope ratios suggests strongly that the four thesis deposits, Red Dog, Drenchwater, Story Creek, and Ginny Creek, all had a common origin. This might be inferred from regional geology and major mineral similarity, but the lead isotope message is much more specific: for such very similar lead isotope ratios to have arisen coincidentally from unrelated metals sources over such a broad area at different times would require a complicated set of circumstances that is highly improbable. What is needed, therefore, is a model for the emplacement of very similar ore both syngenetically, and discordantly in older rocks.

The lead model age for the Red Dog deposit is about the same as that of the Carboniferous host rocks. Vein and stockwork ore could have been emplaced slightly later but almost certainly was in place before deposition of the overlying veinless Etivluk Group rocks. The veins are generally taken to be a preserved feeder system for the podiform ore and barite cap, if not for the disseminated ore.

In contrast to Red Dog, sulfides at Drenchwater are closely associated with volcanic and intrusive rocks. Though most ore minerals occur principally in dark shales and cherts of the Kuna Formation much like those at Red Dog, sphalerite, galena, pyrite and marcasite are also found in tuff, tuffaceous sandstone, and metaquartzite. Again, the mixture of volcanic and pelagic rocks indicates an orogene environment. The lead model age of 310-320 m.y. for Drenchwater agrees well with the accepted age of the host rocks, which was determined from fossil evidence, lithologic affinity of the sediments, and by biotite K/Ar ages of 319 ± 10 m.y. and 330 ± 17 m.y.

for a keratophyre and a pyroxene andesite, respectively, rocks which are intimately associated with ore-bearing sediments (Nokleberg and Winkler, 1982)(these rocks were originally termed quartz latite and basalt, respectively, by Mayfield and others, 1979).

However, the implication that the hydrothermal solutions responsible for Drenchwater sulfide mineralization came directly from near-surface igneous rocks is troublesome. Igneous rocks generated during Carboniferous time would not be expected to produce ore deposits with the observed lead isotope ratios, especially the somewhat radiogenic analysis #7 (Table 6, Fig. 27). The alternative should be considered that a deposit was first formed at Drenchwater by a submarine exhalative mechanism similar to that at Red Dog, and that only later was this deposit penetrated by the igneous rocks now exposed at Drenchwater. An origin like this would not affect the lead model age but would better allow for mixing of lead from deep hydrothermal sources with older lead from a thick sedimentary pile to produce the observed orogene lead isotope ratios.

The Ginny Creek and Story Creek sulfide deposits are hosted in rocks significantly older than those of the Kuna Formation. Yet galenas from these two deposits yield the same lead isotope ratios, and therefore the same lead model age for mineralization, as do galenas from the younger Red Dog and Drenchwater deposits. If either Ginny Creek or Story Creek mineralization showed any strong evidence of being syngenetic, their lead isotope contents would have to be considered to be anomalous. However, both deposits appear to be epigenetic. It is suggested that sulfide mineralization at Ginny Creek and Story Creek could have been generated from the same Carboniferous-aged reservoir that produced the Red Dog and Drenchwater syngenetic deposits, giving them the same lead isotope contents. However, at Ginny Creek and Story Creek this mineralization was either emplaced directly into the older rocks in which it is now found, or was later remobilized after its older host rocks had been thrust over sulfide concentrations in Kuna Formation rocks. It could be difficult to distinguish between these two explanations in the case of an individual epigenetic sulfide deposit, and both types of deposit could be widespread in the Key Creek sequence.

# VIII. DISCUSSION, CONCLUSIONS, AND RECOMMENDATIONS

The purpose of this final chapter is to bring together information from throughout the thesis to arrive at conclusions about the origins of the Red Dog, Drenchwater, Story Creek, and Ginny Creek zinc-lead-silver±barite deposits.

## A. Red Dog characteristics compared to those of other sediment-hosted stratiform zinc-lead deposits

The Red Dog zinc-lead-silver-barite deposit has numerous important characteristics of the sediment-hosted stratiform lead-zinc deposit as defined and modeled by Finlow-Bates (1980), Mitchell and Garson (1981), Large (1983), Lydon (1978; 1983), Russell (1978; 1983), and Russell and others (1981). The class of sediment-hosted stratiform zinc-lead deposits (also known sedimentary exhalative, or submarine exhalative) includes such deposits as Mt. Isa, McArthur River, Broken Hill, Rammelsberg, Meggen, the Irish base-metal/silver deposits, Gamsberg (South Africa), and Sullivan. Closer to Alaska, most of the zinc, lead, and silver deposits in the Selwyn Basin of the Canadian Cordillera belong in this category (Carne and Cathro, 1982). Large (1983) prefers to group these deposits into a class rather than refer to a type deposit precisely because there is wide variation in details between members of the class. A number of the features which put Red Dog in this group are now discussed. Where no specific reference is given, the information is composit but taken mostly from Finlow-Bates (1980), Russell and others (1981), Large (1983), and Russell (1983).

1) Host rocks: Sequences of clastic rocks deposited either in epicratonic embayments into the continental margin, or in intracratonic basins; volcanic rocks are subordinate to absent (Large, 1983). Mayfield and others (1983) interpret the Brooks Range allochthon, including the Key Creek sequence and the Kuna Formation, as having originated in such an extensional basin upon continental crust; all of the thesis deposits occur in clastic rocks of this basinal sequence.

2) Syngenesis: Sedimentary exhalative deposits form, at least initially, with the enclosing sediments. Red Dog and Drenchwater are syngenetic deposits, Ginny Creek and Story Creek are epigenetic.

3) Morphology: Stratabound tabular bodies, commonly underlain by stockwork and vein mineralization (Large, 1983). Red Dog has this form, Drenchwater probably does, and Ginny Creek and Story Creek do not.

4) Contemporaneous igneous activity: Commonly, but not necessarily present; indicates an elevated geothermal gradient in the region (Large, 1983). No igneous activity tied to mineralization at Red Dog, abundant igneous rocks at Drenchwater, none reported from Ginny Creek or Story Creek.

5) Ore petrology and geochemistry: The main sulfide minerals of this class of deposits are pyrite and/or pyrrhotite, sphalerite, and galena, with minor chalcopyrite, arsenopyrite, and marcasite; a wide range of Zn/(Zn + Pb) is possible; copper content is usually less than 1%; silver content ranges from insignificant to 180 g/tonne (about 5.3 tr.oz./ton); iron content is usually high. All of the thesis deposits fit these criteria. The Red Dog Zn/(Zn + Pb) ratio of 0.77, calculated from reported grades, is about medium for sedimentary exhalative deposits, as is the Red Dog silver content of about 83 g/tonne (2.4 tr.oz./ton). No grades have been reported for the other thesis deposits.

6) Barite and chert: Commonly, but not necessarily, present. Both abundant at Red Dog, less so at Drenchwater, and not reported from Ginny Creek or Story Creek.

7) Alteration: May be absent from sedimentary exhalative deposits, and takes a variety of forms when present. Silicification is widespread at Red Dog and Drenchwater, and several other low-grade metamorphic minerals have been identified from both deposits. Alteration, other than sulfide mineralization, has not been reported from Ginny Creek or Story Creek.

8) Lead isotope ratios: Generally fit the plumbotectonics orogene growth curve, indicating a composit source. Lead isotope ratios from all of the thesis deposits fit this curve.

Taken together, these criteria define the class of sedimentary exhalative zinc-lead deposits. Red Dog fits all of the criteria, and clearly belongs to the class. The Drenchwater deposit also meets all of the criteria, but the predominance of igneous rocks associated with mineralization at Drenchwater complicates interpretation, and it is not definite whether this deposit belongs to the class of sedimentary exhalative deposits. The Ginny Creek and Story Creek deposits do not meet criteria 2, 3, 6, or 7, and clearly do not belong to this class, though their mineralogy, geochemistry, host rock sequence, and lead isotope ratios seem to link them to the Red Dog and Drenchwater deposits.

B. Aspects of sedimentary exhalative ore genesis with respect to Red Dog

The rock sequences that host sedimentary exhalative deposits consist of successions of virtually all kinds of marine sediments, which may be up to 10 km thick under some of the largest sedimentary exhalative ore bodies (e.g. Sullivan and Mt. Isa)(Sawkins, 1976). As distance from the continental shelf and water depth increase, so does the proportion of shale and chert. That sequences of shale and chert are commonly the host rocks for these deposits is probably due to the fact that the depositional basin must widen and deepen before ore fluids can be generated by whatever mechanism is at work.

It is questionable whether the Key Creek sequence of the Brooks Range allochthon is anywhere as thick as 10,000 m. In their type section (Fig. 3, Chapter III) Mayfield and others (1983) show approximately 1,750 m of rocks from the top of the Kuna Formation down to the bottom of the section. However, the section bottoms at a thrust fault. Elsewhere in their report, Mayfield and others (1983, plate 5) indicate that the Key Creek sequence was deposited on continental crust. Whether or not this is true is part of the Kagvik controversy (Chapter III) and cannot be resolved by this thesis. However, a significant thickness of continental crust beneith the Key Creek sequence in the region around Red Dog would help to make up the thick sedimentary pile required by models of ore fluid generation for large low-Cu, high-zinc-lead sedimetary exhalative deposits (Large, 1983; Lydon, 1983; Russell, 1983).

Tuffaceous horizons are fairly common in the Kuna Formation (Sterne and others, 1984), and several kinds of igneous intrusive and extrusive rocks are present in the Kuna Formation at Drenchwater Creek (Nokleberg and Winkler, 1982). Some contribution of lead from a deep, juvenile source would help to explain the near-perfect fit of DeLong Mountains lead isotope ratios to the plumbotectonics lead growth curve for the orogene (Doe and Zartman, 1979). Existence of intrusives at depth below Red Dog, though speculative, is another way to account for the generation of a large-scale hydrothermal mineralizing system there in spite of the supposedly shallow nature of the Key Creek sequence.

Lange and others (1981) describe the Red Dog deposit as having "formed during a short-lived period of Mississippian submarine volcanism [including submarine eruption of keratophyre and andesite] ... in an incipient Andean-type arc environment or in a mature island arc environment." This interpretation is in part an artifact of these authors trying to force the Red Dog and Drenchwater deposits into a single "type" despite important differences between the two, and partly due to a rather superficial interpretation of the lead isotope ratios. Their interpretation of Red Dog as a Kuroko-type deposit ignores both the lack of igneous rocks in the area and the fact that

copper is very low in the deposit. The interpretation of Lange and others (1981) may be correct for Drenchwater, if it is granted that the small quantity of igneous rocks present there constitute some sort of island arc; their model is not appropriate for Red Dog.

The Red Dog ore fluid probably formed in a downward-excavating hydrothermal cell, as in the model of Russell (1983). In this model, a thick sequence of basinal sedimentary rocks is subjected to an extremely high rate of extentional strain caused by accelerated rifting. The brittle upper crust is suddenly filled with high-angle fractures, which increase permeability by something like two orders of magnitude. This in turn leads to convection in pore waters and draw-down of surface (i.e. ocean) water into the convection system. Convection might not be vigorous at first but has the effect of cooling the rocks through which it circulates, thereby depressing the brittle-ductile transition zone, assuming a constant, high rate of extentional strain. With deepening of fractures, convecting brines encounter progressively hotter rocks, which leads to more vigorous convection, and so on. Russell (1983) estimates that such a system would bottom at about 15 km as load pressure effectively closes pore spaces, ending brittle fracture.

In Russell's (1983) model, ordinary rocks are the source of metal ions, silica, and reduced sulfur, concentrations of which are controlled by temperature, oxidation state, and reactions with minerals in the rocks. Pore waters and down-drawn sea water contribute chloride that forms complexes to carry lead and zinc in solution. As the cell grows and deepens, the temperature increases to around 200°C, lead and zinc leach ever more easily into solution, and the oxidation state becomes too low to allow the appreciable solution of copper. The degree to which this process has progressed is termed the relative "maturity" of the convection cell (Russell, 1983). Only in what Russell (1983) calls maximal conditions, in which the cell "bottoms out," will the solubility of copper increase significantly. This could help to account for what little chalcopyrite is present in Red Dog ore. Convection and deepening of the cell continue until it bottoms, after which it cools for a length of time comparable to that of the heating phase, or until the extentional stress is relieved, which could prevent the system from reaching maximal maturity.

This model of Russell (1983) seems preferrable for Red Dog mainly because of lack of evidence for a thick pile of unlithified sediments in the region during Carboniferous time as required by the Lydon (1983) model. Presumably the Russell mechanism could operate fairly well in only a few thousand meters of sedimentary section, especially with a possibly elevated geothermal gradient due to rifting. Even this few thousand meters of pre-Kuna Formation sedimentary rock is not proven to be present at Red Dog but it seems more likely given the assessment by Mayfield and others (1983) of Key Creek sequence stratigraphy and structure (Fig. 3, Ch. III).

A possible obstacle to complete acceptance of the Russell (1983) model for Red Dog ore fluid generation is the question of temperature. This model seem to rely on temperatures within the reservoir remaining below about 200°C to prevent significant solution of copper. Harrover and others (1982) report $\delta^{18}O$ equilibration temperatures of 60° to 80° ± 10°C for cherts from around the deposit, but calculate a range of 270° to 395°C from chert crystallite sizes. Lange and others (1982) report sulfur isotope temperatures of 115° to 305°C for galena-sphalerite pairs from Red Dog. Determination of temperature from crystallite size is a new technique and Harrover and others (1982) admit that their calculated range of 270° to 395°C for Red Dog could be on the high side, though by how much they do not estimate. Only two out of seven sphalerite-galena pairs gave sulfur isotope temperatures for Red Dog mineralization significantly above 200°C (Lange and others, 1982). It is usually not easy to prove that a pair of sphalerite and galena grains is truly in isotopic equilibrium but the data of Lange and others (1982) cannot be dismissed simply because they do not agree with a certain theory of ore formation. It is unfortunate and surprising that no one has yet reported any fluid inclusion data from Red Dog. Acceptance of the Russell (1983) model for ore fluid generation is therefore tentative pending publication of fluid inclusion or other reliable temperature data from Red Dog.

As a first approximation, the Zn/(Zn + Pb) ratio in a sedimentary exhalative deposit is an indication of conditions in the reservoir (Lydon, 1983). A high ratio indicates relative immaturity (incompleteness) of leaching and vice versa in the terminology of Russell (1983). This also goes for distinct parts of a deposit individually. Although there are no quantitative data on the subject, it is clear from outcrop, hand specimen, and polished section examination that the Red Dog ore types designated here as disseminated and vein have a high Zn/(Zn + Pb), while the breccia and podiform ore types are comparatively rich in lead. This indicates that the veins and disseminated ore may have come early, the breccia and podiform ore later in the development of the deposit, perhaps controlled by the time required for a hydrothermal cell to excavate downward (Russell, 1983).

Since zinc is more soluble than lead, particularly at lower temperatures (Russell, 1983), brines from an immaturely leached reservoir, that is, one in which circulation and therefore temperature are still low, are expected to contain a high proportion of zinc relative to lead. If such a system also contains sufficient reduced sulfur to precipitate most of the dissolved metals, then the high Zn:Pb ratio will be reflected in the resulting mineral assemblage. This probably accounts for the high proportion of sphalerite in disseminated and vein ore at Red Dog.

The smooth, rhythmic zoning of the Red Dog massive sphalerite veins, with relatively little fragmentation of once-deposited sulfides, suggests laminar flow of mineralizing fluids upward through the fractures with even, regular deposition of sphalerite on the fracture walls, possibly even from colloidal gels. Precipitation could have been caused mainly by adiabatic cooling due to relaxation of hydrostatic pressure as the ore brine moved upward, perhaps through widening fractures, with little or no addition of fresh sea water. Most of the necessary sulfide ion would come from that already in the solution. Lange and others (1981) report that $\delta^{34}S$ values of the Red Dog vein sulfides cluster very close to 0 per mil, indicating mostly hydrothermal sulfide. In this way, although some galena is also precipitated from solution, its amount is small and masked by the high proportion of sphalerite. Periodic deposition of iron-sulfide laminae in the veins is due to even lower temperatures in the system; probably sphalerite (+ galena) is deposited at the same time but deeper in the vein system (Finlow-Bates, 1980).

The problem with this scenario is that the mineralizing solution may actually cool very little by merely rising through fractures if it does not boil. Although Solomon and Walshe (1979) refer to precipitation by reaction with wall rocks, Large (1983) believes that cooling by interaction with wall rock will be insignificant due to the low heat conductivity of rock. The latter author insists that boiling in the conduit is required for sufficient adiabatic cooling to break chloride compexes and precipitate base-metal sulfides in submarine veins.

There is very little data from Red Dog with which to address the question of boiling in the veins. The highest galena-sphalerite sulfur isotope temperature reported by Lange and others (1982) for Red Dog veins is 255°C. At this temperature a brine with a salinity of 15 weight percent NaCl would boil at a water depth of about 400 m or less; rising 5%, 10%, and 20% solutions at 255°C would boil at about 465 m, 430 m, and 350 m, respectively (Haas, 1971). Finlow-Bates (1980), taking exception to part of Haas' argument, has a 5% NaCl solution already boiling at greater than 500 m depth. The only independent indication of water depth at Red Dog around the time of mineralization is the presence of hexactinelid sponge spicules in the Kuna Formation shales. As pointed out in Chapter IV, these sponges generally live at depths of greater than 500 m, so there may have been at least that much water above the Red Dog deposit while it formed. Until fluid inclusion data are available from Red Dog, there is no indication of the salinity of the mineralizing solution. All that can be concluded on this point at present is that water depth and the temperature and salinity of the Red Dog ore solution could have combined to put the system close to the boiling point in the veins, say within a few ten's of degrees C.

The Red Dog fine-grained laminated and "buckshot" sphalerite may have formed from the same ore solution that deposited sphalerite in the veins but at a lower temperature. Mineralizing brine can pond on the sea floor and react with sediments to produce sulfide minerals (Ridge, 1973; Lydon, 1983). Lamination, where present, might be due to any of several factors causing cyclic concentration and dilution in the brine pool. The buoyant rise, cooling, and collapse of a hydrothermal plume, described by Solomon and Walshe (1979), is one. Repeated low-pressure exhalation of saturated ore fluid by seismic pumping along active faults is another (Sibson and others, 1975). Subsequent degeneration of the brine by cooling and dilution then occurs, with sulfide precipitation, until the next plume or pulse recharges the pool (Lydon, 1983).

Alternatively, the pulses of fresh ore solution might diffuse up through uncompacted sediment from buried conduits until pore water encountered is cool and/or dilute enough to break chloride complexes and cause precipitation. Lambert and Bubela (1970) experimentally produced thin monomineralic sulfide bands in natural sediments of various kinds by mixing either sodium sulfide or a culture of sulfate-reducing bacteria with the sediments and percolating aqueous solutions of zinc, copper, and lead through the mixtures. Temple and Roux (1964) produced similar metal sulfide bands in layers of agar separating clay or ferric hydroxide with adsorbed metal ions from a saline, sulfate-reducing bacteria culture. The coarse-grained "buckshot" ore could have formed in a similar way.

Diffusion of ore-forming fluids through soft sediments may be responsible for precipitation of the Red Dog disseminated sphalerite. This allows massive mineralization to form before the veins. As shown in Chapter IV, at least some of the disseminated sulfides were already in place before the onset of veining; fragments of the former are contained in the latter. Diffuse upward percolation of mineralizing brine could flood the sediments with silica to produce the widespread silicification of the Kuna Formation shales at Red Dog. Silicification apparently accompanied disseminated mineralization and was well underway before vein formation became important at Red Dog.

Breccia and podiform ores are both richer in galena than either of the other two types. As discussed in Chapter IV, the breccia ores have a texture that can be viewed as transitional between that of the veins and that of the podiform ore, and can be found adjacent to either of the latter two types. Both vertical and lateral mineralogical zonation in sedimentary exhalative deposits is common and well documented (Large, 1983). Upon quenching of a hot lead- and zinc-saturated solution, the precipitation of galena is favored over that of sphalerite due to the greater affinity of lead than zinc for sulfide ion. Thus, galena is likely to be more abundant near a submarine vent, declining relative to sphalerite away from the vent.

Galena enrichment in the proximal portion of a deposit can, under some circumstances, be further enchanced by sulfide deficiency in the solution, since, when precipitation begins, lead is better able to capture the limited sulfide ion than is zinc (Lydon, 1983).

It is possible that the breccia and podiform ores were deposited from a solution somewhat richer in lead than that which formed the sphalerite veins and disseminated sulfides. In either the model of Lydon (1983) or that of Russell (1983), a solution relatively enriched in lead with respect to zinc would evolve during a more mature (advanced), and probably somewhat higher-temperature, stage of leaching in the reservoir zone. In this more mature stage, not only has part of the zinc in the reservoir been depleted by earlier leaching, but elevated temperature raises the solubility of lead. The more mature solution can be expected to contain higher concentrations of both lead and zinc; if generated in a reservoir with a relatively high $fO_2$, the solution will contain little barium, and may be sulfide-deficient, which promotes fractional precipitation of galena (Lydon, 1983). This is what is observed in the Red Dog breccia and podiform ores.

No sulfide deposit forming from a modern submarine hot spring has been reported to have the same mineral content that the Red Dog deposit has, particularly its low copper and high lead contents. Undoubtedly this is due to the fact that most reported modern, active deposits are forming on fresh ocean crust with their source of mineralizing solutions in hot basalt and similar rock types rich in copper and low in lead (Bischoff and Dickson, 1975), rather than in ordinary sedimentary rocks. In addition, modifications to a sedimentary exhalative deposit due to burial, compaction, and later groundwater circulation can be profound (Large, 1983; Lydon, 1983). However, many of the microscopic and macroscopic sulfide textures in Red Dog ore are common in active submarine hydrothermal deposits. "Smokers" and basal mounds at the active sites are composed of open meshworks of small crystals and botryoidal growths, many of which closely resemble Red Dog breccia and podiform ore textures (Lonsdale, 1979; Koski and others, 1984; Zierenberg and others, 1984). If allowance is made for an ore-forming solution with a different composition, arising from a different kind of reservoir, and for some post-mineralization modification of the Red Dog deposit, then the resemblance of Red Dog to several of the modern deposits is even closer.

Conclusions about Red Dog ore precipitation are shown schematically in Figure 28. Disseminated sphalerite with minor galena was first to form, either by downward precipitation from a sea bottom pool just above the sediment-water interface zone, or by upward percolation through soft sediments from buried fractures; some bacteriogenic sulfide was probably involved. Most of the silicifica-

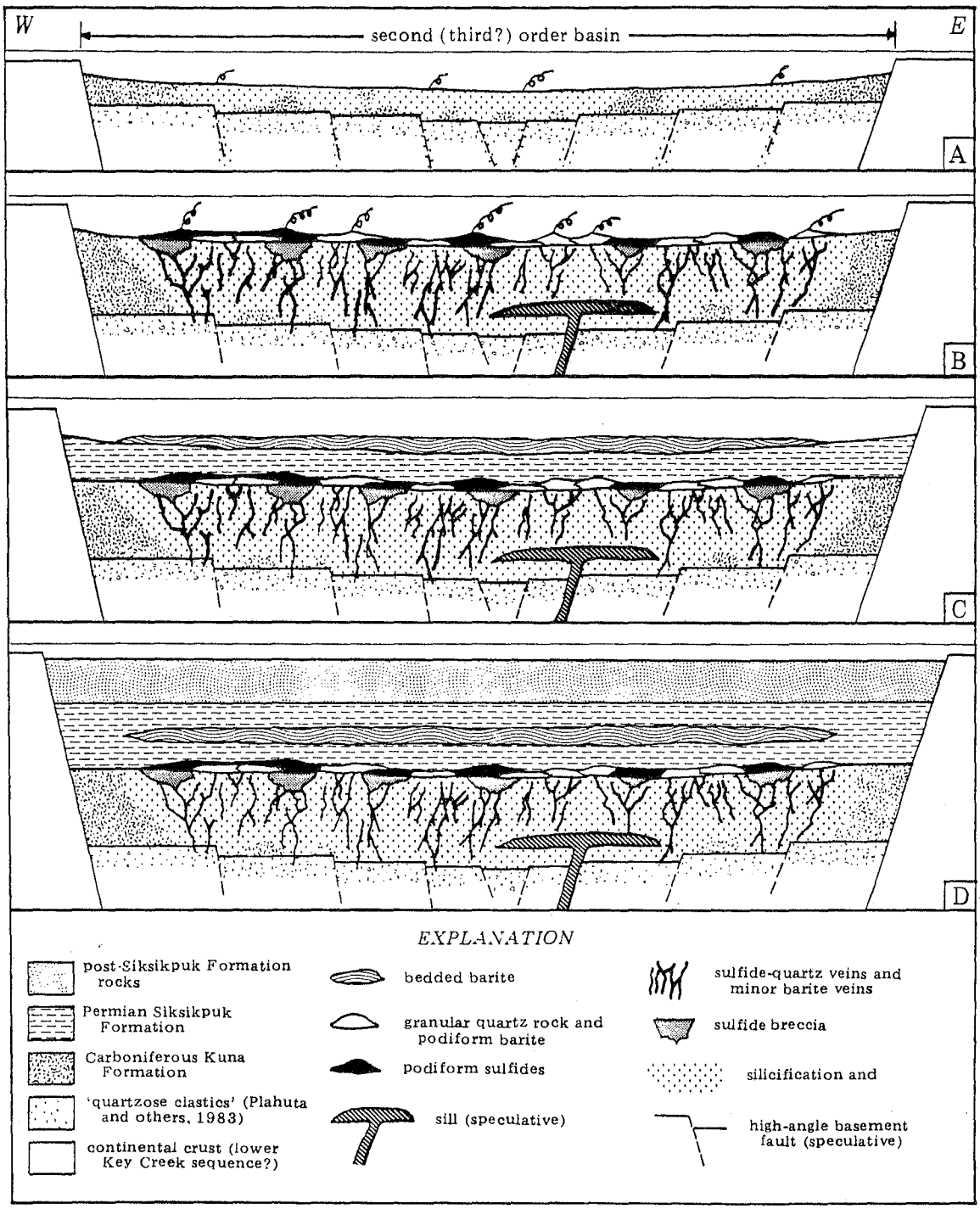


Figure 28. Schematic model of main stages of development of the Red Dog deposit: A, early stages - disseminated ore and silicification; B, later stages - active smokers, basal mounds, veining and brecciation; continued silicification; C, emplacement of bedded barite within Siksikpuk Formation shales; D, burial. See text for discussion.

tion must have occurred together with deposition of the disseminated sulfides (Fig. 28A). The sphalerite veins were emplaced in sediments already lithified but from a zinc-rich solution still very similar to that which deposited the disseminated ore; boiling may have been the cause of precipitation (Fig. 28B). By the time emplacement of the breccia and podiform ores began, the mineralizing solution had evolved to higher lead content and higher temperature, probably reflecting deepening and maturing of the reservoir zone. Exhalation of hydrothermal fluids at the sea floor was more violent than in the case of the veins, causing cataclasis in the vent(s). The podiform ore came from the same later mineralizing fluid that deposited the breccia ore (Fig. 28B).

The reason for the presence of barite in some sedimentary exhalative deposits but not in others is not well known and requires further study, but it is common for barite to be concentrated in sediments above such deposits (Large, 1983). Lydon (1983) suggests that leaching of barium can be enhanced in the same reservoir that produced the sulfide mineralization if conditions in the reservoir become more reducing. At Red Dog, deposition of barite seems to have begun with vein- and podiform-style barite emplacement near the close of sulfide mineralization (Fig. 28B). Later, in Permian time, conditions had changed to allow the deposition of large volumes of barite with very little sulfide mineral content (Fig. 28C). Relaxation of tensional strain, lowered temperature, and impeded circulation of water through the hydrothermal cell could have changed conditions in the reservoir such that barium was leached in preference to base metals. At the same time, conditions at the seafloor must have become more oxygenated to provide the large quantities of sulfate ion required for massive barite deposition. A similar order of events could account for the barite in shales at Drenchwater Creek.

As noted above, sedimentary exhalative deposits typically form in sequences of mainly clastic rocks deposited in extensional epicontinental basins (Large, 1983). The Key Creek sequence of the Brooks Range allochthon appears to have been deposited in such a basin (Mayfield and others, 1983). Not enough is yet known about this basin for it to be discussed in much detail. The presence of submarine exhalative zinc-lead deposits of the Red Dog type within rocks of the Key Creek sequence, however, is independent evidence that the basin formed as a tensional graben or aulacogen upon continental crust.

Host rocks at Drenchwater Creek, though interpreted in this thesis as belonging to the Kuna Formation of the Key Creek sequence mainly because of their location and Carboniferous age, are not easily interpreted if they originated in an extensional epicontinental basin. On the other hand, a collisional mechanism for local magma generation at Drenchwater, as favored by Lange and others (1981) and Nokleberg and Winkler (1982), does not agree with the overall extensional regime

indicated by the stratigraphy and known structure of the Key Creek basin, or with the presence of sedimentary exhalative zinc-lead deposits within rocks of the same sequence. Therefore, the two deposits, Red Dog and Drenchwater, seem to represent conflicting evidence as to the tectonic environment in the DeLong Mountains during the Carboniferous period. Many explanations could be suggested to resolve this apparent contradiction but each would be merely speculative at present.

## C. Conclusions and recommendations

The Red Dog deposit is a syngenetic submarine exhalative deposit related through numerous features to famous ore deposits like Sullivan, Mt. Isa, McArthur River, and deposits in the Selwyn Basin. It also has many characteristics that can be explained by reference to one or another modern submarine exhalative center like the Guaymas Basin and the South San Clemente Basin. The fact that Red Dog has important features not found in modern deposits could be because deposits have not yet been observed forming in just the same setting that produced the Red Dog mineralization. More detailed mapping, probably plane tabling, of the deposit should be done to definitely establish the relationship between the various ore and rock types. Morphology of the deposit as discussed in this thesis, though probably correct in general, is based on very brief field work. With a detailed map in hand, fluid inclusion studies for temperatures and salinities would be useful in determining the deposit's origin, as would quantitative studies of trace elements in ore and country rock. Studies of strontium isotopes from the deposit and associated rocks, especially the igneous outcrops to the northeast, might throw considerable light on the source of the Red Dog barite (Dunham and Hanor, 1967). Microprobe determination of the inclusions or exsolutions in Red Dog sphalerite and galena might answer questions about the nature of the deposit; at least it would help to round out the inventory of Red Dog minerals conducted by microscope and X-ray diffraction for this thesis.

The Drenchwater Creek deposit may have formed by a relatively simple submarine volcanogenic/exhalative process. However, important discrepancies in this model suggest that the mechanism may have been somewhat more complicated. Evidence suggests that the deposit may have been produced by hydrothermal fluids from a deep igneous source penetrating and leaching sediments, or by remobilization of a sedimentary exhalative sulfide concentration by slightly later volcanism. Detailed mapping, sampling, and fluid inclusion studies again might help to determine a more satisfactory explanation for the origin of this deposit.

The Story Creek and Ginny Creek epigenetic deposits are less well

known but share host rock sequence, mineralogy, and lead isotope ratios with the two syngenetic deposits, suggesting a common source for all four. Emplacement of the Story and Ginny deposits could have occurred in a Carboniferous plumbing system or adjacent aquifer, or later by remobilization, yet available evidence indicates that they share an ultimate origin with Red Dog and Drenchwater.

Other known deposits in the Key Creek sequence include the disseminated sphalerite-galena of Lik, located near Red Dog and also hosted in the black shales and cherts of the Kuna Formation; the Nimiuktuk barite deposit, isolated but perhaps hosted in the Kuna Formation; and Whoopee Creek, located near, and very similar to, Story Creek, according to very brief reports. These deposits have not been studied or reported in sufficient detail for them to be fitted into the overall scheme of this thesis with any certainty.

Further lead isotope analyses from DeLong Mountains deposits would be just as valuable as the fluid inclusion data. Many questions are yet to be answered on this topic, for example: How do lead isotope ratios from sphalerite, iron sulfide, barite, and country rock from the various deposits compare to lead ratios of galenas from the same deposits? Would they be similar enough to indicate a common source, or would they be different enough to indicate a separate source for the galena, which appears to be paragenetically late at Red Dog and which up till now has provided all the DeLong Mountains lead ratios? What are the lead ratios from Lik, Nimiuktuk, Whoopee and various lesser-known deposits? Could they continue to be the same as those already reported, indicating a truly large-scale and unusually uniform mineralizing event, or would enough variation eventually emerge to indicate more than one event in the region? At present, the large, uniform event seems easier to believe than that nine galena samples, all with nearly identical lead isotope ratios, have accidentally been chosen from an actually heterogeneous lead isotope population among deposits in the Key Creek sequence. Further analyses of lead compositions from the region could alter that belief.

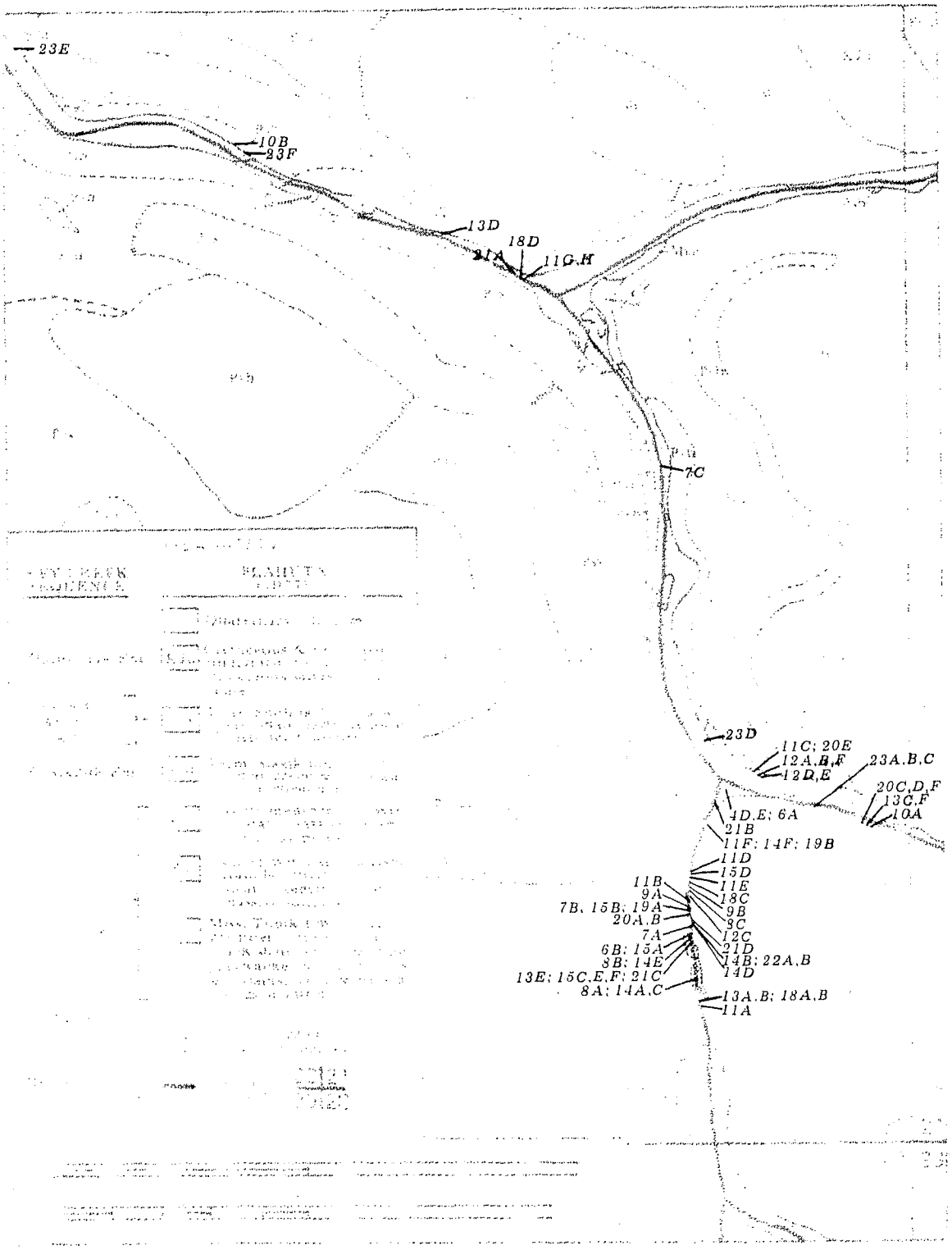


Appendix A, Figure 1. Sample locations for Red Dog hand specimen photographs and photomicrographs; numbers are thesis figure numbers. Geologic map after Plahuta (1978).

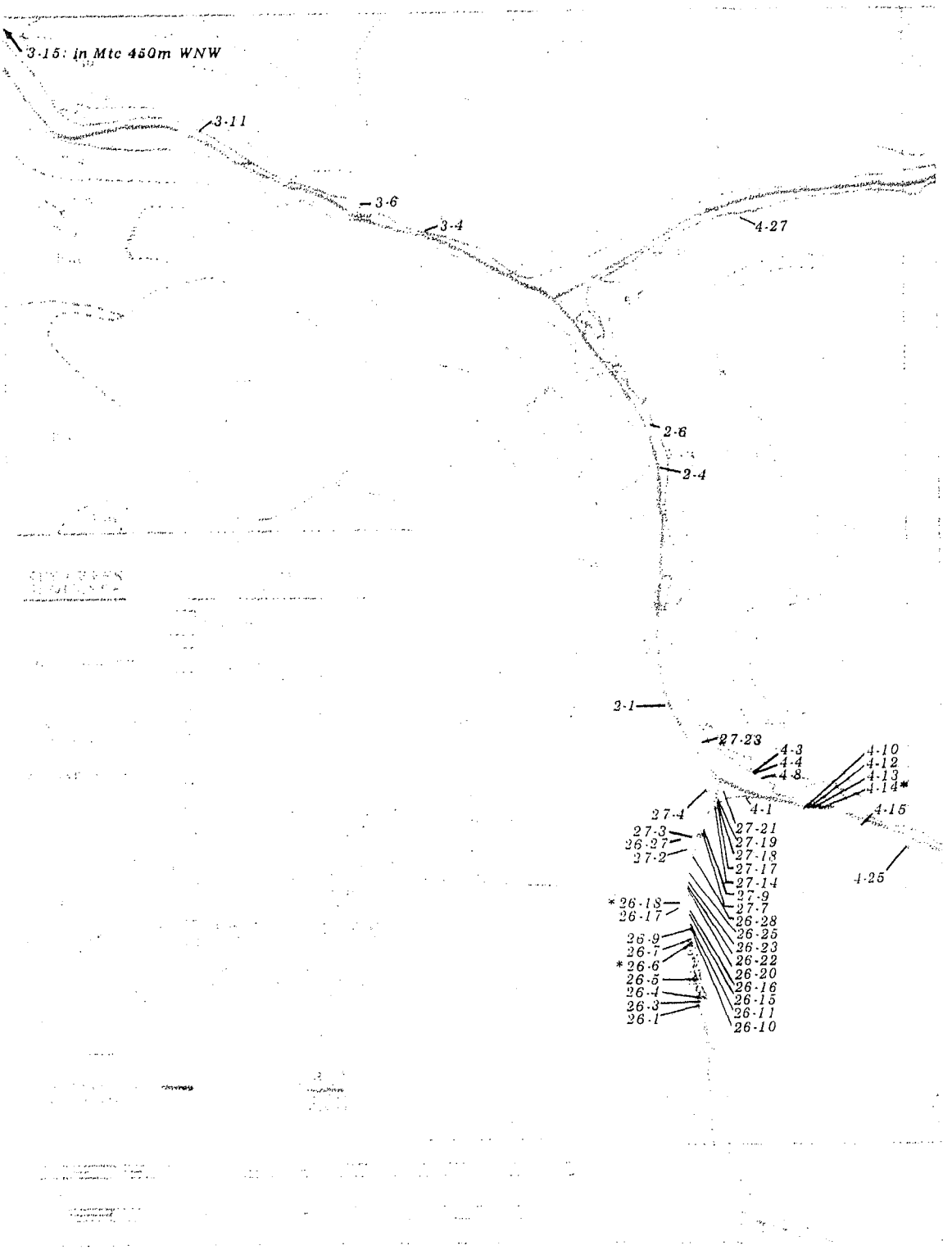


Appendix A, Figure 2. Locations of Red Dog samples analyzed for trace elements and lead isotopes(*). Numbers as in Appendix B, Table 1. Geologic map after Plahuta (1978).

Appendix B, Table 1. Emission spectrographic analyses of Red Dog minerals and host rock by sample type and number.[a]

| Sample[b] Number | Element[c] | | | | | | | | | | | | | | |
|---|---|---|---|---|---|---|---|---|---|---|---|---|---|---|---|
| | Ag | Cd | Cu | Sb | As | Pb | Zn | Fe | Sn | Co | Mn | Mo | Ni | Ti | Cr |
| **A. Sphalerite** | | | | | | | | | | | | | | | |
| 26-3 | 500 | >500 | 200 | 350 | 200 | 2,000 | - | .3 | 50 | 10 | <5 | 10 | 5 | 100 | <20 |
| 26-4A | 75 | >500 | 500 | 500 | 500 | 1,000 | - | 1.5 | <20 | 50 | 5 | 10 | 2 | 150 | <20 |
| 26-7 | 150 | 500 | 150 | 500 | 350 | 10,000 | - | 1 | 20 | 20 | <5 | <10 | 3.5 | <50 | <20 |
| 26-9A | 100 | >500 | 750 | 2,000 | 1,500 | 1,000 | - | 5 | 75 | 200 | 10 | 20 | <2 | 100 | <20 |
| 26-11A | 150 | >500 | 750 | 500 | 750 | 1,000 | - | 1 | <20 | 50 | <5 | <10 | <2 | 100 | <20 |
| 26-23 | 500 | >500 | 750 | 750 | 750 | 7,500 | - | 5 | 20 | 50 | <5 | <10 | 3.5 | 50 | <20 |
| 26-25B | 75 | >500 | 750 | 2,000 | 1,000 | 5,000 | - | 5 | 75 | 75 | <5 | 10 | 3.5 | 150 | <20 |
| 27-9L | 100 | >500 | 750 | 750 | 500 | 1,500 | - | 1.5 | 20 | 75 | 5 | <10 | <2 | 50 | <20 |
| 27-9D | 35 | >500 | 1,000 | 1,000 | 3,500 | 750 | - | 7 | 150 | 20 | 10 | 15 | <2 | 200 | <20 |
| 27-17B | 50 | 500 | 1,000 | 2,000 | 1,000 | 750 | - | 5 | 100 | 150 | 10 | 10 | 3.5 | 150 | 20 |
| 27-19B | 200 | >500 | 1,000 | 750 | 1,000 | 1,000 | | 1.5 | <20 | 350 | <5 | <10 | <2 | <50 | <20 |
| 27-21B | 75 | >500 | 750 | 100 | 750 | 1,500 | | 1.5 | <20 | 75 | <5 | <10 | <2 | 150 | <20 |
| 4-13 | 500 | >500 | 750 | 750 | 750 | 15,000 | | 1.5 | 100 | <10 | <5 | 50 | 2 | 100 | <20 |
| 2-4 | 150 | >500 | 1,000 | 500 | 500 | 2,000 | | 1 | <20 | 50 | 5 | 20 | 2 | 50 | <20 |
| 4-25B | 35 | >500 | 200 | 1,000 | 2,000 | 3,500 | | 5 | 20 | 350 | 5 | 10 | <2 | 50 | <20 |
| **B. Fe sulfide** | | | | | | | | | | | | | | | |
| 26-3 | 150 | <100 | 150 | 3,500 | 5,000 | 5,000 | >10,000 | - | 100 | 10 | 100 | 50 | <2 | 200 | 200 |
| 26-6A | 500 | <100 | 500 | 10,000 | 7,500 | 10,000 | >10,000 | - | 150 | 750 | 100 | 75 | 10 | 75 | 1,000 |
| 26-22 | 150 | <100 | 150 | 5,000 | 10,000 | 5,000 | >10,000 | - | 50 | 750 | 200 | 75 | 500 | 750 | 1,500 |
| 26-10 | 500 | <100 | 500 | 5,000 | >10,000 | 5,000 | 2,000 | - | 75 | 750 | 1,000 | 35 | 15 | 100 | 500 |
| 27-18B | 1,000 | <100 | 500 | 3,500 | 5,000 | 15,000 | 10,000 | - | 50 | 500 | 750 | 75 | 150 | 100 | 1,500 |
| 26-15 | 150 | <100 | 75 | 5,000 | 10,000 | 10,000 | 1,500 | - | 50 | 750 | 200 | 75 | 500 | 200 | 1,500 |
| 26-20 | 150 | 100 | 100 | 5,000 | 10,000 | 7,500 | >10,000 | - | 100 | 350 | 150 | 50 | 7.5 | 200 | 7,500 |
| 4-4B | 20 | <100 | 35 | 3,500 | 7,500 | <20 | 750 | - | 35 | 200 | 100 | 35 | <2 | 50 | 75 |
| 2-4A | 750 | <100 | 500 | 3,500 | 7,500 | >20,000 | 10,000 | - | 150 | 500 | 1,000 | 100 | 75 | 150 | 750 |
| 4-25B | 150 | 100 | n.d. | 5,000 | 10,000 | 1,500 | >10,000 | - | 50 | 200 | 750 | 20 | <2 | 500 | 200 |

Appendix B, Table 1. continued

C. Galena

| | Ag | Cd | Cu | Sb | As | Pb | Zn | Fe | Sn | Co | Mn | Mo | Ni | Ti | Cr |
|---|---|---|---|---|---|---|---|---|---|---|---|---|---|---|---|
| 26-3A | 1,000 | 100 | 35 | 75 | <200 | - | >10,000 | 1 | 20 | 35 | <5 | 10 | <2 | 50 | <20 |
| 26-3C | 2,000 | <100 | 100 | 100 | <200 | - | >10,000 | .5 | <20 | 50 | <5 | 10 | <2 | 150 | <20 |
| 26-6B | >5,000 | 350 | 100 | 100 | <200 | - | >10,000 | .3 | <20 | 50 | <5 | 15 | 2 | 50 | <20 |
| 26-18 | >5,000 | <100 | 35 | 20 | <200 | - | 2,000 | <.1 | 20 | 20 | <5 | <10 | <2 | 100 | <20 |
| 4-13 | 3,500 | 100 | 150 | 100 | <200 | - | >10,000 | .5 | <20 | 50 | <5 | <10 | <2 | 75 | <20 |
| 4-14A | 2,000 | 500 | 200 | 500 | 500 | - | >10,000 | 1.5 | 100 | 20 | <5 | 50 | 2 | 200 | <20 |
| 4-14C | 2,000 | 150 | 75 | 50 | <200 | - | >10,000 | .1 | 75 | <10 | <5 | 10 | <2 | 50 | <20 |
| 4-15B | 2,000 | <100 | 35 | 200 | <200 | - | >10,000 | .5 | <20 | 50 | <5 | <10 | 2 | 75 | <20 |
| 2-4 | >5,000 | <100 | 350 | 1,000 | 1,000 | - | >10,000 | 7 | 350 | 50 | 1,500 | 100 | 5 | 500 | 1,000 |

D. Barite

| | | | | | | | | | | | | | | | |
|---|---|---|---|---|---|---|---|---|---|---|---|---|---|---|---|
| 27-23 | 7 | <100 | n.d. | 50 | <200 | 15,000 | 10,000 | .1 | 100 | 20 | <5 | 50 | 5 | 350 | <20 |
| 3-6B | 100 | <100 | 20 | 100 | 200 | >20,000 | 5,000 | .7 | <20 | <10 | <5 | 50 | 7 | 350 | 150 |
| 3-11 | 2 | <100 | 2 | 50 | <200 | 750 | 750 | .1 | <20 | <10 | <5 | 35 | <2 | 350 | <20 |
| 4-10A | 75 | <100 | 15 | 750 | 750 | 7,500 | 1,500 | 5 | 100 | 20 | <5 | 20 | 2 | 500 | <20 |
| 4-12A | 15 | <100 | 7 | 350 | 200 | 7,500 | 3,500 | 1.5 | 20 | 75 | <5 | 20 | 2 | <50 | <20 |
| 4-13 | 20 | >500 | 50 | n.d. | n.d. | 500 | 1,000 | 1 | <20 | 10 | <5 | <10 | 10 | 2,000 | 20 |
| 4-27 | 750 | <100 | 100 | n.d. | n.d. | >20,000 | 2,000 | 5 | <20 | 350 | 350 | 150 | 500 | 1,000 | 2,000 |

E. Host rock

| | | | | | | | | | | | | | | | |
|---|---|---|---|---|---|---|---|---|---|---|---|---|---|---|---|
| 26-1 | 50 | <100 | 75 | n.d. | n.d. | 5,000 | 1,000 | 1.5 | <20 | 20 | 50 | <10 | 15 | 1,000 | <20 |
| 26-5 | 75 | <100 | 750 | n.d. | n.d. | 10,000 | >10,000 | 10 | 20 | 350 | 500 | <10 | 500 | 2,000 | 2,000 |
| 26-16 | <1 | <100 | 75 | n.d. | n.d. | 1,000 | 1,000 | 5 | <20 | 20 | 5 | <10 | 100 | 3,500 | 150 |
| 26-17 | 10 | 150 | 10 | n.d. | n.d. | <20 | 1,000 | 1 | <20 | 10 | 1,000 | 10 | 2 | 5,000 | <20 |
| 26-28 | 2 | <100 | 10 | n.d. | n.d. | 3,500 | 1,000 | 2 | <20 | 20 | 100 | <10 | 100 | 3,500 | 1,000 |
| 27-14 | 35 | <100 | 20 | n.d. | n.d. | 1,500 | 1,000 | 2 | <20 | 50 | 75 | <10 | 100 | 5,000 | 1,000 |
| 2-6 | 75 | 150 | 200 | n.d. | n.d. | 10,000 | >10,000 | 5 | 20 | 10 | <5 | <10 | 7 | 50 | <20 |
| 3-15 | 15 | <100 | 50 | n.d. | n.d. | 750 | 500 | 5 | 20 | 500 | 150 | <10 | 500 | 1,500 | 750 |
| 4-1 | 15 | <100 | 5 | n.d. | n.d. | 750 | 750 | 1.5 | <20 | 50 | 5 | <10 | 150 | 2,000 | 75 |
| 4-3 | 750 | 100 | 750 | n.d. | n.d. | >20,000 | >10,000 | 7 | 20 | 10 | 75 | <10 | 7 | 2,000 | <20 |
| 4-8A | 50 | 500 | 500 | n.d. | n.d. | 10,000 | >10,000 | 7 | <20 | 20 | 5 | <10 | 200 | 2,000 | 500 |
| 4-12B | <1 | <100 | 10 | n.d. | n.d. | 1,000 | 1,500 | 1.5 | <20 | 20 | <5 | <10 | 75 | 1,500 | 20 |
| 26-6C | 35 | <100 | 75 | 500 | 500 | 5,000 | >10,000 | 1.5 | <20 | 20 | <5 | 10 | 100 | 500 | 100 |
| 27-7 | 10 | <100 | 15 | 200 | <200 | 1,000 | 2,000 | .5 | <20 | 20 | <5 | 10 | 10 | 750 | <20 |

Appendix B, Table 1. continued

F. Quartz-barite rock

| | Ag | Cd | Cu | Sb | As | Pb | Zn | Fe | Sn | Co | Mn | Mo | Ni | Ti | Cr |
|---|---|---|---|---|---|---|---|---|---|---|---|---|---|---|---|
| 2-1 | 100 | <100 | 500 | n.d. | n.d. | 1,500 | 500 | 5 | <20 | 150 | 20 | <10 | 150 | 3,500 | 1,500 |
| 26-27 | 75 | <100 | 35 | 200 | <200 | 7,500 | n.d. | .5 | <20 | <10 | 75 | 10 | 200 | 150 | <20 |
| 27-2 | 35 | <100 | 15 | 200 | <200 | 7,500 | 1,500 | .2 | <20 | <10 | 50 | 10 | 50 | 150 | <20 |
| 27-3 | 150 | <100 | 35 | 350 | <200 | 10,000 | 5,000 | .5 | <20 | 100 | 20 | <10 | 200 | 100 | 75 |
| 3-4B | 50 | 100 | 75 | 150 | 200 | 20,000 | >10,000 | .2 | 20 | 20 | 20 | 10 | 150 | 100 | 20 |
| 27-4 | 75 | <100 | 500 | 500 | 500 | 10,000 | >10,000 | 1.5 | <20 | <10 | <5 | 10 | 10 | 50 | <20 |

a. All analyses performed by the author according to the procedure described by Stevens (1971).
b. Except for samples 27-9L and 27-9D, where L = light-colored sphalerite and D = dark-colored sphalerite from bands within the same sample, the capital letter part of a sample number merely denotes a certain hand specimen from a given station. Station locations are shown in Appendix A, Figure 2.
c. Analytical limits: Ag 1-5,000 ppm; Cd 100-500 ppm; Cu 1-20,000 ppm; Sb 20-10,000 ppm; As 200-10,000 ppm; Pb 20-20,000 ppm; Zn 200-10,000 ppm; Fe 0.1-20%; Sn 20-1,000 ppm; Co 10-2,000 ppm; Mn 5-5,000 ppm; Mo 10-2,000 ppm; Ni 2-5,000 ppm; Ti 50-10,000 ppm; Cr 20-5,000 ppm; n.d. = no data.

## APPENDIX C

## SUMMARY OF LEAD ISOTOPE THEORY

Lead has four common, naturally occurring isotopes of atomic weight 204, 206, 207, and 208. $^{204}Pb$ is primordial, having no known parent isotopes, and thus its amount is constant in the earth as a whole. $^{232}Th$ decays through a series of daughter products to $^{208}Pb$. $^{235}U$ similarly decays to $^{207}Pb$, and $^{238}U$ to $^{206}Pb$. These decay series occur at different but precisely known rates. It is therefore theoretically possible to date a sample of lead containing all four isotopes by extropolating the observed proportions back to an assumed uranium/thorium/lead composition of a source and calculating how long it would have taken the observed lead isotope proportions to have formed by known decay rates.

Several assumptions are necessary in any such calculation:

1. That the reservoir containing thorium, uranium, and lead is very large and homogeneous so that the initial composition can be considered constant and uniform;

2. That this initial Th/U/lead composition, including proportions of all four lead isotopes present at the formation of the earth, can be quantitatively estimated with some confidence;

3. That lead found in deposits and rocks has been derived directly from this large, homogeneous source or reservoir without any kind of contamination on the way and left undisturbed by geochemical processes since the time of emplacement;

4. That the composition of the large, homogeneous source or reservoir has not changed since the formation of the earth.

Until recently, the large, homogeneous source was taken by most investigators to be the mantle. Evidence from meteorites and elsewhere led to estimates of the age of the earth and its initial composition. Radioactive decay rates, though periodically refined, were known on theoretical grounds to be unchanging with time. Galena, feldspar, and some other minerals do tend to exclude uranium and thorium from their crystal lattices while including lead without respect to isotopes, thus locking in Pb/Pb isotope ratios present during ore or rock formation. And significant geochemical fractionation of lead isotopes after emplacement has not been demonstrated; the only paper claiming fractionation (Boyle, 1959) is seldom cited.

These ideas were first applied to the problem of age dating of ore deposits by A.O. Nier and others in the late 1930's and early 1940's (Faure, 1977). In 1946 A. Holmes and F.G. Houtermans independently formulated a set of equations relating assumed primordial lead isotope ratios and assumed U/Pb and Th/Pb ratios by known decay constants to measured lead isotope ratios from rocks and ore deposits. This set of algorithms, the so-called Holmes-Houtermans model, can generate any number of lead growth curves depending on values assigned for the age of the earth, initial isotope compositions of the large homogeneous source or reservoir, and the decay constants. Any age for a lead sample determined from plotting observed ratios against such a theoretical growth curve is called a "lead model age."

Use of the Holmes-Houtermans model led to some successful dating of lead from rocks and ore deposits of known age but to even more exceptions, or anomalies. It was gradually recognized that only stratiform ore deposits, and not all of those, yielded lead isotope ratios conforming to any one reasonable growth curve. Many anomalies fell into two broad categories, J-type and B-type. The former give model ages younger than the host rocks, even ages millions of years from the present. The B-type gives ages older than the host rocks.

It had to be recognized that juvenile lead (from the deep, large source) is often mixed with crustal lead during magmatism and ore emplacement (Doe, Hedge, and White, 1966). Even more revolutionary was growing evidence that the supposed large, deep, homogeneous lead source was not homogeneous in either mineral or isotope composition. Armstrong (1968), Armstrong and Hein (1973), Hedge (1974), and Vollmer (1983), among others, have shown that the earth's mantle could not be as homogeneous as previously thought. If the mantle is significantly heterogeneous, due to incomplete mixing since planetary accretion or to plate tectonic subduction or both, even leads derived directly from this deep, relatively stable reservoir could not be expected to fit a simple, uniform model. Together with crustal mixing during emplacement this initial inhomogeneity explains in general why the great majority of leads do not fit any single model growth curve well.

Stacey and Kramers (1975) and Cumming and Richards (1975) developed lead evolution models which assumed, without postulating specifically how, that the deep, more or less homogeneous lead source was at some time in the past reset, that the U/Pb, Th/Pb, and U/Th ratios were changed. In both models this reset leads to a two-stage growth, with lead isotope development continuing along one Holmes-Houtermans-type curve from the formation of the earth to a point at which the mantle composition changed, after which lead evolution occurred along a different curve. Stacey and Kramers' changeover is abrupt at 3,700 million years ago, thought to be a time of major crustal formation. That of Cumming and Richards occurs gradually, probably also due to crustal accretion. Both of these

models work better than single-stage growth curves by accommodating more deposits of known age. But on either one the majority of lead-containing deposits still do not fit well nor yield reasonable model ages, in other words, they are anomalous. There does not seem to be any way to make most lead isotope ratios fit any single growth curve.

More recently Doe and Zartman (1979) and Zartman and Doe (1981) incorporated lead evolution systematics with the geologic processes of plate tectonics to derive the model they call plumbotectonics. This model recognizes that, since the onset of continental accretion about 4,000 m.y. ago, the earth has had not one but three large, long-term environments or reservoirs, the mantle, the upper crust, and the lower crust. Each of these reservoirs remains separate and distinct for certain periods in its proportions of thorium, uranium, and lead. During these periods, averaging 400 m.y., each of the reservoirs evolves in isolation by radioactive decay, producing a distinctive suite of lead isotope ratios. However, since 4,000 m.y. ago periodic orogenies, more or less evenly spaced in time, have mixed together some fraction of the mantle with preexisting portions of upper and lower crust to form new segments of crust. This mixing produces a fourth, relatively short-term environment or reservoir, the orogene. The model has this isolation-mixing alternation occurring at regular intervals, with the mantle contribution declining by one half in each orogeny. Theoretical lead isotope composition for each of the four broad environments just mentioned is shown by the four pairs of growth curves in Figure 27, A and B.

Plumbotectonics is not the final word in lead isotope theory. It does not treat in any detail the possibility of an originally, inhomogeneous mantle, from which the crust and juvenile leads arise. It cannot account for all the myriad subenvironments which must exist, or for many sets of lead isotope ratios which still are anomalous, nor can it dispense with all assumptions. However, where they are still necessary these assumptions are better justified, more reasonable, and individually less critical to the model as a whole than were those of earlier models. The four pairs of plumbotectonics growth curves in Figure 27 essentially constitute a set of models for lead evolution that gives a choice for interpretation of new data and a better chance of deriving meaningful lead model ages.

Finally, there are more important and achievable applications of lead isotope theory than age dating. Though dating can be enlightening, even the best-conforming lead isotope ratios carry an inherent age uncertainty of ±150 m.y. (Cannon and others, 1961), or even ±200 m.y. (R.E. Zartman, pers. comm., 1981). The primary function is that of "fingerprinting," or characterizing a lead occurrence by its three lead isotope ratios. This has some application worldwide, although deposits which vary in age and

geologic environment need to be compared carefully and tentatively on the basis of their lead isotope composition. It is more useful to examine lead isotopes from a geologically limited terrain with a view to drawing conclusions about sources and genetic connections between related deposits. This has recently been done, for example, by Kish and Feiss (1982) and LeHurray (1982) for parts of the southeast United States, and by Godwin and Sinclair (1982), Godwin and others (1982), and Andrew and others (1984) for geologically well-defined parts of the Canadian Cordillera. These studies have, in fact, led to the development of refined lead growth curves for the areas covered. No new growth curve is proposed in this thesis, but the lead isotope "fingerprinting" approach is considered crucial.

## REFERENCES CITED


Andrew, Anne, Godwin, C.I., and Sinclair, A.J., 1984, Mixing line isochrons: A new interpretation of galena lead isotope data from southeastern British Columbia: Economic Geology, v. 79, p. 919-932.

Armstrong, R.L., 1968, A model for the evolution of strontium and lead isotopes in a dynamic earth: Reviews of Geophysics, v. 6, p. 175-199.

Armstrong, R.L., and Hein, S.M., 1973, Computer simulation of Pb and Sr isotope evolution of the earth's crust and upper mantle: Geochemica et Cosmochimica Acta, v. 37, p. 1-18.

Barnes, D.F., Mayfield, C.F., Morin, R.L., and Brynn, Sean, 1982, Gravity measurements useful in the preliminary evaluation of the Nimiuktuk barite deposit, Alaska: Economic Geology, v. 77, p. 185-198.

Barton, P.B., Jr., and Skinner, B.J., 1979, Sulfide mineral stabilities, in Barnes, H.L., ed., Geochemistry of hydrothermal ore deposits (2nd ed.): New York, Wiley-Interscience, p. 278-403.

Barton, P.B., Jr., and Toulmin, Priestly, III, 1966, Phase relations involving sphalerite in the Fe-Zn-S system: Economic Geology, v. 61, p. 815-849.

Berner, R.A., 1969, The synthesis of framboidal pyrite: Economic Geology, v. 64, p. 383-384.

Bischoff, J.L., and Dickson, F.W., 1975, Seawater-basalt interaction at 200°C and 500 bars: Implications for origin of sea-floor heavy-metal deposits and regulation of seawater chemistry: Earth and Planetary Science Letters, v. 25, p. 385-397.

Boyle, R.W., 1959, Some geochemical considerations on lead-isotope dating of lead deposits: Economic Geology, v. 54, p. 130-135.

Browne, P.R.L., and Lovering, J.F., 1973, Composition of sphalerites from the Broadlands geothermal field and their significance to sphalerite geothermometry and geobarometry: Economic Geology, v. 68, p. 381-387.

Campbell, F.A., and Williams, K.L., 1968, Composition of sphalerite from Quemont Mine, Quebec: Economic Geology, v.63, p.824-831.

Cannon, R.S., Jr., Pierce, A.P., Antweiler, J.C., and Buck, K.L., 1961, The data of lead isotope geology related to problems of ore genesis: Economic Geology, v. 56, p. 1-38.

Carne, R.C., and Cathro, R.J., 1982, Sedimentary exhalative (sedex) zinc-lead-silver deposits, northern Canadian cordillera: C.I.M. Bulletin, v. 75, p. 66-78.

Churkin, Michael, Jr., Mayfield, C.F., Teobald, P.K., Bartow, Harlan, Nokleberg, W.J., Winkler, G.R., and Huie, Carl, 1978, Geological and geochemical appraisal of metallic mineral resources, southern National Petroleum Reserve in Alaska: U.S. Geological Survey Open-file Report 78-70A, 82 p.

Churkin, Michael, Jr., Nokleberg, W.J., and Huie, Carl, 1979, Collision-deformed Paleozoic continental margin, western Brooks Range, Alaska: Geology, v. 7, p. 379-383.

Crane, R.C., 1980, Comments and replies on "Collision-deformed Paleozoic continental margin, western Brooks Range, Alaska," in Forum: Geology, v. 8, p. 354.

Cumming, G.L., and Richards, J.R., 1975, Ore lead isotope ratios in a continuously changing earth: Earth and Planetary Science Letters, v. 28, p. 155-71.

Curtis, S.M., Ellersieck, Inyo, Mayfield, C.F., and Tailleur, I.L., 1982, Reconnaissance geologic map of southwestern Misheguk Mountain quadrangles, Alaska: U.S. Geological Survey Open-file Report OF 82-611, 42 p., scale 1:63,360.

Deer, W.A., Howie, R.A., and Zussman, J., 1966, An introduction to the rock forming minerals: London, Longman, 528 p.

Doe, B.R., Hedge, C.E., and White, D.E., 1966, Preliminary investigation of the source of lead and strontium in deep geothermal brines underlying the Salton Sea geothermal area: Economic Geology, v. 61, p. 462-483.

Doe, B.R., and Zartman, R.E., 1979, Plumbotectonics, the Phanerozoic, in Barnes, H.L., ed., Geochemistry of hydrothermal ore deposits, 2nd ed.: New York, Wiley-Interscience, p. 22-70.

Dunham, A.C., and Hanor, J.S., 1967, Controls on barite mineralization in the western United States: Economic Geology, v. 62, p. 82-94.

Dutro, J.T., Jr., 1980, Comments and replies on "Collision-deformed Paleozoic continental margin, western Brooks Range, Alaska," in Forum: Geology, v. 8, p. 355.

Edmond, J.M., and Von Damm, Karen, 1983, Hot springs on the ocean floor: Scientific American, v. 248, p. 79-93.

Einsele, G., Gieskes, J.M., Curray, J., Moore, D.M., Aguayo, E., Aubry, M.-P., Fornari, D., Guerrero, J., Kastner, M., Kelts, K., Lyle, M., Matoba, Y., Molina-Cruz, A., Niemitz, J., Rueda, J., Saunders, A., Schader, H., Simoneit, B., and Vacquier, V., 1980, Intrusion of basaltic sills into highly porous sediments, and resulting hydrothermal activity: Nature, v. 283, p. 441-445.

Ellersieck, Inyo, Curtis, S.M., Mayfield, C.F., and Tailleur, I.L., 1983, Reconnaissance geologic map of the DeLong Mountains A2, B2, and part of C2 quadrangles, Alaska: U.S. Geological Survey Open-File Report OF 83-184, 53 p., scale 1:63,360.

Ellersieck, I.F., Jansons, Uldis, Mayfield, C.F., and Tailleur, I.L., 1981, The Story Creek and Whoopee Creek lead-zinc-silver occurrences, western Brooks Range, Alaska: The United States Geological Survey in Alaska: Accomplishments during 1980, Warren L. Coonrad, ed.: U.S. Geological Survey Circular 844, p. 35-38.

Facca, G., and Tonani, F., 1967, The self-sealing geothermal field: Bulletin volcanologique, v. 30, p. 271-273.

Farrand, M., 1970, Framboidal sulfides precipitated synthetically: Mineralium Deposita, v. 5, p. 237-247.

Faure, Gunter, 1977, Principles of isotope geology: New York, John Wiley, 464 p.

Finlow-Bates, Terence, 1980, The chemical and physical controls on the genesis of submarine exhalative orebodies and their imlpications for formulating exploration concepts. A review: Geologisches Jahrbuch, D40, p. 131-168.

Godwin, C.I., and Sinclair, A.J., 1982, Average lead isotope growth curves for shale-hosted zinc-lead deposits, Canadian Cordillera: Economic Geology, v. 77, p. 675-690.

Godwin, C.I., Sinclair, A.J., and Ryan, B.D., 1982, Lead isotope models for the genesis of carbonate-hosted Zn-Pb, shale hosted Ba-Zn-Pb, and silver-rich deposits in the northern Canadian Cordillera: Economic Geology, v. 77, p. 82-94.

Haas, J.L., 1971, The effect of salinity on the maximum thermal gradient of a hydrothermal system at hydrostatic pressure: Economic Geology, v. 66, p. 940-946.

Harrover, R.D., Norman, D.I., Savin, S.M., and Sawkins, F.J., 1982, Stable oxygen isotope and crystallite size analysis of DeLong Mountain, Alaska, cherts: an exploration tool for submarine exhalative deposits: Economic Geology, v. 77, p. 1761-1766.

Haymon, R.M., 1983, Growth history of hydrothermal black smoker chimneys: Nature, v. 301, p. 695-698.

Hedge, C.E., 1974, Strontium isotopes in economic geology: Economic geology, v. 69, p. 823-825.

Hodgson, C.J., and Lydon, J.W., 1977, Geologic setting of volcanogenic massive sulphide deposits and active hydrothermal systems: Some implications for exploration: CIM Bulletin, October, p. 95-106.

Jansons, Uldis, and Park, M.A., 1981, 1978 Mineral investigations in the Misheguk Mountain and Howard Pass Quadrangles, Alaska: U.S. Bureau of Mines Open-file Report 26-81, 193 p.

Jones, Allan, 1982, Red Dog deposit said spectacular: The Northern Miner, v. 67, no. 51, p. 1-2.

Kanasewich, E.R., 1968, The interpretation of lead isotopes and their geological significance, in Hamilton, E.I., and Farquhar, R.M., eds., Radiometric dating for geologists: New York, Interscience, p. 147-223.

Kish, S.A., and Feiss, P.G., 1982, Application of lead isotope studies to massive sulfide and vein deposits of the Carolina slate belt: Economic Geology, v. 77, p. 352-363.

Koski, R.A., Clague, D.A., and Oudin, Elisabeth, 1984, Mineralogy and chemistry of massive sulfide deposits from the Juan de Fuca Ridge: Geological Society of America Bulletin, v. 95, p. 930-945.

Krauskopf, K.B., 1967, Introduction to geochemistry: New York, McGraw-Hill, 721 p.

Lambert, I.B., and Bubela, B., 1970, Banded sulphide ores: The experimental production of monomineralic sulphide bands in sediments: Mineralium Deposita, v. 5, p. 97-102.

Lambert, I.B., and Sato, Takeo, 1974, The Kuroko and associated ore deposits of Japan: A review of their features and metallogenesis: Economic Geology, vol. 69, p. 1215-1236.

Lange, I.M., Nokleberg, W.J., Plahuta, J.T., Krouse, H.R., Doe, B.R., and Jansons, Uldis, 1981, Isotopic geochemistry of stratiform zinc-lead-barium deposits, Red Dog Creek and Drenchwater Creek

areas, northwestern Brooks Range, Alaska: in Proceedings of the Symposium on Mineral Deposits of the Pacific Northwest, Geological Society of America, Cordilleran Section Meeting at Corvallis, Oregon, March 20-21, 1980: U.S. Geological Survey Open-file Report 81-355, p. 2-16.

Large, D.E., 1983, Sediment-hosted massive sulphide lead-zinc deposits, in Sangster, D.F., ed., Short course in sediment-hosted stratiform lead-zinc deposits: Mineralogical Association of Canada, Short Course Handbook, v. 8, p. 1-29.

Larter, R.C.L., Boyce, A.J., and Russell, M.J., 1981, Hydrothermal pyrite chimneys from the Ballynoe barite deposit, Silvermines, County Tipperary, Ireland: Mineralium Deposita, v. 16, p. 309-318.

LeHuray, A.P., 1982, Lead isotopic patterns of galena in the Piedmont and Blue Ridge ore deposits, southern Appalachians: Economic Geology, v. 77, p. 335-351.

Lonsdale, Peter, 1979, A deep-sea hydrothermal site on a strike-slip fault: Nature, v. 281, p. 531-534.

Lonsdale, Peter, and Lawver, L.A., 1980, Immature plate boundary zones studied with a submersible in the Gulf of California: Geological Society of America Bulletin, v. 91, p. 555-569.

Lueck, Larry, 1980, Lead isotope ratios from the Red Dog and Drenchwater Creek lead-zinc deposits, DeLong Mountains, Brooks Range, Alaska: Short Notes on Alaskan Geology 1979-1980, Geologic Report 63, Alaska Division of Geological and Geophysical Surveys, p. 1-5.

Lydon, J.W., 1978, Some criteria for categorizing hydrothermal base metal deposits: Current Research, Part A, Geological Survey of Canada Paper 78-1A, p. 299-302.

Lydon, J.W., 1983, Chemical parameters controlling the origin and deposition of sediment-hosted stratiform lead-zinc deposits, in Sangster, D.F., ed., Mineralogical Association of Canada, Short Course Handbook, v. 8, p. 175-250.

McQuat, J.F., 1982, History of the Red Dog deposit discovery: The Northern Miner, v. 68, p. A29.

Martin, A.J., 1970, Structure and tectonic history of the western Brooks Range, DeLong Mountains and Lisburne Hills, northern Alaska: Geological Society of America Bulletin, v. 81, p. 3605-3622.

Mayfield, C.F., 1980, Comments and replies on "Collision-deformed Paleozoic continental margin, western Brooks Range, Alaska," in Forum: Geology, v. 8, p. 357-359.

Mayfield, C.F., Curtis, S.M., Ellersieck, I.F., and Tailleur, I.L., 1979, Reconnaissance geology of the Ginny Creek zinc-lead-silver and Nimiuktuk barite deposits, northwestern Brooks Range, Alaska: U.S. Geological Survey Open-file Report 79-1092, 20 p.

Mayfield, C.F., Tailleur, I.L., and Ellersieck, Inyo, 1983, Stratigraphy, structure, and palinspastic synthesis of the western Brooks Range, northwestern Alaska: U.S. Geological Survey Open-file Report OF 83-779.

Metz, P.A., 1980, Comments and replies on "Collision-deformed Paleozoic continental margin, western Brooks Range, Alaska," in Forum: Geology, v. 8, p. 360.

Metz, P.A., Robinson, M.S., and Lueck, Larry, 1979a, Baseline geochemical studies for resource evaluation of D-2 lands - geophysical and geochemical investigations of the Red Dog and Drenchwater Creek mineral occurrences: Juneau, Alaska, U.S. Bureau of Mines, Alaska Field Operations Center unpublished report, 21 p.

Metz, P.A., Robinson, M.S., Peace, J., and Lueck, L., 1979b, Carboniferous metallogeny of the northern Brooks Range, Alaska and the Arctic Rim: Alaska Geological Society Symposium, Anchorage, Alaska, April 22-25

Metz, P.A., Egan, Alyce, and Johansen, Otto, 1982, Landsat linear features and incipient rift system model for the origin of base metal and petroleum resources of northern Alaska: in Embry, A.F., and Balkwill, H.R., eds., Arctic geology and geophysics; Proceedings of the Third International Symposium on Arctic Geology; Canadian Society of Petroleum Geologists Memoir 8, p. 101-112.

Mitchell, A.H.G., and Garson, M.S., 1981, Mineral deposits and global tectonic settings: New York, Academic Press, 405 p.

Moore, R.C., Lalicker, C.G. and Fischer, A.G., 1952, Invertebrate fossils: New York, McGraw Hill, 766 p.

Mull, C.G., 1980, Comments and replies on "Collision-deformed Paleozoic continental margin, western Brooks Range, Alaska," in Forum: Geology, v. 8, p. 361-362.

Mull, C.G., Tailleur, I.L., Mayfield, C.F., Inyo Ellersieck, and Curtis, S., 1982, New upper Paleozoic and lower Mesozoic

stratigraphic units, central and western Brooks Range, Alaska: American Association of Petroleum Geologists Bulletin, v. 66, p. 348-362.

Nelson, S.W., 1980, Comments and replies on "Collision-deformed Paleozoic continental margin, western Brooks Range, Alaska," in Forum: Geology, v. 8, p. 364-365.

Nokleberg, W.J., and Churkin, M., Jr., 1980, Comments and replies on "Collision-deformed Paleozoic continental margin, western Brooks Range, Alaska," in Forum: Geology, v. 8, p. 360-361.

Nokleberg, W.J., and Winkler, G.R., 1982, Stratiform zinc-lead deposits in the Drenchwater Creek area, Howard Pass Quadrangle, northwestern Brooks Range, Alaska: U.S. Geological Survey Professional Paper 1209, 22 p.

Plahuta, J.T., 1978, Geologic map and cross sections of the Red Dog prospect, DeLong Mountains, northwestern Alaska: U.S. Bureau of Mines Open-file Report 65-78, 11 p., scale 1:20,000.

Plahuta, J.T., Young, L.E., Modene, J.S., and Moore, D.W., 1983, Geology of the Red Dog zinc/lead deposit, DeLong Mountains [abs., 8th Annual Convention of the Alaska Miners Association, Anchorage, Alaska, October 19-22]: The Alaska Miner, v. 11, no. 12, p. 11.

Raiswell, R., and Plant, J., 1980, The incorporation of trace elements into pyrite during diagenesis of black shales, Yorkshire, England: Economic Geology, v. 75, p. 684-699.

Ramdohr, P., 1969, The ore minerals and their intergrowths: New York, Pergamon, 1174 p.

Rickard, D.T., 1970, The origin of framboids: Lithos, v. 3, p. 269-293.

Ridge, J.D., 1973, Volcanic exhalations and ore deposition in the vicinity of the sea floor: Mineralium Deposita, v. 8, p. 332-348.

Roeder, Dietrich, and Mull, C.G., 1978, Tectonics of the Brooks Range ophiolites, Alaska: American Association of Petroleum Geologists Bulletin, v. 62, p. 1696-1702.

Russell, M.J., 1978, Downward-excavating hydrothermal cells and Irish-type ore deposits: importance of an underlying thick Caledonian prism: Transactions of the Institute of Mining and Metallurgy (Section B: Applied earth science), v. 87, p. B168-B171.

Russell, M.J., 1983, Major sediment-hosted zinc + lead deposits: formation from hydrothermal convection cells that deepen during crustal extension, in Sangster, D.F., ed., Short course in sediment-hosted stratiform lead-zinc deposits: Mineralogical Association of Canada, Short Course Handbook, v. 8, p. 251-282.

Russell, M.J., Solomon, M., and Walshe, J.L., 1981, The genesis of sediment-hosted, exhalative zinc + lead deposits: Mineralium Deposita, v. 16, p. 113-127.

Sawkins, F.J., 1976, Metal deposits related to intracontinental hotspot and rifting environments: Journal of Geology, v. 84, p. 653-671.

Scott, S.D., and Barnes, H.L., 1971, Sphalerite geothermometry and geobarometry: Economic Geology, v. 66, p. 653-669.

Scott, S.D., and Kissin, S.A., 1973, Sphalerite composition in the Zn-Fe-S system below 300°C: Economic Geology, v. 68, p. 475-479.

Sibson, R.H., Moore, J.McM., and Rankin, A.H., 1975, Seismic pumping - a hydrothermal fluid transport mechanism: Journal of the Geological Society of London, v. 131, p. 653-659.

Sims, P.K., and Barton, P.B., Jr., 1961, Some aspects of the geochemistry of sphalerite, Central City district, Colorado: Economic Geology, v. 56, p. 1211-1237.

Solomon, M., and Walshe, J.L., 1979, The formation of massive sulphide deposits on the sea floor: Economic Geology, v. 74, p. 797-813.

Stacey, J.S., and Kramers, J.D., 1975, Approximation of terrestrial lead isotope evolution by a two-stage model: Earth and Planetary Science Letters, v. 26, p. 207-21.

Sterne, E.J., Zantop, Half, and Reynolds, R.C., 1984, Clay mineralogy and carbon-nitrogen geochemistry of the Lik and Competition Creek zinc-lead-silver prospects, DeLong Mountains, Alaska: Economic Geology, v. 79, p. 1406-1411.

Stevens, D.L., 1971, Geology and geochemistry of the Denali Prospect, Clearwater Mountains, Alaska: unpublished Ph.D. dissertation, University of Alaska, Fairbanks, 81 p.

Sweeney, R.E., and Kaplan, I.R., 1973, Pyrite framboid formation: laboratory synthesis and marine sediments: Economic Geology, v. 68, p. 618-634.

Tailleur, I.L., Kent, B.H., Jr., and Reiser, H.N., 1966, Outcrop/geology maps of the Nuka-Etivluk region, northern Alaska:

U.S. Geological Survey Open-File Report 66-128, scale 1:63,360, 7 sheets.

Tailleur, I.L., 1970, Lead-, zinc-, and barite-bearing samples from the western Brooks Range, Alaska, with a section on Petrography and mineralogy, by G.D. Eberlein and Ray Wehr: U.S. Geological Survey Open-file Report, 16 p.

Tailleur, I.L, and Brosgé, W.B., 1970, Tectonic history of northern Alaska, in Adkison, W.L., and Brosgé, W.W., eds., Geological seminar on the north slope of Alaska: American Association of Petroleum Geologists, Pacific Section, Menlo Park, California, Proceedings, p. E1-E19.

Tailleur, I.L., Ellersieck, I.F., and Mayfield, C.F., 1977, Mineral resources of the western Brooks Range, in Blean, K.M., ed., The United States Geological Survey in Alaska: Accomplishments during 1976: U.S. Geological Survey Circular 751-B, p. B24-B25.

Taylor, C.M., and Radtke, A.S., 1969, Micromineralogy of silver-bearing sphalerite from Flat River, Missouri: Economic Geology, v. 64, p. 306-318.

Temple, K.L., and Le Roux, N.W., 1964, Syngenesis of sulfide ores: Desorption of adsorbed metal ions and their precipitation as sulfides: Economic Geology, v. 59, p. 647-655.

Urabe, T., and Sato, T., 1978, Kuroko deposits of the Kosaka Mine, northeast Honshu - products of submarine hot springs on Miocene sea floor: Economic Geology, v. 73, p. 161-179.

Vollmer, R., 1983, Earth degassing, mantle metasomatism, and isotopic evolution of the mantle: Geology, v. 11, p. 452-454.

Williams, K.L., 1974, Compositions of sphalerites from the zoned hydrothermal lead-zinc deposits in Zeehan, Tasmania: Economic Geology, v. 69, p. 657-672.

Winkler, H.G.F., 1976, Petrogenesis of metamorphic rocks (4th ed.): New York, Springer-Verlag, 334 p.

Zartman, R.E., and Doe, B.R., 1981, Plumbotectonics - the model: Tectonophysics, v. 75, p. 135-162.

Zierenberg, R.A., Shanks, W.C.,III, and Bischoff, J.L., 1984, Massive sulfide deposits at 21°N, East Pacific Rise: Geological Society of America Bulletin, v. 95, p. 922-929.